

**ESTIMATION OF ABSOLUTE PERMEABILITY
IN MULTILAYERED PETROLEUM RESERVOIRS
WITH TWO- AND THREE-PHASE FLOW**

Thesis by
Eliana Mary Makhoul

In Partial Fulfillment of the Requirements
for the Degree of
Doctor of Philosophy

California Institute of Technology
Pasadena, California

1990

(Submitted January 12, 1990)

ACKNOWLEDGEMENTS

I would like to express my deep appreciation to my advisor, Professor John Seinfeld, without whose generous and patient support this work would not have been completed. I would like to thank Drs. Ernest Chung, Wen Chen, Mel Wasserman and Fred Kelsey for providing many valuable suggestions, and the Chevron Oil Field Research Company for providing access to their lab facilities and their Cray X-MP/48.

I also thank my family and friends, particularly Professor Ares Rosakis and Mr. David Olson for their continuous love and encouragement.

ABSTRACT

A numerical algorithm is developed to estimate absolute permeability in multiphase, multilayered petroleum reservoirs based upon noisy observation data, such as pressure, water cut, gas-oil ratio and rates of liquid and gas production from individual layers. The industrial Black-Oil code, CLASS, (Chevron Limited Application Simulation System), is used as the basic reservoir simulator in conjunction with this history matching algorithm. Since the history matching inverse problem is ill-posed due to its large dimensionality and the insensitivity of the permeability to measured well data, regularization and spline approximation of the spatially varying absolute permeability are employed to render the problem computationally well behaved. A stabilizing functional with a gradient operator is used to measure the non-smoothness of the parameter estimates in the regularization approach, and the regularization parameter is determined automatically during the computation. The numerical minimization algorithm is based on the partial conjugate gradient method of Nazareth. Numerical examples are considered in two- and three-phase reservoirs with three layers. The effects of the degree of regularization, spline approximation versus zonation, and differing true areal permeability distributions on the performance of the method are considered.

Table of Contents

	Page
Acknowledgements	ii
Abstract	iii
Table of Contents	iv
List of Figures	vii
List of Tables	xiv
 Chapter I: Introduction	 1
References	8
 Chapter II: Determination of Individual Layer Properties in Multilayered Reservoirs with Two-Phase Flow	 12
1. Introduction	12
2. Reservoir Model	13
3. Production Strategies	19
4. Sensitivity of Measured Production Variables to Vertical Heterogeneities	24
5. Conclusion	38
Nomenclature	41
References	43
 Chapter III: A General History Matching Code for Three-Phase, Three-Dimensional Petroleum Reservoirs	 45
1. Introduction	45
2. Reservoir Model	46

3. The History Matching Problem	49
4. Spline Approximation of the Areal Permeability Distribution	56
5. The History Matching Algorithm	58
6. Computational Examples	61
7. Conclusions	127
Nomenclature	130
References	134
Appendices	137
A. Finite Difference Reservoir Equations	137
B. Functional Derivative of J_{LS}	141
Chapter IV: Conclusions	146
Appendices	148
A. Derivation of the History Matching Algorithms	148
1. Derivation and Solution of the Reservoir Equations	148
2. Derivation of the Adjoint System	153
3. Calculation of the Derivatives of J_{SM}	159
with respect to $W_{l,k}$	
4. Minimization Algorithm	160
B. User's Guide to the AUTOHM Program	163
1. Introduction	163
2. Discussion of Method	163
3. Generation of the Input and Output Data	164
Files for Use with the AUTOHM Program	
3.1 Input File for CLASS, *.DECK	164
3.2 Generation of the Observation Files	165

from Program RSVRS.FOR	
3.3 Input and Output Files for Step 1 of the AUTOHM Program, RSVR1.FOR	170
3.4 Input and Output Files for Step 2 of the AUTOHM Program, RSVR2.FOR	172
3.5 Input and Output Files for Step 3 of the AUTOHM Program, RSVR3.FOR	178
4. Implementation	184
5. Definition of Programs	186
6. Definition of Subroutines	187
7. Discussion of Options	191

List of Figures

		Page
Chapter II		
Fig. 1 -	Vertical cross section of a petroleum reservoir between an injection and production well	18
Fig. 2	Production wellbore pressure for cases (1.A)-(1.C)	25
Fig. 3	Production wellbore pressure for cases (1.D)-(1.F)	26
Fig. 4	Production wellbore pressure for cases (2.A)-(2.B)	28
Fig. 5	Production wellbore pressure for cases (3.A)-(3.B)	29
Fig. 6	Production wellbore pressure for cases (4.A)-(4.D)	32
Fig. 7	Rate of production from layer two for cases (4.A)-(4.D)	33
Fig. 8	Production wellbore pressure for cases (5.A)-(5.C)	35
Fig. 9	Rate of production from layer one for cases (5.A)-(5.C)	37
Chapter III		
Fig. 6.1	Reservior shape and well locations	65

Fig. 6.2 (a)	True absolute permeability distribution for layer 1	66
Fig. 6.2 (b)	True absolute permeability distribution for layer 3	67
Fig. 6.3	History match of bottomhole pressure from well P3 for 2-phases	79
Fig. 6.4	History match of water cut from well P3 for 2-phases	80
Fig. 6.5 (a)	History match of liquid flow rate from well P3 from completion 1 for 2-phases	81
Fig. 6.5 (b)	History match of liquid flow rate from well P3 from completion 2 for 2-phases	82
Fig. 6.5 (c)	History match of liquid flow rate from well P3 from completion 3 for 2-phases	83
Fig. 6.6 (a)	Estimated permeability distribution of layer 1 for 2-phases after Step 3 using bicubic splines	84
Fig. 6.6 (b)	Estimated permeability distribution of layer 2 for 2-phases after Step 3 using bicubic splines	85

Fig. 6.6 (c)	Estimated permeability distribution of layer 3 for 2-phases after Step 3 using bicubic splines	86
Fig. 6.7 (a)	Estimated permeability distribution of layer 1 for 2-phases after Step 3 using zonation	87
Fig. 6.7 (b)	Estimated permeability distribution of layer 2 for 2-phases after Step 3 using zonation	88
Fig. 6.7 (c)	Estimated permeability distribution of layer 3 for 2-phases after Step 3 using zonation	89
Fig. 6.8 (a)	Estimated permeability distribution of layer 1 for 2-phases after Step 2 using zonation	90
Fig. 6.8 (b)	Estimated permeability distribution of layer 2 for 2-phases after Step 2 using zonation	91
Fig. 6.8 (c)	Estimated permeability distribution of layer 3 for 2-phases after Step 2 using zonation	92
Fig. 6.9 (a)	Estimated permeability distribution of layer 1 for 2-phases after Step 2 using bicubic splines	93
Fig. 6.9 (b)	Estimated permeability distribution of layer 2 for 2-phases after Step 2 using bicubic splines	94

Fig. 6.9 (c)	Estimated permeability distribution of layer 3 for 2-phases after Step 2 using bicubic splines	95
Fig. 6.10.1	History match of bottomhole pressure from well P3 for 3-phases: Example 1	99
Fig. 6.10.2	History match of bottomhole pressure from well P3 for 3-phases: Example 2	100
Fig. 6.11.1	History match of water cut from well P3 for 3-phases: Example 1	101
Fig. 6.11.2	History match of water cut from well P3 for 3-phases: Example 2	102
Fig. 6.12.1 (a)	History match of liquid flow rate from well P3 from completion 1 for 3-phases: Example 1	103
Fig. 6.12.1 (b)	History match of liquid flow rate from well P3 from completion 2 for 3-phases: Example 1	104
Fig. 6.12.1 (c)	History match of liquid flow rate from well P3 from completion 3 for 3-phases: Example 1	105
Fig. 6.12.2 (a)	History match of liquid flow rate from well P3 from completion 1 for 3-phases: Example 2	106

Fig. 6.12.2 (b)	History match of liquid flow rate from well P3 from completion 2 for 3-phases: Example 2	107
Fig. 6.12.2 (c)	History match of liquid flow rate from well P3 from completion 3 for 3-phases: Example 2	108
Fig. 6.13.1 (a)	History match of gas flow rate from well P3 from completion 1 for 3-phases: Example 1	109
Fig. 6.13.1 (b)	History match of gas flow rate from well P3 from completion 2 for 3-phases: Example 1	110
Fig. 6.13.1 (c)	History match of gas flow rate from well P3 from completion 3 for 3-phases: Example 1	111
Fig. 6.13.2 (a)	History match of gas flow rate from well P3 from completion 1 for 3-phases: Example 2	112
Fig. 6.13.2 (b)	History match of gas flow rate from well P3 from completion 2 for 3-phases: Example 2	113
Fig. 6.13.2 (c)	History match of gas flow rate from well P3 from completion 3 for 3-phases: Example 2	114
Fig. 6.14.1	History match of gas-oil ratio from well P3 for 3-phases: Example 1	115

Fig. 6.14.2	History match of gas-oil ratio from well P3 for 3-phases: Example 2	116
Fig. 6.15 (a)	Estimated permeability distribution of layer 1 for 3-phases after Step 3 using bicubic splines: Example 2	117
Fig. 6.15 (b)	Estimated permeability distribution of layer 2 for 3-phases after Step 3 using bicubic splines: Example 2	118
Fig. 6.15 (c)	Estimated permeability distribution of layer 3 for 3-phases after Step 3 using bicubic splines: Example 2	119
Fig. 6.16 (a)	Estimated permeability distribution of layer 1 for 3-phases after Step 2 using bicubic splines: Example 1	120
Fig. 6.16 (b)	Estimated permeability distribution of layer 2 for 3-phases after Step 2 using bicubic splines: Example 1	121
Fig. 6.16 (c)	Estimated permeability distribution of layer 3 for 3-phases after Step 2 using bicubic splines: Example 1	122

Fig. 6.17 (a)	Estimated permeability distribution of layer 1 for 3-phases after Step 2 using bicubic splines: Example 2	123
Fig. 6.17 (b)	Estimated permeability distribution of layer 2 for 3-phases after Step 2 using bicubic splines: Example 2	124
Fig. 6.17 (c)	Estimated permeability distribution of layer 3 for 3-phases after Step 2 using bicubic splines: Example 2	125
Appendix A		
Fig. A-1	Flow chart of Nazareth's partial conjugate gradient algorithm	163

List of Tables

	Page
Chapter I	
Table 1 Prior Papers on Automatic History Matching	7
Chapter II	
Table 1 Physical Properties of the Reservoir	14
Table 2 Production Scenarios for Determining Sensitivity of Measured Variables to Reservoir Heterogeneities	23
Chapter III	
Table 1 Physical Properties of the Reservoir	64
Table 2 Performance of the Estimation for the Two-Phase Case Using Bicubic Spline Approximation	70
Table 3 Performance of the Estimation for the Two-Phase Case Using the Zonation Approach	71
Table 4 Performance of the Estimation for the Three-Phase Case Using Bicubic Spline Approximation: Example 1	72
Table 5 Performance of the Estimation for the Three-Phase Case Using Bicubic Spline Approximation: Example 2	73

CHAPTER I

INTRODUCTION

Estimation of the properties of multilayered, multiphase reservoirs remains an important problem in reservoir analysis. The knowledge of these properties, such as absolute permeability, forms the basis for determining an optimal strategy of oil recovery. The process of estimating unknown properties in a mathematical reservoir model to give the best fit to measured well data is called history matching.

The history matching problem is a notoriously difficult one for several reasons: (1) In a reservoir, properties vary with location; thus, conceptually an infinite number of parameters are required for a full description of the reservoir. Computationally, a reservoir simulator contains a finite number of parameters corresponding to the number of grid blocks, and in field-scale simulations, a simulator may contain on the order of 10,000 grid blocks. (2) The history matching problem is theoretically ill-posed, which means that small instabilities in the data can lead to large perturbations in the estimated parameters^{1,2}. (3) Many actual reservoirs involve significant vertical as well as horizontal property variations, requiring the estimation of property distributions in both directions. (4) History matching situations may involve full three-phase (oil, water and gas) behavior, wherein traditional observations at wells may not be adequate to enable property estimation; this problem has not been addressed previously in the literature.

There exist a number of prior papers on automatic history matching, which have been organized according to reservoir dimensionality and number of phases considered in Table 1. The goal of the present work is to develop a general history matching code applicable for three-dimensional, three-phase reservoirs.

To alleviate the ill-conditioning in the history matching problem, several approaches have been tried, such as decreasing the number of parameters to be estimated and, in addition, utilizing any available information to constrain the choice of the unknown parameters. One way of reducing the number of parameters is to divide the reservoir into a relatively small number of zones and to assume that the properties are uniform within each zone. While this approach is effective in reducing the number of unknowns, sufficient *a priori* information is not usually available to enable specification of the zones on any physical basis. A modification to zonation is to use prior information expressed as an assumed probability distribution for the zonal reservoir properties. If certain *a priori* knowledge is assumed about the mean values and correlations of the parameters, the history matching performance index can be modified to include a term that penalizes the weighted deviations of the parameters from their assumed mean values¹. Although it has been shown that better-conditioned estimates may be obtained when *a priori* statistical information is used, sufficient knowledge of the nature of the unknown parameters is not generally available to specify the parameters needed to carry out such a Bayesian estimation.

Kravaris and Seinfeld^{3,4} have shown that the concept of regularization can be applied to the estimation of spatially varying parameters in partial differential equations of the parabolic type. Regularization of an ill-posed, inverse problem refers to solving a well-posed inverse problem whose solution approximates that of the original problem in a physically meaningful way. In particular, parameter estimation by regularization is performed by minimizing a smoothing functional that is a weighted sum of the conventional least-squares functional and a stabilizing functional which measures the degree of non-smoothness with respect to the parameter estimates. The weighting factor or regularization parameter represents the degree of smoothing desired. Furthermore, spline approximation, which provides a convenient way of representing the spatially varying parameters, also helps circumvent some of the ill-conditioning inherent in the finite difference or zonation representation of the unknown parameters by imparting a degree of smoothness to the parameter distribution.

Estimation of porosity and absolute permeability, in single-phase, two-dimensional reservoirs using regularization and bicubic spline approximation has been investigated by Lee et al⁵. The effects of the degree of spline approximation and regularization on the parameter estimation were considered. In applying the spline approximation to the parameter estimation problem, the number of coefficients for spline representation should not exceed either the number of grid cells for the PDE's or the number of available observation data. If too few coefficients are employed, the spline approximation cannot represent the spatial details of the permeability distribution adequately. Estimation of absolute permeability and simultaneous estimation of absolute and relative permeability in two-phase (oil and water), two-dimensional reservoirs were also investigated by Lee et al^{6,7}. As in the

single-phase case, both bicubic spline approximation and regularization techniques were used in parameter estimation.

Chen et al.⁸ have applied a so-called generalized pulse spectrum technique (GPST) inversion algorithm for history matching in two-dimensional, two-phase simulator models. The GPST method involves solving the history matching problem using a multigrid technique in which the estimation is performed on successively finer grids starting with a single cell model until convergence is reached. In this work, Chen assumes that both pressure and saturation data are available at each observation point in the history match. In actual field applications, saturation data are not generally available. Lee et al.^{6,7} assumed only measurable production data, such as water-oil ratio and wellbore pressure, to be available at observation locations. In addition, Lee's method can be applied directly to any two-dimensional, two-phase simulator model not only to those using a multigrid method for solution.

A number of investigations aimed at estimating parameters in multilayered reservoirs have been carried out in the field of well testing⁹⁻²⁵. All the prior work in multilayered reservoirs, conducted for the case of single-phase flow, demonstrates that the properties of individual layers cannot be estimated by conventional transient well tests if all the layers are producing simultaneously. To determine individual layer parameters and interlayer crossflow parameters, it is necessary to conduct well tests in which some layers are produced and others are shut-in. The above listed references provide a variety of strategies for determining layered properties together with analytical solutions for transient well tests on single-phase reservoirs.

Although single- and two-phase, two-dimensional reservoirs are clearly the first step in addressing parameter estimation problems, from the point of practical application, it is necessary to consider three-phase, three-dimensional reservoirs. Chen et al.^{26,27} have applied the GPST algorithm to idealized three-dimensional, two- and three-phase simulator models. In this work, as in their two-dimensional, two-phase work, the permeability distribution is estimated assuming pressure, water and gas saturation data are available at the wells. In general, data of this type are not available; rather only field production data are available.

This thesis represents in many respects the culmination of many years of work by the Caltech group together with that at the Chevron Oil Field Research Company in the field of parameter estimation in petroleum reservoirs. We develop, in this work, a multilayered, three-phase history matching algorithm for use with an industrial Black Oil simulator. The permeability distribution is estimated by matching production data such as the wellbore pressure, the water cut, the gas-oil ratio and the flow rates of liquid and gas from individual completions. The techniques of regularization and bicubic spline approximation are used to convert the ill-posed inverse problem into one that is computationally well behaved.

Chapter II is an initial examination of the question of determining the properties of individual layers in multilayered reservoirs using two-phase flow information. The situation considered here is a simple water flood in which a vertically stratified, oil-bearing reservoir cross section between two wells is subjected to water injection at one of the wells. The ability of layer-by-layer measurements at the producing well, such as well pressure and water-oil ratio, to reflect the reservoir's vertical heterogeneity is examined through reservoir simulation. Thus, the object is to assess the

feasibility of estimating properties of layered reservoirs on the basis of waterflood-
ing data. Various types of production scenarios are examined and the sensitivity of
measured production data to reservoir properties is analyzed.

In Chapter III, the determination of absolute permeability in multilayer reser-
voirs using two- and three-phase well data, such as well pressure, water cut, gas-oil
ratio and rates of liquid and gas production from individual layers is addressed. A
history matching algorithm that employs the industrial Black Oil simulator, CLASS
(Chevron Limited Applications Simulation System), is developed to estimate ab-
solute permeabilities. The effects of bicubic spline approximation versus zonation
and regularization are considered in a series of history matching calculations.

TABLE 1 - PRIOR PAPERS ON AUTOMATIC HISTORY MATCHING

No. of Dim.	Number of Phases		
	One-Phase	Two-Phase	Three-Phase
1-D	1,24,29	30	
2-D	2-5,9-19, 21-25,28	6-8	
3-D		26, This work	27, This work

REFERENCES

- (1) Shah, P. C., Gavalas, G. R., and Seinfeld, J. H.: "Error Analysis in History Matching: The Optimum Level of Parameterization," *SPEJ* (June 1978) 219-28.
- (2) Yakowitz, S., and Duckstein, L.: "Instability in Aquifer Identification: Theory and Case Studies," *Water Resources Research*, **16**, No. 198, 1054-64.
- (3) Kravaris, C., and Seinfeld, J. H.: "Identification of Parameters in Distributed Parameter Systems by Regularization," *SIAM J. Control and Optimization*, **23**, No. 2, 217-41.
- (4) Kravaris, C., and Seinfeld, J. H.: "Identification of Spatially-Varying Parameters in Distributed Parameter Systems by Discrete Regularization," *J. Mathematical Analysis and Appl.*, (1986) **118**, No. 9.
- (5) Lee, T., Kravaris, C., and Seinfeld, J. H.: "History Matching by Spline Approximation and Regularization in Single-Phase Areal Reservoirs," *SPE Reservoir Engineering*, **1**, 521 (1986).
- (6) Lee, T., and Seinfeld, J. H.: "Estimation of Two-Phase Petroleum Reservoir Properties by Regularization," *J. Computational Physics*.
- (7) Lee, T., and Seinfeld, J. H.: "Estimation of Absolute and Relative Permeabilities in Petroleum Reservoirs," *Inverse Problems*.
- (8) Chen, Y. M. *et al.*: "GPST Inversion Algorithm for History Matching in 2-D, Two-Phase Simulator Models," *Appl. Numer. Math.*, **4**, 83, (1988).

- (9) Bremer, R. E., Winston, H., and Vela, S.: "Analytical Model for Vertical Interference Tests Across Low-Permeability Zones," *SPEJ* (June 1985) 407-418.
- (10) Dogru, A. H., and Seinfeld, J. H.: "Design of Well Tests to Determine the Properties of Stratified Reservoirs," paper SPE 7694 presented at the 1979 SPE of AIME Fifth Symposium on Reservoir Simulation held in Denver, CO, Feb. 1-2.
- (11) Earlougher, R. C. Jr., Kersch, K. M., and Kunzman, W. J.: "Some Characteristics of Pressure Buildup Behavior in Bounded Multiple-Layered Reservoirs Without Crossflow," *JPT* (Oct. 1974) 1178-1186; *Trans.*, AIME, **257**.
- (12) Ehlig-Economides, C. A., and Ayoub, J. A.: "Vertical Interference Testing Across a Low-Permeability Zone," *SPEFE* (Oct. 1986) 497-510.
- (13) Ehlig-Economides, C. A., and Joseph, J.: "A New Test for Determination of Individual Layer Properties in a Multilayered Reservoir," *SPEFE* (Sept. 1987) 261-283.
- (14) Foss, B. A.: "Well Test Analysis and Design: A Parameter Identification Approach," Report No.1, The Norwegian Institute of Technology (June 1986).
- (15) Gao, C. T.: "Single-Phase Fluid Flow in a Stratified Porous Medium with Crossflow," *SPEJ* (Feb. 1984) 97-106.
- (16) Kazemi, H., and Seth, M. S.: "Effect of Anisotropy and Stratification on Pressure Transient Analysis of Wells with Restricted Flow Entry," *JPT* (May 1969) 639-647.

- (17) Lefkovits, H. C. *et al.*: "A study of the Behavior of Bounded Reservoirs Composed of Stratified Layers," *SPEJ* (March 1961) 43-58; *Trans.*, AIME, **222**.
- (18) Pendergrass, J. D., and Berry, V. J. Jr.: "Pressure Transient Performance of a Multilayered Reservoir with Crossflow," *SPEJ* (Dec. 1962) 347-354.
- (19) Prijambodo, R., Raghavan, R., and Reynolds, A. C.: "Well Test Analysis for Wells Producing Layered Reservoirs with Crossflow," *SPEJ* (June 1985) 380-396.
- (20) Raghavan, R. *et al.*: "Well Test Analysis for Wells Producing from Two Commingled Zones of Unequal Thickness," *JPT* (Sept. 1974) 1035-1043; *Trans.*, AIME, **257**.
- (21) Russell, D. G., and Prats, M.: "Performance of Layered Reservoirs with Crossflow - Single-Compressible-Fluid Case," *SPEJ* (March 1962) 53-67.
- (22) Russell, D. G., and Prats, M.: "The Practical Aspects of Interlayer Crossflow," *JPT* (June 1962) 589-594.
- (23) Streltsova, T. D.: "Pressure Drawdown in a Well with Limited Flow Entry," *JPT* (Nov. 1979) 1469-1476.
- (24) Streltsova, T. D.: "Buildup Analysis for Interference Tests in Stratified Formations," *JPT* (Feb. 1984) 301-310.
- (25) Chen, W. H. *et al.*: "A New Algorithm for Automatic History Matching," *SPEJ*, **14**, (Dec. 1974) 593 - 608.

- (26) Chen, Y. M. *et al.*: “Application of GPST to History Matching In Multiphase Simulator Models,” *IMACS Trans. Sci. Comput. - 1988; 1.1 and 1.2: Numer. and Appl. Math.*, ed. by W. F. Ames and C. Brezinski, in press.
- (27) Zhu, J. P. and Chen, Y. M.: “GPST for History Matching In 1-Parameter, 3-D, Three-Phase Simulator Models,” to appear in *J. Comp. Phys.*
- (28) Wasserman, M. L., Emanuel, A. S., and Seinfeld, J. H.: *SPEJ* , **15**, 347 (1975).
- (29) Chavent, G., Dupuy, M., and Lemonnier, P.: “History Matching by Use of Optimal Control Theory,” *SPEJ* , (Feb. 1975), 74-86; *Trans., AIME* , 251.
- (30) Van der Bosch, B., and Seinfeld, J. H.: *SPEJ* , **17**, 398, (1977).

CHAPTER II

DETERMINATION OF INDIVIDUAL LAYER PROPERTIES IN MULTILAYER RESERVOIRS WITH TWO-PHASE FLOW

1. INTRODUCTION

Estimation of the properties of multilayer reservoirs remains an important problem in reservoir analysis. A number of investigations of this problem have appeared in the petroleum engineering literature¹⁻¹⁶. All the prior work, conducted for the case of single-phase flow, demonstrates that the properties of individual layers cannot be estimated by conventional transient well tests if all the layers are producing simultaneously. To determine individual layer parameters and interlayer crossflow parameters, it is necessary to conduct well tests in which some layers are produced and others are shut-in. The above listed references provide a variety of strategies for determining layered properties together with analytical solutions for transient well tests on single-phase reservoirs.

The present paper is an initial examination of the question of the determination of the properties of individual layers in multilayer reservoirs using two-phase flow information. The situation considered here is a simple waterflood in which a vertically stratified, oil-bearing reservoir cross section between two wells is subjected to water injection at one of the wells. The ability of layer-by-layer measurements at the producing well, such as well pressure and water-oil ratio, to reflect the reservoir's vertical heterogeneity is examined through reservoir simulation. Thus, the object of the present paper is to assess the feasibility of estimating properties of layered reservoirs on the basis of waterflooding data.

This work begins with a brief statement of the reservoir model employed and then discusses the types of production scenarios that will be examined. The major body of the paper consists of an analysis of the sensitivity of measured production data to the reservoir properties.

2. RESERVOIR MODEL

The two-dimensional, unsteady flow of oil and water in a vertical cross section of a reservoir with thickness Δy in which water is injected at one well and oil and water are produced from the other well is considered. If the capillary pressure is assumed to be zero, and the fluids are both slightly compressible, the pressure and saturation distributions in the reservoir are governed by

$$\begin{aligned} \frac{\partial}{\partial x} \left[\frac{k_x(x, z) k_{r,l}(S_w) b_l(p)}{\mu_l} \frac{\partial p}{\partial x} \right] + \frac{\partial}{\partial z} \left[\frac{k_z(x, z) k_{r,l}(S_w) b_l(p)}{\mu_l} \frac{\partial (p - \rho_l g z)}{\partial z} \right] = \\ \phi \frac{\partial}{\partial t} [b_l(p) S_l] - Q_l, \quad l = o, w \end{aligned} \quad (1)$$

$$S_w + S_o = 1 \quad (2)$$

$$\frac{\partial p}{\partial x} = 0 \quad \text{at } x = 0 \text{ and } x = L_x \quad (3)$$

$$k_z(x, z) = 0 \quad \text{at } z = 0 \text{ and } z = L_z \quad (4)$$

$$p(x, z, 0) = p_0(x, z) \quad (5)$$

TABLE 1 - PHYSICAL PROPERTIES OF THE RESERVOIR**(1) Fluid properties**

	<u>Water</u>	<u>Oil</u>
Compressibility, atm^{-1}	1.0×10^{-4}	1.5×10^{-4}
Viscosity, g cm^{-3}	0.305	0.5
Relative permeability	$a_w = 1.0$	$a_o = 1.0$
	$b_w = 2.0$	$b_o = 2.0$
	$S_{iw} = 0.12$	$S_{ro} = 0.10$

(2) Rock and reservoir properties

Porosity	0.3
Initial pressure, atm	325.0

The physical properties of the reservoir are shown in Table 1. Furthermore, the relative permeabilities of the oil and water phases are assumed to be functions of saturation and can be written as

$$k_{ro}(S_w) = a_o \left(\frac{1.0 - S_{ro} - S_w}{1.0 - S_{ro} - S_{iw}} \right)^{b_o} \quad (6)$$

$$k_{rw}(S_w) = a_w \left(\frac{S_w - S_{iw}}{1.0 - S_{iw} - S_{ro}} \right)^{b_w} \quad (7)$$

Since the wellbore size is small relative to the reservoir dimensions, the production and injection well flow rates are treated as sink or source terms in the governing equations. The fully implicit finite-difference approximation of the reservoir equations can be written as

$$\begin{aligned} & \left(\frac{\Delta z_k}{\Delta x} \right) \left(\frac{k_x k_{r,l} b_l}{\mu_l} \right)_{i+1/2,k}^{n+1} (p_{i+1,k} - p_{i,k})^{n+1} \\ & + \left(\frac{\Delta z_k}{\Delta x} \right) \left(\frac{k_x k_{r,l} b_l}{\mu_l} \right)_{i-1/2,k}^{n+1} (p_{i-1,k} - p_{i,k})^{n+1} \\ & + \left(\frac{\Delta x}{\Delta z_{k+1/2}} \right) \left(\frac{k_z k_{r,l} b_l}{\mu_l} \right)_{i,k+1/2}^{n+1} [p_{i,k+1} - p_{i,k} + \rho_l g(z_k - z_{k+1})]^{n+1} \\ & + \left(\frac{\Delta x}{\Delta z_{k-1/2}} \right) \left(\frac{k_z k_{r,l} b_l}{\mu_l} \right)_{i,k-1/2}^{n+1} [p_{i,k-1} - p_{i,k} + \rho_l g(z_k - z_{k-1})]^{n+1} \\ & + Q_{l,i,k} - \frac{\phi}{\Delta t} [(b_l S_l)^{n+1} - (b_l S_l)^n]_{i,k} = 0 \end{aligned} \quad (8)$$

In order to draw quantitative conclusions, it is necessary to assume a certain number of layers for the reservoir simulation. The reservoir will be assumed to consist of three layers in which the horizontal permeabilities as well as the vertical permeabilities between layers one and two and layers two and three are assumed to be uniform. (See Fig. 1.) Three layers are sufficient for us to draw general conclusions about the behavior of layered reservoirs and are a compromise in the representation of layered reservoir behavior.

One of several variables that govern the behavior of the wellbore such as the wellbore pressure, total liquid flow rate and the oil or water flow rates can be specified. In this study, the total liquid flow rate in the production well and the total water flow rate in the injection well are assumed to be known. In all cases considered here, water is injected into all three layers simultaneously, and the number of layers that are being produced at a given time is varied. Two equations governing the injection and production wellbores are needed to calculate the wellbore pressures when the overall well flow rates are specified. The equations governing the injection and production wells are

$$\sum_{k=NZP(1)}^{NZP(NZL)} Q_{w,k}^{INJ} - Q_{TOTAL}^{INJ} = 0 \quad (9)$$

where

$$Q_{w,k}^{INJ} = \frac{-\Delta z_k}{\ln(\frac{r_e}{r_w})} \frac{b_{w,k}^{INJ}}{\mu_l} [p_{1,k} - p_{wb}^{INJ} + \alpha g \sum_{j=k}^{NZ-1} (\rho_w \Delta z)_{j+1/2}] \quad (10)$$

and

$$\sum_{k=NZP(1)}^{NZP(NZL)} (Q_{w,k}^{PROD} + Q_{o,k}^{PROD}) - Q_{TOTAL}^{PROD} = 0 \quad (11)$$

where

$$Q_{l,k}^{PROD} = \frac{-\Delta z_k}{\ln(\frac{r_e}{r_w})} \left(\frac{k_x k_{r,l} b_l}{\mu_l} \right)_{NX,k} [p_{NX,k} - p_{wb}^{PROD} + \alpha g \sum_{j=k}^{NZ-1} (\bar{\rho} \Delta z)_{j+1/2}] \quad (12)$$

Newton's method was used to solve the nonlinear system of $2N + 2$ equations generated by Eqs. (8),(9) and (11).

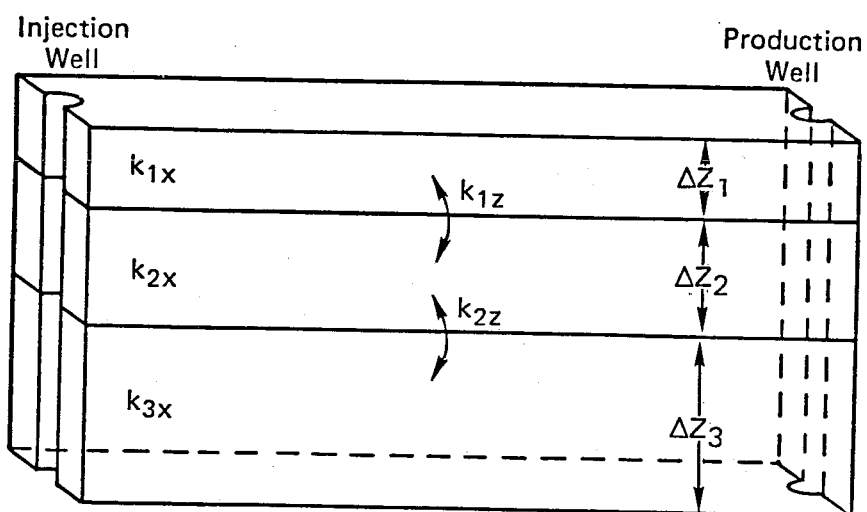


Fig. 1 - Vertical cross-section of a petroleum reservoir between an injection and production well

3. PRODUCTION STRATEGIES

It is assumed that at $t = 0$, water is injected and fluid produced at equal volumetric flow rates. Although water is injected into all three layers simultaneously, gravitational forces tend to cause the water to sink to the bottommost layer with a corresponding displacement of oil into the layers above. When the value of the vertical permeabilities is $O(10^{-2}$ darcies or more) (i.e., the layers are communicating), for the conditions we will simulate, all of the water injected sinks to the bottom layer well before reaching the producing well. When the vertical permeabilities are extremely small, $O(10^{-4}$ darcies or less), (i.e., the layers are uncommunicating), the water tends to remain in the layer into which it has been injected. If production occurs only from layer three (the bottom layer), for example, communicating layers lead to a decrease in the water breakthrough time over that if the layers do not communicate, since the water migrates along the bottom layer. If the well is producing at layer two only, water production does not occur until the bottom layer is nearly saturated with water, and the oil is eventually displaced by water migrating upward into layer two. When producing from layer two, if the layers are noncommunicating ($k_z \leq O(10^{-4}$ darcies)), then water breakthrough occurs sooner than if the layers communicate since the water injected into layer two does not sink towards the bottom of the reservoir before reaching the production well. Thus, for the conditions we will consider, because gravitational forces redistribute the water and oil in the reservoir well before water breakthrough occurs, if the layers are communicating, the effect of small changes in the values of vertical permeabilities on the production parameters is expected to be negligible, and only a large reduction in the vertical permeabilities, $k_z \leq O(10^{-4}$ darcies), can be expected to cause noticeable changes in production behavior.

A variety of measurements can be made in both the injection and production wells depending upon the number of layers being produced or injected. In the production well with only one layer producing, the wellbore pressure and the water-oil ratio can be measured. With two layers producing, the rate of liquid production from only one of the layers needs to be monitored since the total flow is specified. Several cases with different numbers and combinations of producing layers are considered in which various measurements are made, such as the production wellbore pressure, the rate of liquid production from a producing layer and the water-oil ratio. Note that the water breakthrough time can be determined without measuring the water-oil ratio directly by monitoring the sudden decrease in the production wellbore pressure that occurs at water breakthrough. In general, the production measurements will be found to be more sensitive to changes in the horizontal than the vertical permeabilities. When producing from only one layer at a specified total rate of liquid production, the wellbore pressure at the producing layer is most sensitive to changes in the permeability of that layer. (Note that the wellbore pressure is always measured at the bottom hole, i.e., the bottommost producing layer.) Because the rate of production is proportional to the pressure drop between the reservoir and the wellbore, as in Eqs. (10) and (12), the larger the pressure drop necessary to produce at a specified rate of total liquid production, the smaller the permeability of the producing layer. Furthermore, since specifying the same volumetric flow rates of injection and production keeps the reservoir pressure distribution constant with time, the bottom hole pressure is indicative of the behavior of the pressure drop across the wellbore. Since the pressure drop decreases as the bottom hole pressure increases, the larger the permeability of the sole producing layer, the larger the bottom hole pressure measured at that layer. Thus, a larger

permeability in the producing layer creates a correspondingly larger bottom hole pressure.

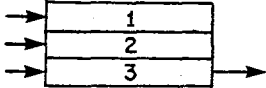
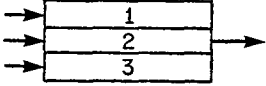
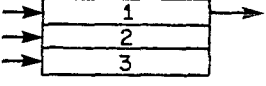
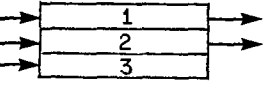
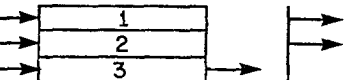
The horizontal permeabilities of the nonproducing layers do not affect the wellbore pressure when producing from only one layer, but tend only to delay or enhance water breakthrough times. In particular, when producing from layer three, the larger the permeability of the producing layer, k_{3x} , the sooner water breakthrough occurs; while the larger the horizontal permeabilities in layers one and two (the nonproducing layers), the longer the water injected remains in those layers without sinking to the bottommost layer. In general, with communicating layers, most of the water injected sinks to the bottom of the reservoir then flows through the bottommost layer until water breakthrough occurs. Hence, regardless of which layer is producing, the larger the permeability of the bottommost layer, the sooner water breakthrough occurs. The water breakthrough times behave similarly when producing only from layer one. Again, a larger permeability in layer three (a non-producing layer) decreases the water breakthrough time. Whereas, the larger the permeability in either layer one (the producing layer), or layer two, the later water breakthrough occurs.

When producing from two or more layers simultaneously, the wellbore pressure at the bottom hole depends upon the permeabilities of all the producing layers not just that of the bottommost producing layer where the wellbore pressure is measured. Although the sum of the rates of liquid production from all the layers is specified (i.e., the total rate of liquid production), the individual rates of production from a particular layer depend upon the ratio of the permeabilities of the two layers. In particular, since the total rate of production is specified, when producing from layers one and two, for example, the larger the ratio ($\frac{k_{1x}}{k_{2x}}$), the lower the rate of production from layer two versus layer one and the higher the wellbore

pressure measured. In other words, the wellbore pressure depends upon both the value of the permeability at the bottommost producing layer where the pressure is measured, as well as the ratio of that permeability to the permeabilities of the other producing layers. When two or more layers are producing, the water breakthrough time depends upon both the ratios of the permeabilities of all the layers (producing and nonproducing) and the value of the permeabilities. For example, if the ratios of k_{1x} to k_{2x} and k_{2x} to k_{3x} in one case are identical to those of another case, even if the values of the permeabilities are different in the two cases, the water breakthrough time is the same. In two cases in which the values of k_{1x} and k_{2x} are the same, the larger the value of k_{3x} , the sooner water breakthrough occurs for the reasons discussed earlier. In general, the analysis of the sensitivity of measured production parameters to vertical heterogeneity is more difficult in cases where more than one layer is produced simultaneously.

The specific cases that will be considered here are defined in Table 2. In cases (1) - (3), fluid is produced from only one layer at a time. Both the wellbore pressure at the producing layer and the water-oil ratio are measured. In case (4), fluid is produced from two layers simultaneously. Although the total rate of liquid production is specified, the rate of liquid production from an individual layer is measured at the bottommost layer produced. In case (5), fluid is produced from layer three only; however, after the first 100 time steps, fluid is produced from layers one and two simultaneously until water breakthrough occurs.

TABLE 2 - PRODUCTION SCENARIOS FOR DETERMINING SENSITIVITY OF MEASURED VARIABLES TO RESERVOIR HETEROGENEITIES

Case Number		Permeability (darcies)					
		k_{1x}	k_{2x}	k_{3x}	k_{1z}	k_{2z}	
1		A	0.7	0.3	0.5	0.03	0.03
		B	0.4	0.6	0.3	0.03	0.03
		C	0.4	0.6	0.5	0.03	0.03
		D	0.4	0.3	0.5	0.03	0.03
		E	0.4	0.6	0.3	0.0003	0.0003
		F	0.4	0.2	0.3	0.03	0.03
2		A	0.5	0.2	0.6	0.02	0.02
		B	0.5	0.2	0.4	0.02	0.02
3		A	0.4	0.5	0.3	0.02	0.02
		B	0.4	0.5	0.3	0.02	0.01
4		A	0.7	0.35	0.35	0.035	0.035
		B	0.35	0.7	0.35	0.035	0.035
		C	0.35	0.7	0.7	0.035	0.035
		D	0.35	0.7	0.35	0.0035	0.0035
5		A	0.5	0.6	0.3	0.025	0.025
		B	0.5	0.4	0.3	0.025	0.025
		C	0.5	0.4	0.3	0.00025	0.00025

4. SENSITIVITY OF MEASURED PRODUCTION VARIABLES TO VERTICAL RESERVOIR HETEROGENEITIES

In this section, the sensitivity of production parameters, such as the production wellbore pressure, the water-oil ratio and the rate of production from individual layers, to differences in the horizontal and the vertical permeabilities is examined. The various production strategies discussed in the previous section, as shown in Table 2, are considered here.

In cases (1) - (3), in Table 2, fluid is produced from only one of the three layers. Since the wellbore pressure is most sensitive to the permeability of the producing layer, it is indicative of the permeability of that layer only. Hence, little information can be determined about the horizontal permeabilities of the nonproducing layers and vertical permeabilities between layers. In general, if the total rate of production is specified, the larger the permeability of the producing layer, the larger the wellbore pressure measured at that layer. This behavior is seen by examining the following cases. For example, as shown in Figs. 2 and 3, the wellbore pressure of case (1.C) is higher than that of case (1.B). In these cases, fluid is produced from layer three only, and hence, the wellbore pressure behavior in cases (1.B) and (1.C) implies that $k_{3x}^{(1.C)} > k_{3x}^{(1.B)}$. Furthermore, as shown in Figs. 2 and 3, the absence of marked differences between the wellbore pressure curves of cases (1.A) and (1.C) indicates that $k_{3x}^{(1.A)} \approx k_{3x}^{(1.C)}$. Although $k_{3x}^{(1.A)} \approx k_{3x}^{(1.C)}$, $k_{1x}^{(1.A)} > k_{1x}^{(1.C)}$ and $k_{2x}^{(1.A)} < k_{2x}^{(1.C)}$ which shows the insensitivity of the wellbore pressure measured at the producing layer to the permeabilities of the nonproducing layers in cases where only one layer is producing.

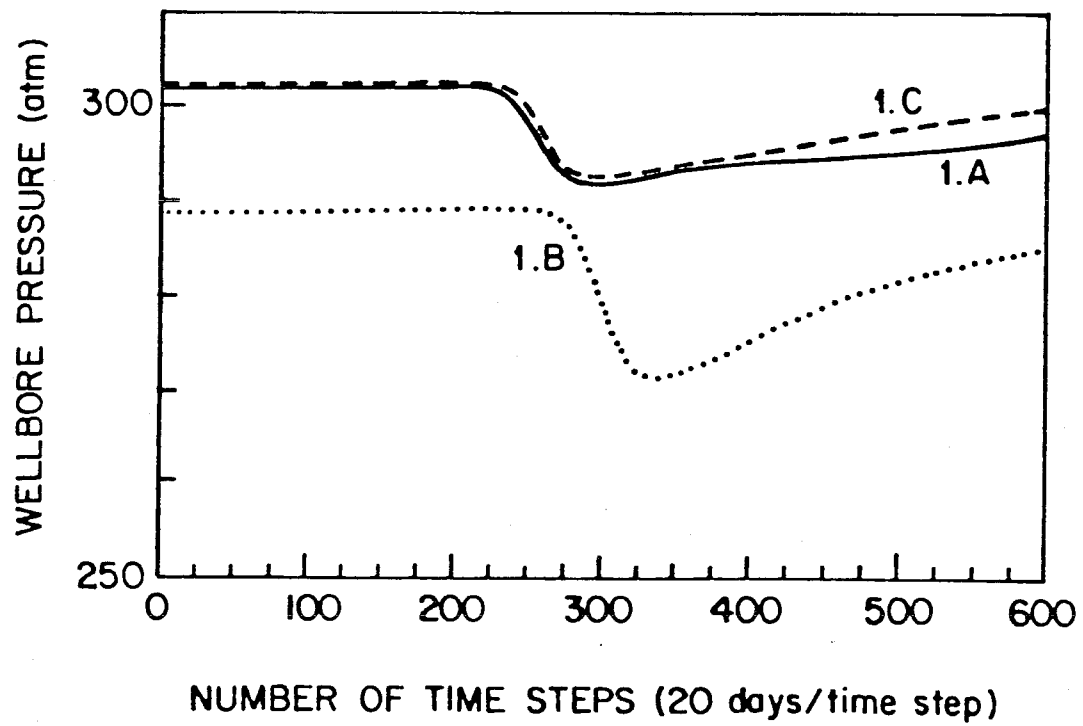


Fig. 2 - Production wellbore pressure for cases (1.A)-(1.C)

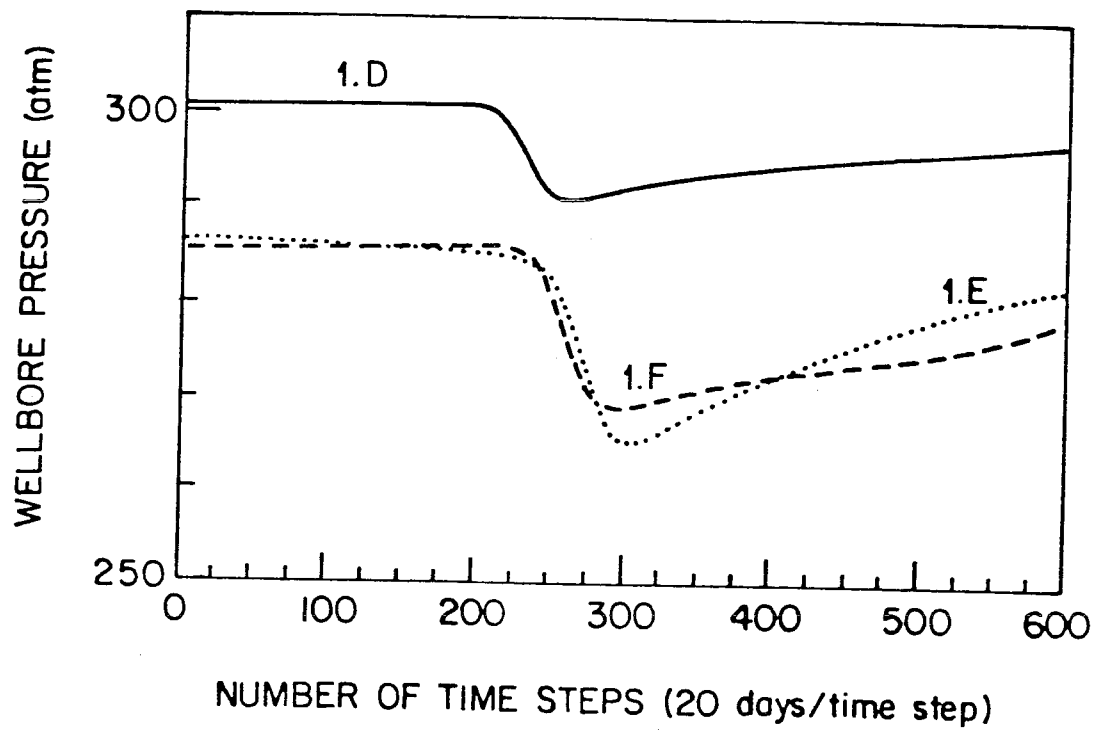


Fig. 3 - Production wellbore pressure for cases (1.D)-(1.F)

Although vertical permeabilities also affect the reservoir production parameters, the wellbore pressure and the water breakthrough time are less sensitive to their differences than to those of the horizontal permeabilities. This insensitivity is illustrated by a comparison of the wellbore pressure curves for cases (3.A) and (3.B). The horizontal permeabilities and the vertical permeability between layers one and two are identical in both cases; however, $k_{2z}^{(3.A)} = 2k_{2z}^{(3.B)}$. Even though the value of the vertical permeability between layers two and three in case (3.B) is half that in case (3.A), the wellbore pressures are the same except near water breakthrough. (See Fig. 5.)

Since water breakthrough time depends on the horizontal permeabilities of the producing and nonproducing layers as well as the vertical permeabilities between layers, other aspects of the vertical structure are difficult to determine. In order to understand how the water breakthrough time is affected by horizontal and vertical permeabilities, several examples are considered. When the layers are communicating the water injected sinks to the bottommost layer before water breakthrough occurs, and hence, most of the water flows to the producing well through layer three. Thus, when producing from layer one, two or three, regardless of which layer is the producing one, the larger the permeability of layer three, k_{3x} , the sooner water breakthrough occurs. For example, when layer two is producing, as in cases (2.A) and (2.B), (where $k_{1x}^{(2.A)} = k_{1x}^{(2.B)}$ and $k_{2x}^{(2.A)} = k_{2x}^{(2.B)}$), water breakthrough occurs sooner in case (2.A) than in case (2.B), since $k_{3x}^{(2.A)} > k_{3x}^{(2.B)}$. (See Fig. 4.) As discussed in the previous section, the larger the permeabilities of layers one and two, k_{1x} and k_{2x} , the later water breakthrough occurs, regardless of which layer is producing. When layer three is producing, water breakthrough occurs sooner in case (1.D) than (1.C), (where $k_{1x}^{(1.C)} = k_{1x}^{(1.D)}$ and $k_{3x}^{(1.C)} = k_{3x}^{(1.D)}$), since $k_{2x}^{(1.D)} < k_{2x}^{(1.C)}$, as shown in Figs. 2 and 3.

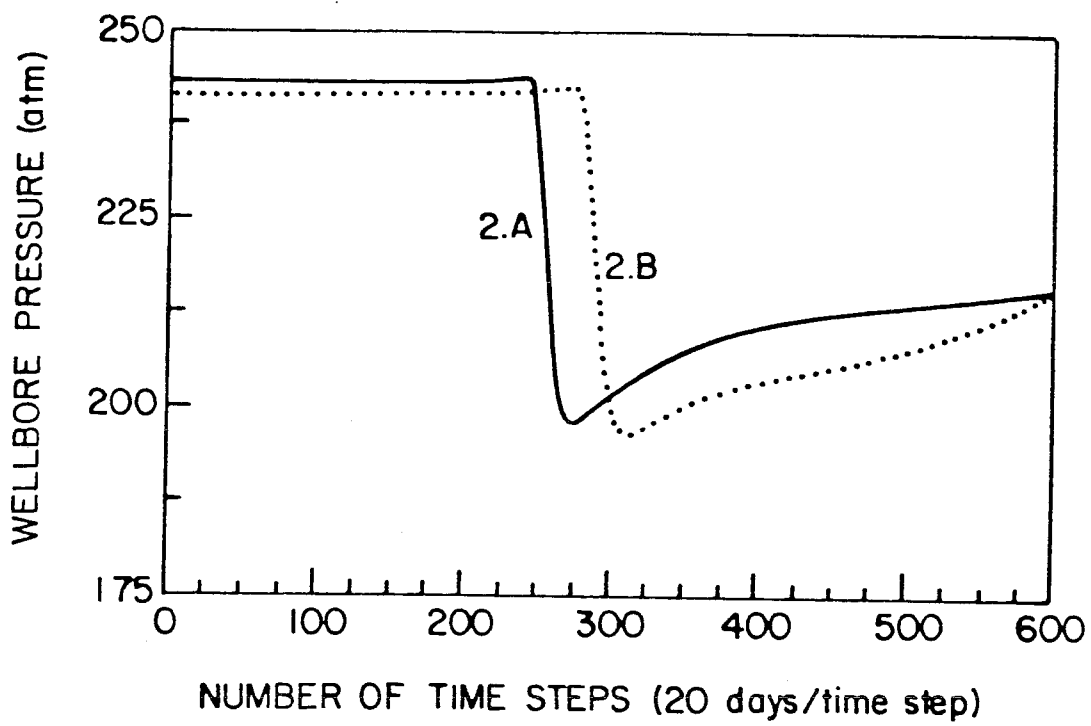


Fig. 4 - Production wellbore pressure for cases (2.A)-(2.B)

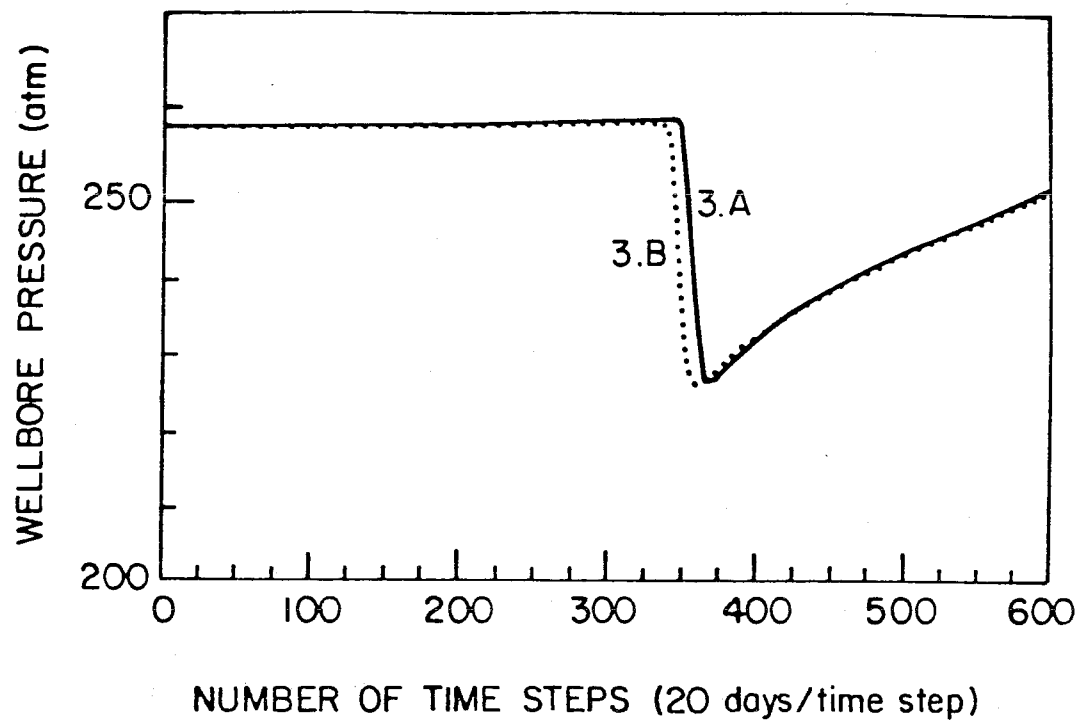


Fig. 5 - Production wellbore pressure for cases (3.A)-(3.B)

When the layers are noncommunicating as in case (1.E), the fluid flow in the vertical direction is negligible; therefore, fluid flows in the horizontal direction more quickly causing water breakthrough to occur sooner. See for example, cases (1.B) and (1.E), in which the horizontal permeabilities are identical, but $k_{1z}^{(1.E)} = 0.001k_{1z}^{(1.B)}$ and $k_{2z}^{(1.E)} = 0.001k_{2z}^{(1.B)}$. (See Figs. 2 and 3.) As discussed previously, when producing from layer three only, as in case (1), the smaller the permeabilities in the nonproducing layers, one and two, the earlier water breakthrough occurs. Consider case (1.F), in which the permeability of layer three, k_{3x} , (the producing layer), is the same in cases (1.B) and (1.E). Since the permeabilities of layer three are the same in cases (1.B), (1.E) and (1.F), the wellbore pressures behave similarly. In case (1.F), the permeability of layer two is less than that in case (1.B), (i.e., $k_{2x}^{(1.F)} < k_{2x}^{(1.B)}$), and hence, as in case (1.E), water breakthrough for case (1.F) occurs sooner than in case (1.B). In fact, the water breakthrough times for cases (1.E) and (1.F) are very similar, but due to different vertical structure. In particular, in case (1.E), because the layers are noncommunicating, water breakthrough occurs sooner than in case (1.B). Whereas, in case (1.F), water breakthrough occurs sooner than in case (1.B) because the horizontal permeability of layer two is smaller in case (1.F) than in case (1.B). Although the wellbore pressure for cases (1.E) and (1.F) indicates that the permeability of layer three is the same in both cases, the time at which water breakthrough occurs is affected by both the horizontal and vertical permeabilities. Therefore, it is difficult to distinguish between the vertical structure in cases (1.E) and (1.F) where both the wellbore pressure behavior and the water-oil ratios are similar. Thus, the analysis of the production parameters measured while producing from only one layer from $t = 0$ until water breakthrough can be ambiguous and inconclusive.

In case (4), where fluid is produced from layers one and two simultaneously, in addition to the wellbore pressure and the water breakthrough time, the rate of production from an individual layer can be measured. Hence, when two layers are produced simultaneously, a combined analysis of the wellbore pressure and the rate of production from an individual layer can be used to estimate the horizontal permeabilities of the producing layers. When the total rate of production is specified, both the wellbore pressure, which is measured at the bottommost producing layer, and the rate of production from an individual layer are sensitive not only to the value of the permeability at that layer, but also to the ratio between the permeabilities of the two producing layers. As discussed in the previous section, (See Eq. (12)) since the rate of production from a layer is proportional to the pressure drop between the reservoir and the wellbore, and since the reservoir pressure remains constant with time due to equal total rates of injection and production, the wellbore pressure increases as the rate of production from that layer decreases. Furthermore, the larger the ratio of the permeabilities between layers one and two, the smaller the rate of production from layer two versus layer one.

For example, consider cases (4.A) and (4.B) where $\frac{k_{1x}^{(4.A)}}{k_{2x}} = 2.0$ and $\frac{k_{1x}^{(4.B)}}{k_{2x}} = 0.5$. An examination of the rate of production from layer two which is smaller in case (4.A) than in case (4.B), indicates that $\frac{k_{1x}^{(4.A)}}{k_{2x}} \gg \frac{k_{1x}^{(4.B)}}{k_{2x}}$. Since the rate of production from layer two is smaller in case (4.A) than in case (4.B), the wellbore pressures measured at layer two are similar (except at water breakthrough) even though $k_{2x}^{(4.A)} < k_{2x}^{(4.B)}$. In case (4.C), both the rate of production from layer two and the wellbore pressure behave similarly to case (4.B) (See Figs. 6 and 7).

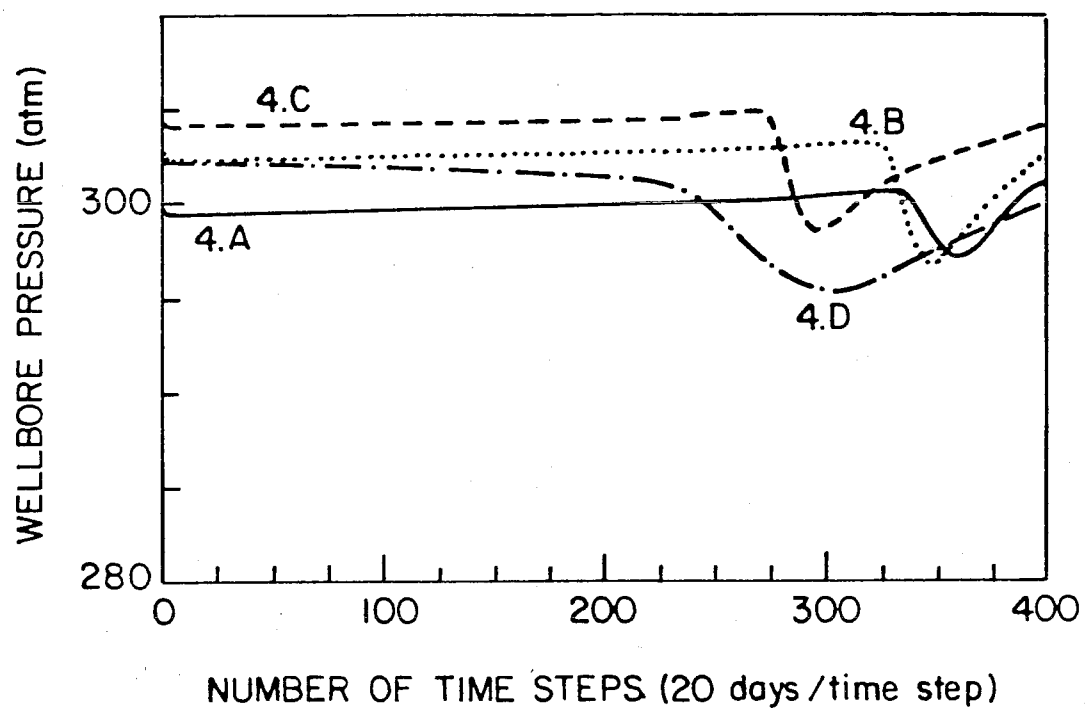


Fig. 6 - Production wellbore pressure for cases (4.A)-(4.D)

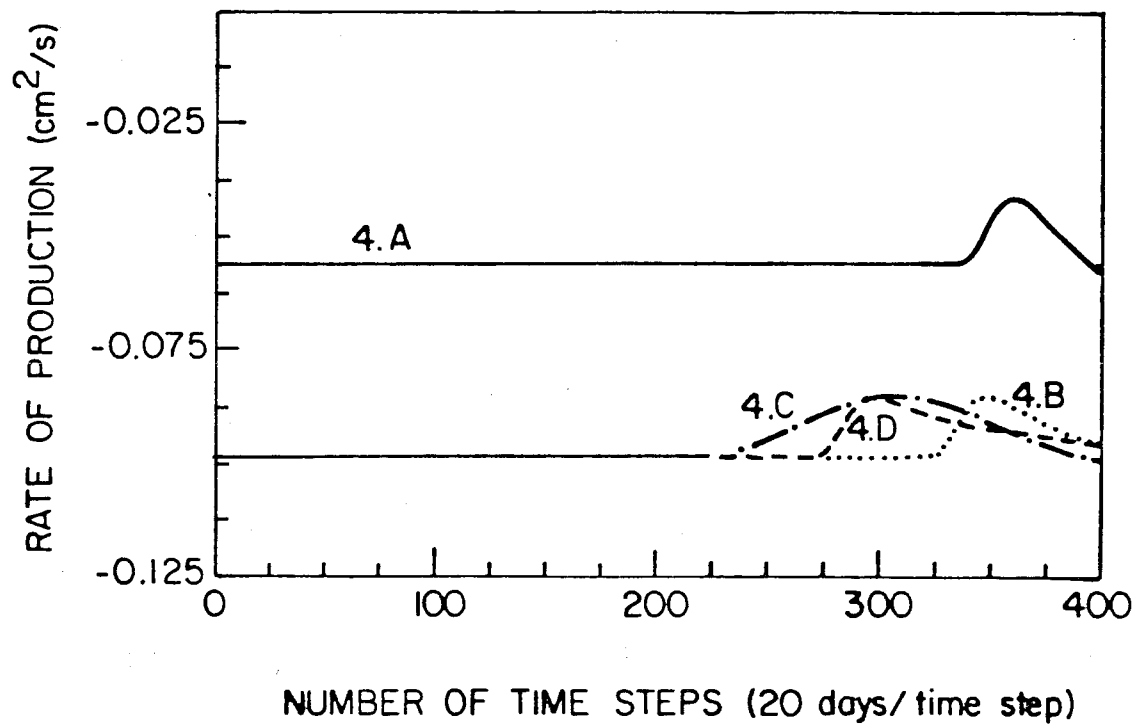


Fig. 7 - Rate of production from layer two for cases (4.A)-(4.D)

Since both the rates of production and the wellbore pressures are similar in cases (4.B) and (4.C), both the ratios of the permeabilities between the layers one and two and the values of the permeabilities of the producing layers are the same. (i.e., $\frac{k_{1x}^{(4.B)}}{k_{2x}} = \frac{k_{1x}^{(4.C)}}{k_{2x}}$ and $k_{1x}^{(4.B)} = k_{1x}^{(4.C)}$, $k_{2x}^{(4.B)} = k_{2x}^{(4.C)}$).

As we have shown, when producing from two layers simultaneously, the permeabilities of the two producing layers can be estimated by a combined analysis of the rate of production from an individual layer and the wellbore pressure measured at the bottommost producing layer. On the other hand, the water breakthrough time depends upon the horizontal permeabilities of the producing and nonproducing layers as well as the vertical permeabilities between layers. As a result, it is difficult to draw any additional conclusions about the permeabilities of the nonproducing layers and the vertical permeabilities between layers. For example, the water breakthrough times of cases (4.C) and (4.D) are similar. Furthermore, they are both shorter than the water breakthrough time for case (4.B), but because of different vertical structures. In all three cases, the wellbore pressures and the rates of production from layer two are similar which indicates that the horizontal permeabilities in layers one and two are the same. In case (4.C), water breakthrough occurs sooner because the horizontal permeability of layer three is larger than in case (4.B), whereas the water breakthrough time is shorter in case (4.D) because the layers are noncommunicating.

In case (5), fluid is produced solely from layer three for the first 100 time steps; then, after this initial period, fluid is produced from layers one and two simultaneously until water breakthrough occurs. In cases (5.A), (5.B) and (5.C), as shown in Fig. 8, the wellbore pressures behave similarly for the first 100 time steps.

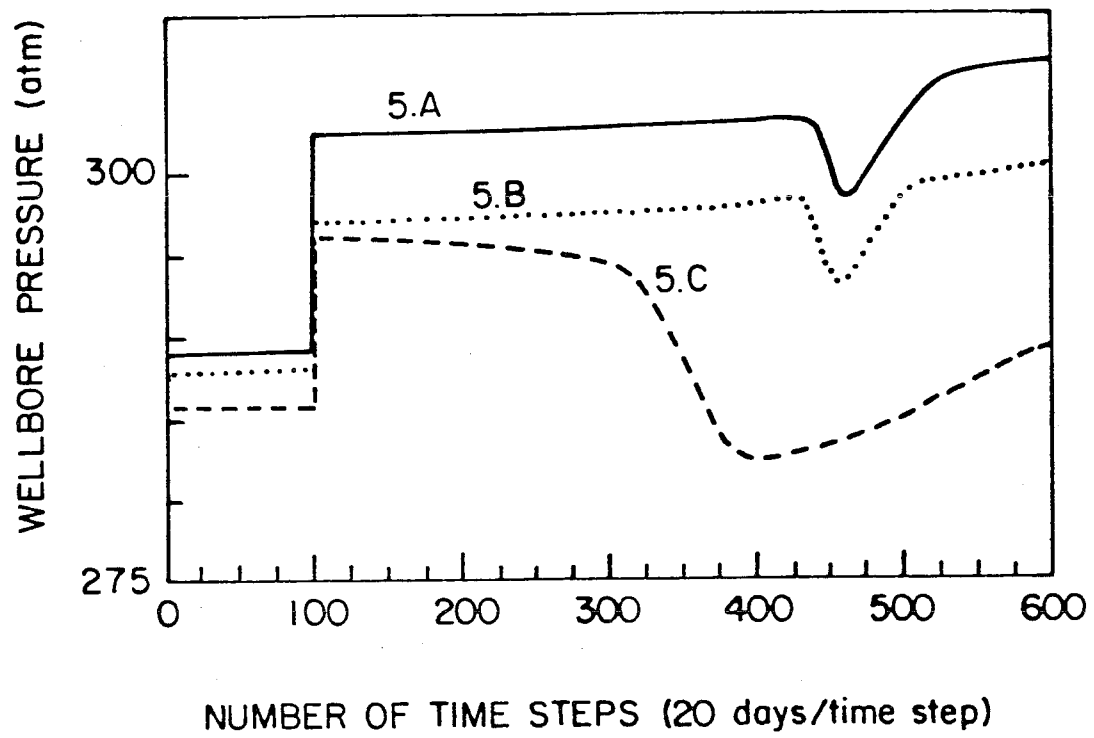


Fig. 8 - Production wellbore pressure for cases (5.A)-(5.C)

As discussed before, since fluid is produced solely from layer three during this period, this similarity indicates that the permeabilities in layer three are identical in all three cases. After the first 100 time steps, since fluid is produced from two layers simultaneously, the rate of production from layer one is measured. Since the rate of production from layer one in case (5.A) is smaller than that in cases (5.B) and (5.C), it is clear that $\frac{k_{1x}^{(5.A)}}{k_{2x}} < \frac{k_{1x}^{(5.B),(5.C)}}{k_{2x}}$. Furthermore, as shown in Fig. 9, the rate of production from layer one is the same in cases (5.B) and (5.C) implying that $\frac{k_{1x}^{(5.B)}}{k_{2x}} = \frac{k_{1x}^{(5.C)}}{k_{2x}}$. Since, in cases (5.B) and (5.C), from $t = 100$ time steps to $t \approx 250$ time steps, both the wellbore pressures and the rates of production from layer one behave similarly, the permeabilities of layer one and layer two must be the same in both cases. Thus, since the horizontal permeabilities are the same in all three layers in cases (5.B) and (5.C), differences in the vertical permeabilities must cause the shorter water breakthrough time in case (5.C). As discussed previously, because the layers are noncommunicating in case (5.C), water breakthrough occurs sooner. By producing from all three layers, more information about the vertical structure can be determined in cases (5.B) and (5.C). In general, a production strategy in which fluid is produced from each of the three layers (but not more than two simultaneously) is the most useful in determining both horizontal and vertical permeabilities.

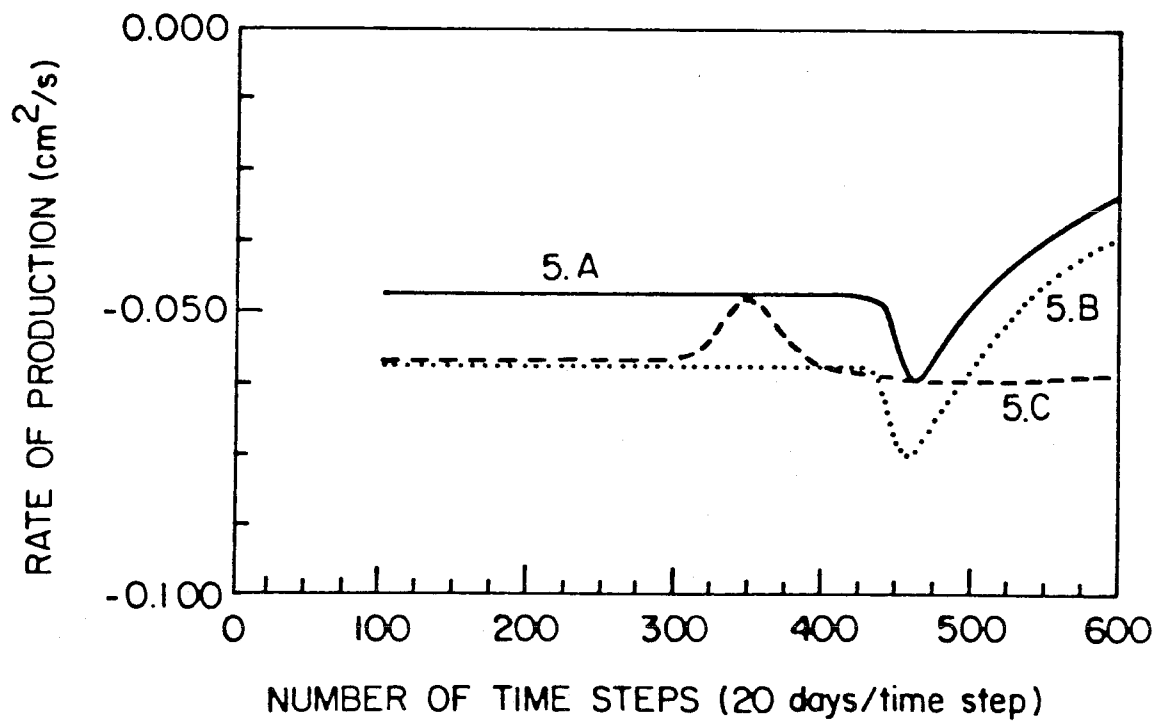


Fig. 9 - Rate of production from layer one for cases (5.A)-(5.C)

5. CONCLUSION

In this paper, the determination of the horizontal and vertical permeabilities of the individual layers in a multilayer, oil-bearing reservoir during a simple waterflood has been examined. Since two-phase flow exists in this case, the analysis of the sensitivity of measured production parameters is different from that when only one phase is flowing. In particular, the water breakthrough time can be used to examine certain aspects of the formation's vertical structure. Several production strategies are examined to discover those most suitable for determining horizontal and vertical permeabilities. All the results are based on an assumed three-layer reservoir, but the conclusions can be generalized to any number of layers.

In the first production strategy examined, fluid is produced solely from only one of the layers. When producing from only one layer until water breakthrough occurs, the production wellbore pressure is indicative of the permeability of that layer only. Since the horizontal and vertical permeabilities of all layers affect the water breakthrough time, the vertical permeabilities between layers one and two and between layers two and three and the horizontal permeabilities of the nonproducing layers are difficult to determine individually. Thus, although an analysis of the wellbore pressure when fluid production occurs from only one layer leads to a clear determination of the permeability of the producing layer, the water breakthrough time is insufficient to estimate other aspects of the vertical structure.

When producing from two layers simultaneously until water breakthrough occurs, the wellbore pressure that is measured at the bottommost producing layer depends upon both the value of the permeability of that layer and the ratio of the permeabilities of the two producing layers. If the total rate of liquid production is specified, the individual rate of production from a particular layer depends upon the ratio of the permeability of that layer to the permeability of the other producing layer. Thus, a combined analysis of the wellbore pressure and the rate of production from an individual layer can be used to determine the horizontal permeabilities of both producing layers. Since the water breakthrough time depends upon the horizontal and vertical permeabilities of all the layers, the horizontal permeability of the nonproducing layer as well as the vertical permeabilities between layers cannot be uniquely determined. Clearly a production strategy in which two layers are produced is more useful in determining vertical structure than one in which fluid is produced from only one layer.

In the last case, fluid is produced solely from layer three for a certain period of time, and then after this initial period, fluid production occurs from both layers one and two simultaneously until water breakthrough. During the initial period, an analysis of the wellbore pressure, measured at layer three, determines conclusively the permeability of this layer. After this initial period, when fluid is produced from layers one and two simultaneously, a combined analysis of the wellbore pressure and the rate of production from one of the layers leads to a determination of the permeabilities of layers one and two. Since all three horizontal permeabilities can be determined from a combined analysis of the wellbore pressure and the rate of production from layer one, an examination of the water breakthrough time leads to knowledge about other aspects of the vertical structure such as the communication

between layers. Since the horizontal permeabilities of all three layers and the communication between layers can be determined, a production strategy in which fluid is eventually produced from all three layers is the most advantageous in determining a formation's vertical structure.

NOMENCLATURE

- b_l = formation volume factor of phase l
 g = gravitational acceleration
 $k_{r,l}$ = relative permeability of phase l
 $k_x(x, z)$ = absolute horizontal permeability
 $k_z(x, z)$ = absolute vertical permeability
 L_x = length of the reservoir
 L_z = depth of the reservoir
 NX = total number of grid blocks in the x – direction
 NZ = total number of grid blocks in the z – direction
 NZL = total number of producing layers
 $NZP(k)$ = index of the producing layer
 p = reservoir pressure
 p_{wb}^{INJ} = bottom hole pressure in the injection well
 p_{wb}^{PROD} = bottom hole pressure in the production well
 Q_l = injection or production rate of phase l
 $Q_{w,k}^{INJ}$ = rate of water injection into layer k
 $Q_{l,k}^{PROD}$ = rate of fluid production from layer k
 Q_{TOTAL}^{INJ} = total rate of water injection
 Q_{TOTAL}^{PROD} = total rate of fluid production
 r_e = effective radius
 r_w = wellbore radius
 S_l = saturation of phase l
 S_{iw} = irreducible water saturation
 S_{ro} = residual oil saturation

GREEK

- α = conversion factor
 Δt = time step
 Δx = grid block length
 Δz_k = grid block height
 μ_l = viscosity of phase l
 ρ_l = density of phase l
 $\bar{\rho}$ = average fluid density in production wellbore

SUBSCRIPTS

- e = effective
 i = index in the x – direction
 k = index in the z – direction
 l = phase
 o = oil phase
 w = water phase

SUPERSCRIPTS

- INJ = injection
 $PROD$ = production

REFERENCES

- (1) Bremer, R. E., Winston, H., and Vela, S.: "Analytical Model for Vertical Interference Tests Across Low-Permeability Zones," *SPEJ* (June 1985) 407-418.
- (2) Dogru, A. H., and Seinfeld, J. H.: "Design of Well Tests to Determine the Properties of Stratified Reservoirs," paper SPE 7694 presented at the 1979 SPE of AIME Fifth Symposium on Reservoir Simulation held in Denver, CO, Feb. 1-2.
- (3) Earlougher, R. C. Jr., Kersch, K. M., and Kunzman, W. J.: "Some Characteristics of Pressure Buildup Behavior in Bounded Multiple-Layered Reservoirs Without Crossflow," *JPT* (Oct. 1974) 1178-1186; *Trans.*, AIME, **257**.
- (4) Ehlig-Economides, C. A., and Ayoub, J. A.: "Vertical Interference Testing Across a Low-Permeability Zone," *SPEFE* (Oct. 1986) 497-510.
- (5) Ehlig-Economides, C. A., and Joseph, J.: "A New Test for Determination of Individual Layer Properties in a Multilayered Reservoir," *SPEFE* (Sept. 1987) 261-283.
- (6) Foss, B. A.: "Well Test Analysis and Design: A Parameter Identification Approach," Report No.1, The Norwegian Institute of Technology (June 1986).
- (7) Gao, C. T.: "Single-Phase Fluid Flow in a Stratified Porous Medium with Crossflow," *SPEJ* (Feb.1984) 97-106.
- (8) Kazemi, H., and Seth, M. S.: "Effect of Anisotropy and Stratification on Pressure Transient Analysis of Wells with Restricted Flow Entry," *JPT* (May 1969) 639-647.
- (9) Lefkovits, H. C. *et al.*: "A study of the Behavior of Bounded Reservoirs Composed of Stratified Layers," *SPEJ* (March 1961) 43-58; *Trans.*, AIME, **222**.
- (10) Pendergrass, J. D., and Berry, V. J. Jr.: "Pressure Transient Performance of a Multilayered Reservoir with Crossflow," *SPEJ* (Dec. 1962) 347-354.
- (11) Prijambodo, R., Raghavan, R., and Reynolds, A. C.: "Well Test Analysis for Wells Producing Layered Reservoirs with Crossflow," *SPEJ* (June 1985) 380-396.

- (12) Raghavan, R. *et al.*: "Well Test Analysis for Wells Producing from Two Commingled Zones of Unequal Thickness," *JPT* (Sept. 1974) 1035-1043; *Trans.*, AIME, **257**.
- (13) Russell, D. G., and Prats, M.: "Performance of Layered Reservoirs with Crossflow - Single-Compressible-Fluid Case," *SPEJ* (March 1962) 53-67.
- (14) Russell, D. G., and Prats, M.: "The Practical Aspects of Interlayer Crossflow," *JPT* (June 1962) 589-594.
- (15) Streltsova, T. D.: "Pressure Drawdown in a Well with Limited Flow Entry," *JPT* (Nov. 1979) 1469-1476.
- (16) Streltsova, T. D.: "Buildup Analysis for Interference Tests in Stratified Formations," *JPT* (Feb. 1984) 301-310.

CHAPTER III

A GENERAL HISTORY MATCHING ALGORITHM FOR THREE-PHASE, THREE-DIMENSIONAL PETROLEUM RESERVOIRS

1. INTRODUCTION

In the present work, a multilayered, three-phase history matching algorithm is developed for use in conjunction with the industrial Black Oil simulator, CLASS, (Chevron Limited Application Simulation System) for estimating the absolute permeability distribution using measured well data such as pressure, water cut, flow rates of liquid and gas from individual completions, and gas-oil ratio. The algorithm incorporates the latest advances in regularization theory as applied to petroleum reservoir parameter estimation. Numerical examples are considered in a series of history matching calculations on two- and three-phase reservoirs with three layers. The effects of the degree of regularization, spline approximation versus zonation for representing the unknown permeability distribution, and differing true areal permeability distributions on the performance of the method are examined.

2 . RESERVOIR MODEL

We consider the three-dimensional, unsteady flow of oil, water and gas in a petroleum reservoir. If the three phases are immiscible, then the mass conservation equations for the water, oil and gas phases are

$$\begin{aligned}
 R_w \equiv & -\frac{\partial}{\partial t}(\rho_w(p_o)\phi(p_o)S_w) - \nabla \cdot (\rho_w(p_o)v_w) \\
 & + \sum_{\nu=1}^{N_{well}} \rho_w(p_o)q_{w,\nu}\delta(x-x_\nu)\delta(y-y_\nu)\delta(z-z_\nu) = 0
 \end{aligned} \tag{1}$$

$$\begin{aligned}
 R_o \equiv & -\frac{\partial}{\partial t}(\rho_o(p_o, R_s)\phi(p_o)S_o) - \nabla \cdot (\rho_o(p_o, R_s)v_o) \\
 & + \sum_{\nu=1}^{N_{well}} \rho_o(p_o, R_s)q_{o,\nu}\delta(x-x_\nu)\delta(y-y_\nu)\delta(z-z_\nu) = 0
 \end{aligned} \tag{2}$$

$$\begin{aligned}
 R_g \equiv & -\frac{\partial}{\partial t}(\phi(p_o)(\rho_g(p_o)S_g + R_s\rho_o(p_o, R_s)S_o)) \\
 & - \nabla \cdot (\rho_g(p_o)v_g + R_s\rho_o(p_o, R_s)v_o) \\
 & + \sum_{\nu=1}^{N_{well}} \rho_g(p_o)q_{g,\nu}\delta(x-x_\nu)\delta(y-y_\nu)\delta(z-z_\nu) = 0.
 \end{aligned} \tag{3}$$

The volume fractions of oil, water and gas with respect to the total fluid volume, S_o , S_w and S_g , are called oil, water and gas saturations respectively, and satisfy

$$S_w + S_o + S_g = 1. \tag{4}$$

The linear velocities of the three phases are represented by Darcy's Law,

$$v_o = -\frac{k(x, y, z)k_{ro}(S_w, S_g)}{\mu_o(p_o, R_s)} \nabla (p_o - g\rho_o(p_o, R_s)h(x, y)) \tag{5}$$

$$v_w = - \frac{k(x, y, z)k_{rw}(S_w)}{\mu_w(p_o)} \nabla (p_o - g\rho_w(p_o)h(x, y) - P_{cwo}(S_w)) \quad (6)$$

$$v_g = - \frac{k(x, y, z)k_{rg}(S_g)}{\mu_g(p_o)} \nabla (p_o - g\rho_g(p_o)h(x, y) + P_{cog}(S_g)) \quad (7)$$

where $k(x, y, z)$ is the absolute permeability $\mu_o(p_o)$, $\mu_w(p_o)$ and $\mu_g(p_o)$ are the viscosities of oil, water and gas, respectively, and the relative permeabilities of oil, water and gas, $k_{ro}(S_w, S_g)$, $k_{rw}(S_w)$ and $k_{rg}(S_g)$, are functions of the water and gas saturations. The initial conditions are specified pressure and saturations,

$$p(x, y, z, 0) = p_0(x, y, z) \quad (8)$$

$$S_w(x, y, z, 0) = S_{iw} \quad (9)$$

$$S_o(x, y, z, 0) = S_{io} \quad (10)$$

and the typical no flux reservoir boundary conditions are

$$\mathbf{n} \cdot \nabla (p_o - g\rho_o(p_o, R_s)h(x, y)) = 0 \quad (11)$$

$$\mathbf{n} \cdot \nabla (p_o - g\rho_w(p_o)h(x, y) - P_{cwo}(S_w)) = 0 \quad (12)$$

$$\mathbf{n} \cdot \nabla (p_o - g\rho_g(p_o)h(x, y) + P_{cog}(S_g)) = 0. \quad (13)$$

Equations (1) - (13) are generally solved numerically using finite difference approximations. In this study, the particular numerical solutions of Equations (1) - (13) embodied in the Black Oil simulator, CLASS (Chevron Limited Applications Simulation System) developed at the Chevron Oil Field Research Company will be employed. (See Appendix A.)

3. THE HISTORY MATCHING PROBLEM

In a multiphase petroleum reservoir, the parameters to be estimated can in theory be the absolute permeability, porosity, or the relative permeabilities. In the present work, only the estimation of absolute permeability is considered, and the porosity and relative permeabilities are assumed known.

In a two-phase (water and oil), single-layered, areal (two-dimensional) reservoir, the measured data necessary to estimate absolute permeability consist of the wellbore pressure and the water cut. To estimate absolute permeability in a three-phase (gas, oil and water), multilayered (three-dimensional) reservoir gas-oil ratio and the rate of gas production from individual layers must be included as well. In particular, the liquid and gas flow rates from individual layers are crucial to the estimation of vertical heterogeneity in multilayered reservoirs. Hence, in three-dimensional reservoirs exhibiting two-phase flow, the least-squares, history matching objective function consists of three discrepancy terms corresponding to the three types of measured well data (pressures, water cuts and liquid flow rates from individual completions) that are measured at observation wells in the reservoir. In addition to the three discrepancy terms found in the objective function used in two-phase estimations, the least-squares objective function used for estimating the permeability distribution in three-phase reservoirs contains two additional discrepancy terms corresponding to the gas-oil ratio and the flow rate of gas from individual completions.

The mean-square error, σ_p^2 , between the calculated and observed pressure data is defined as,

$$\sigma_p^2 = \frac{1}{N_o N_t} \sum_{n=1}^{N_t} \sum_{\nu=1}^{N_o} (p(x_\nu, y_\nu, z_\nu, t_n) - p_\nu^{obs^n})^2 \quad (14)$$

where (x_ν, y_ν, z_ν) , $\nu = 1, \dots, N_o$ denote the locations of the observations, i.e., the wells, and t_n , $n = 1, \dots, N_t$ are the observation times. Similarly, the mean-square errors in the water cut, the gas-oil ratio, the rate of liquid production from individual layers and the rate of gas production from individual layers are defined as,

$$\sigma_W^2 = \frac{1}{N_o N_t} \sum_{n=1}^{N_t} \sum_{\nu=1}^{N_o} (WCUT(x_\nu, y_\nu, z_\nu, t_n) - WCUT_\nu^{obs^n})^2, \quad (15)$$

$$\sigma_G^2 = \frac{1}{N_o N_t} \sum_{n=1}^{N_t} \sum_{\nu=1}^{N_o} (GOR(x_\nu, y_\nu, z_\nu, t_n) - GOR_\nu^{obs^n})^2, \quad (16)$$

$$\sigma_{Q_l}^2 = \frac{1}{N_o N_t} \sum_{n=1}^{N_t} \sum_{\nu=1}^{N_o} \sum_{k=1}^{N_{LAY}} (Q_l(x_\nu, y_\nu, z_\nu, t_n) - Q_{l,\nu,k}^{obs^n})^2, \quad (17)$$

and

$$\sigma_{Q_g}^2 = \frac{1}{N_o N_t} \sum_{n=1}^{N_t} \sum_{\nu=1}^{N_o} \sum_{k=1}^{N_{LAY}} (Q_g(x_\nu, y_\nu, z_\nu, t_n) - Q_{g,\nu,k}^{obs^n})^2 \quad (18)$$

where N_{LAY} is the number of layers completed in a given well. The overall least-squares objective function is given by the weighted sum of the five contributions

$$J_{LS}(k) = W_p \sigma_p^2 + W_W \sigma_W^2 + W_G \sigma_G^2 + W_{Q_l} \sigma_{Q_l}^2 + W_{Q_g} \sigma_{Q_g}^2 \quad (19)$$

where W_p , W_W , W_G , W_{Q_l} and W_{Q_g} are the weighting coefficients. The calculation of these weighting factors will be discussed later. The performance function, J_{LS} , which is generally non-convex, must be minimized over a large number of variables and is usually insensitive to changes in certain of the parameters. As a consequence, the parameter estimates are frequently dependent upon the initial guess, may be spatially oscillatory and dependent on the grid system chosen for the numerical solution, and generally are not continuously dependent on the measured data. This type of behavior in inverse problems is termed “ill-posed.”

One means of alleviating the ill-posed nature of inverse problems is to solve a “regularized” problem, the solution of which approximates that of the original problem. In general, no single solution exists to problems of the type we consider in this work. Regularization attempts to select one solution that balances the minimization of the discrepancy between predictions and observations while maintaining some degree of smoothness in the estimated parameters. Regularization of an ill-posed parameter estimation problem penalizes the undesired features (non-smoothness) of the parameter estimates through a stabilizing functional, J_{ST} , that characterizes the non-smoothness of the parameter,

$$J_{ST}(k) = \| Lk \|^2_{H^{(L)}(\Omega)}, \quad (20)$$

where L is either identity or a differential operator and $H^{(L)}(\Omega)$ is an appropriate Sobolev space. The total performance index is then the so-called smoothing functional

$$J_{SM}(k; \beta) = J_{LS}(k) + \beta J_{ST}(k), \quad (21)$$

where the regularization parameter, β , measures the relative weight of the penalty on the non-smoothness compared to the error in matching the data. A discussion of how to choose the value of β will follow later.

Tikhonov's stabilizing functional is given by $\|k\|_{H^{(3)}(\Omega)}^2$, where the space, $H^{(3)}(\Omega)$, is the set of functions that are square-integrable over Ω and have square-integrable derivatives up to order 3¹⁻⁴,

$$J_{ST}(k) = \sum_{k=1}^{N_{LAY}} \sum_{m=0}^3 \zeta_m J_{ST_k}^{(m)}(k_k). \quad (22)$$

where $k_k(x, y)$, $k = 0, \dots, N_{LAY}$, is the parameter distribution for each layer and N_{LAY} is the total number of layers in the reservoir. $J_{ST_k}^{(m)}$, $m = 0, \dots, 3$, represents m-th order derivative terms given by

$$J_{ST_k}^{(m)}(k) = \int \int_{\Omega} \sum_{\nu=0}^m \binom{m}{\nu} \left(\frac{\partial^m k_k(\xi, \eta)}{\partial \xi^{\nu} \partial \eta^{m-\nu}} \right)^2 d\xi d\eta \quad (23)$$

with dimensionless spatial variables $\xi = \frac{x}{\Delta x}$ and $\eta = \frac{y}{\Delta y}$, and the coefficients ζ_m , $m = 0, \dots, 3$ satisfy $\zeta_m \geq 0$ for $m = 0, 1, 2$ and $\zeta_3 > 0$ ⁵⁻⁸. Since significant vertical heterogeneity is expected in a multilayered petroleum reservoir, "smoothing" of the parameter distribution is desired only in the areal dimensions and not in the vertical direction.

As Trummer⁹ has pointed out, in practical application of the theory of regularization, Tikhonov's stabilizing functional can lead to underestimation of the parameter value due to the term $J_{ST_k}^{(0)}$ in Eq. (23), which is the Euclidean norm of the parameter. Locker and Prenter¹⁰ have suggested regularization with a differential operator defined by $\| Lk \|^2_{H^{(L)}(\Omega)}$ for the linear least-squares problem, so that the stabilizing functional is the norm of the derivatives of the parameter in the Sobolev space. When the operator L in Eq. (20) is equal to the two-dimensional gradient ∇ , Locker and Prenter's stabilizing functional becomes

$$J_{ST}(k) = \sum_{k=1}^{N_{LAY}} \sum_{m=1}^3 \zeta_m J_{ST_k}^{(m)}(k) \quad (24)$$

where $J_{ST_k}^{(m)}$, $m = 1, \dots, 3$ is the same as above, and the coefficients ζ_m , $m = 1, \dots, 3$ satisfy $\zeta_1 > 0$, $\zeta_2 \geq 0$, and $\zeta_3 > 0$, so that it does not include the Euclidean norm of the parameter. The choice of values for the ζ_m 's in Eqs. (22) and (24) is arbitrary except for the inequality conditions stated above. One possibility is to base the choice of ζ_m 's on the length scales used in the finite difference approximation of the PDE's, Δx and Δy . By using this criterion, the ζ_m 's used in this work are $\zeta_1 = \zeta_2 = \zeta_3 = 1$ ¹¹.

Since, in some cases, the absolute permeability may be known at certain locations it may prove useful to include this local information while estimating the permeability over the whole reservoir. In using a zonation approach, in which the absolute permeability value itself is estimated at each grid cell, one way of accomplishing the inclusion of known permeability information is to minimize the performance index only with respect to the unknown zones. When using a bicubic spline approximation, however, the bicubic spline coefficients do not have a one-to-one relationship with the permeability values at each grid cell, and thus, a direct elimination of a coefficient is not possible. Rather, an additional penalty term

can be included in the performance index, J_{PEN} , which is a weighted sum of the discrepancy between the permeability predicted during the parameter estimation and the “true” value at that location,

$$J_{PEN}(k) = \sum_{i=1}^{N_k} W_{k_i} (k_i^{EST} - k_i^{TRUE})^2 \quad (25)$$

where W_{k_i} is the weighting factor for the i^{th} known value of k and is assumed to be $\frac{1}{\bar{k}_i^2}$ where \bar{k}_i is an upper bound of the known permeability values.

The formulation of the history matching problem as discussed above seeks the minimum of either the smoothing functional, $J_{SM}(k; \beta)$, or the smoothing functional plus a penalty term, $J_{SM}(k; \beta) + J_{PEN}$, in the case that information is known *a priori* about the permeability distribution. In the first case, J_{SM} is composed of six quantities, $W_p \sigma_p^2$, $W_W \sigma_W^2$, $W_G \sigma_G^2$, $W_{Q_l} \sigma_{Q_l}^2$, $W_{Q_g} \sigma_{Q_g}^2$ and βJ_{ST} , where five of the six weighting coefficients W_p , W_W , W_G , W_{Q_l} , W_{Q_g} and β , must be determined independently. In this work, W_p , W_W , W_G , W_{Q_l} and W_{Q_g} have been chosen as $\frac{1}{\bar{\sigma}_p^2}$, $\frac{1}{\bar{\sigma}_W^2}$, $\frac{1}{\bar{\sigma}_G^2}$, $\frac{1}{\bar{\sigma}_{Q_l}^2}$ and $\frac{1}{\bar{\sigma}_{Q_g}^2}$, respectively, where $\bar{\sigma}_p$, $\bar{\sigma}_W$, $\bar{\sigma}_G$, $\bar{\sigma}_{Q_l}$ and $\bar{\sigma}_{Q_g}$ are the upper bounds of the discrepancy terms associated with the observed well data. This particular choice for the weighting coefficients assures that each type of measured well data is weighted equally and have values of approximately order 1.

Determining a suitable value of β for a given set of noisy measured data where the noise level may or may not be known can be done in one of several ways. Clearly, $\beta = 0$ corresponds to the non-regularized problem, while $\beta \rightarrow \infty$ would lead to oversmoothing of the estimated distribution. Craven and Wahba¹² used the method of generalized cross validation (GVC) to find a β at which the parameter estimate gives the best prediction of unobserved data values. To apply GCV to reservoir parameter estimation, one needs the parametric sensitivity of pressure

and production data, the calculation of which is specifically avoided here for computational efficiency. Another possibility, developed by Tikhonov and Arsenin¹³, involves defining a “quasi-optimal” value of the regularization parameter for $\beta > 0$ such that the parameter estimates are minimally sensitive to the logarithmic change of β ; i.e., $J_{ST}(\beta \frac{\partial k}{\partial \beta})$ is a minimum. The numerical algorithm to find such a quasi-optimal β requires repeated solution of the regularized problem for different β 's. Miller¹⁴ suggested a way of determining the regularization parameter from the ratio of an upper bound of J_{LS} values calculated from the measured data to an upper bound of J_{ST} i.e., $\frac{\bar{J}_{LS}}{\bar{J}_{ST}}$. Based upon Miller's idea, Lee and Seinfeld¹¹ developed an algorithm in which the regularization parameter is determined automatically during the estimation process without requiring *a priori* information. In the computational examples considered here, the regularization parameter is calculated automatically using the following relation

$$\beta = \alpha W_p \frac{\bar{J}_{LS}}{\bar{J}_{ST}} \quad (26)$$

where $\alpha = 0.1$ for two-phase cases and $\alpha = 10$ for three-phase cases. By trial and error, it has been found that Miller's method determines a regularization parameter that is too large for two-phase problems and too small for three-phase problems. A regularization parameter that is $\frac{1}{10}$ of the value suggested by Miller has been found to work well in a variety of two-phase cases, and a regularization parameter that is 10 times the value suggested by Miller has been found to work well in a variety of three-phase cases.

4. SPLINE APPROXIMATION OF THE AREAL PERMEABILITY DISTRIBUTION

Several options exist for representing the spatial distribution of the parameters. One such option is the zonation approach in which the absolute permeability itself is assumed uniform in each zone. A zone may be as small as one grid cell or encompass a number of grid cells. Another approach is to use a prespecified function, such as a bicubic spline function, to represent the horizontal variation of the permeability. Spline approximation has several merits including a built-in smoothing of the parameter distribution as well as computational convenience^{5-8,15}. As noted in the previous section, significant vertical heterogeneity is expected in the permeability distribution and thus the bicubic spline approximation is applied to each layer separately.

The spline representation of the spatially varying absolute permeability in each horizontal layer is given by

$$k_k(x, y) = \sum_{l_y=1}^{N_{ys}} \sum_{l_x=1}^{N_{xs}} b_x(l_x, x) b_y(l_y, y) W_{l,k} \quad (27)$$

where $b_x(l_x, x)$ and $b_y(l_y, y)$ are the cubic B-spline functions,

$$b_x(l_x, x) = \chi^{*4} \left(4 - l_x + \frac{x}{\Delta x_s} \right), \quad l_x = 1, \dots, N_{xs} \quad (28)$$

$$b_y(l_y, y) = \chi^{*4} \left(4 - l_y + \frac{y}{\Delta y_s} \right), \quad l_y = 1, \dots, N_{ys} \quad (29)$$

$$\chi^{*4}(\theta) = \begin{cases} \frac{\theta^3}{6}, & \theta \in [0, 1]; \\ \frac{1}{6} + \frac{(\theta-1)}{2} + \frac{(\theta-1)^2}{2} - \frac{(\theta-1)^3}{2}, & \theta \in [1, 2]; \\ \frac{4}{6} - (\theta-2)^2 + \frac{(\theta-2)^3}{2}, & \theta \in [2, 3]; \\ \frac{1}{6} - \frac{(\theta-3)}{2} + \frac{(\theta-3)^2}{2} - \frac{(\theta-3)^3}{6}, & \theta \in [3, 4]; \\ 0, & \text{otherwise;} \end{cases} \quad (30)$$

where Δx_s and Δy_s are the grid spacings for the spline approximation and $l = l_x + N_{xs}(l_y - 1)$, $l = 1, \dots, N_s$ where $N_s = N_{xs} \times N_{ys}$. With this approximation, $k_k(x, y)$ is replaced by the set of unknown coefficients, $W_{l,k}$, $l = 1, \dots, N_s$, $k = 1, \dots, N_{LAY}$.

In applying the spline approximation to the history matching problem, the number of coefficients for spline representation should not exceed either the number of grid cells for the PDE's or the number of available observation data. If too few coefficients are employed, the spline approximation cannot represent the spatial details of the permeability distribution adequately; furthermore, the functional derivative of J_{LS} with respect to the absolute permeability given by Eq. (B.9 - 10) cannot be properly represented by the derivative of J_{LS} with respect to the spline coefficients during the minimization of J_{SM} , and this may slow the rate of convergence. When the spline approximation is used together with regularization, the smoothing power of the spline approximation becomes less important than in its absence and N_{xs} and N_{ys} can be chosen as large as the numbers of grid cells along the x - and y -directions for the solution of the PDE's¹¹.

5 . THE HISTORY MATCHING ALGORITHM

The problem is to minimize subject to Eqs. (1-13) the augmented objective function, J_{SM} , with respect to the spline coefficients, $W_{l,k}$, $l = 1, \dots, N_s$ and $k = 1, \dots, N_{LAY}$. If a zonation approach is used, the minimization is carried out with respect to the zonal permeabilities themselves. To obtain an algorithm to solve this problem, two steps are required. First, the gradient of J_{SM} with respect to each $W_{l,k}$ must be computed, and then this gradient must be used in a numerical minimization method to minimize J_{SM} . The calculation of these gradients represents the most time-consuming part of updating the parameter iterates. In a problem as large as the current one, these derivatives must be calculated directly without first calculating the sensitivity coefficients. The derivation of these derivatives and the expressions describing them shown in Eqs. (B.9 - 11) can be found in Appendix B. The approach that will be used here, based on optimal control theory, requires only first-order functional derivatives of the performance index with respect to the parameter to be estimated^{1,2,16,17}. To compute the functional derivative of J_{LS} with respect to the absolute permeability, the reservoir PDE's are first solved forward in time with the given initial conditions at $t = 0$; then, as described in Appendix B, the adjoint system of equations, Eqs. (B.2 - 5), are solved backward in time with the terminal constraints given by Eqs. (B.6 - 8). At the end of each time step during the solution of the adjoint system of equations, the derivative of J_{LS} with respect to the permeability at each grid cell, $\frac{\partial J_{LS}}{\partial k_i}$, $i = 1, \dots, N$, is computed by Eq. (B.9). Next one computes the derivative of J_{LS} with respect to the spline coefficient, $W_{l,k}$ from Eq. (B.10), the derivative of J_{ST} with respect to $W_{l,k}$ as discussed by Kravaris and Seinfeld¹⁸ and the derivative of J_{SM} with respect to $W_{l,k}$ from Eq. (B.11).

For most multivariate minimization problems, methods that require second-order derivatives of the performance functional are not recommended since they are computationally inefficient. As a result, various methods have been developed that utilize only the first derivatives; these include the conjugate gradient, quasi-Newton and partial conjugate gradient methods. The conjugate gradient algorithm requires an exact line search to compute the length of each descent direction vector. Quasi-Newton methods use the inverse Hessian matrix to compute the descent vector, which requires a substantial amount of memory, although it does not require an exact line search. In general, quasi-Newton methods are preferred for relatively small problems, and conjugate gradients methods for large ones¹⁹. On the other hand, partial conjugate gradient methods have the same memory requirements as conjugate gradient methods, without requiring an exact line search and show good performance over a range of problem sizes. Lee, et al.^{11,20} employed the partial conjugate gradient method of Nazareth²¹ as the core minimization technique in estimating permeabilities in two-dimensional, two-phase problems. In the present study this method will be used also.

As Lee et al.¹¹ discussed, the choice of the initial guess is crucial since convergence difficulties are experienced when the initial guesses of the parameters are far from their actual values. To alleviate this problem and to generate an algorithm that is as automatic as possible, Lee et al.¹¹ suggest beginning the estimation by determining the unknown parameter as uniform over each layer in the region. Thus, to start, a single value of permeability is estimated for each horizontal layer in the entire region which minimizes J_{LS} . These values then serve as a starting point for the multivariable estimation algorithm. The reason behind this strategy is that convergence difficulties should not be encountered in estimating only a few parameters. These uniform parameters values, while not accurate in their spatial detail,

serve as a good starting point for the full algorithm. This initial minimization is carried out using the secant method. To summarize, the following algorithm is used in this work:

- Step 1** In the absence of *a priori* information about the unknown parameters, find the flat initial guess of the permeability for each layer that minimizes J_{LS} .
- Step 2** Using the starting value of the permeability determined in Step 1, find the spatially-varying parameter that minimizes J_{LS} and compute the values of J_{LS} and J_{ST} .
- Step 3** Using the permeability distribution and the values of J_{LS} and J_{ST} determined in Step 2, let $\beta = 0.1W_p \frac{J_{LS}}{J_{ST}}$ for two-phase problems, and $\beta = 10W_p \frac{J_{LS}}{J_{ST}}$ for three-phase problems, and find the spatially-varying permeability distribution that minimizes J_{SM} .

6. COMPUTATIONAL EXAMPLES

The remainder of this work is devoted to the numerical evaluation of the history matching algorithm in a three-layered reservoir in the case of two- and three-phase flow. The algorithm will be evaluated on well-defined test problems for which the true absolute permeability distribution is known. The reservoir simulator is solved with the true permeability distribution to generate observation data, and then the history matching algorithm is used to try to recover the true permeability values. The horizontal permeability distribution in each of the three layers is to be estimated.

From the results in Chapter II, in which the sensitivity of measured well data such as wellbore pressure, water cut and rate of liquid production from individual layers to changes in k_v is examined, it was shown that the measured well data are relatively insensitive to changes in k_v for $k_v > 0$. The reason for this insensitivity is that gravitational forces tend to segregate the fluids rapidly, water sinking to the bottom close to the wells where it is injected and gas rising to the top of the reservoir as soon as it is released from solution in the oil phase. Thus, the gravitational forces outweigh the effect of differences in the value of k_v on the vertical distribution of fluids. As a result, the wellbore pressure, water cut and rate of liquid production from individual layers measured at the production wells where multiphase production takes place are insensitive to changes in k_v since gas is normally produced from the top layers of the reservoir and water from the bottom. Of course, if the layers are noncommunicating, i.e., $k_v = 0$, then fluid remains in the layer in which it is injected or is released from solution and no segregation takes place. In this work, computational examples in which the layers communicate are considered. In a multilayered petroleum reservoir, k_v is usually considerably smaller

than the horizontal permeability due to the deposition history of the sedimentary layers and the existence of shale lenses within these layers. In this work, we have used a rule of thumb, often employed in petroleum reservoir simulation, which is to assume that k_v is $\frac{1}{10}$ of the value of the horizontal permeability in each grid cell^{22,23}.

The physical specification of the reservoir is given in Table 1. Both the reservoir PDE's and the adjoint system are solved on a 15×10 grid, and a spline grid of the same dimensions is employed for the bicubic spline representation of the permeability distribution in each layer. The geometry of the reservoir with the well locations is shown in Fig. 6.1, and the true absolute permeability distributions for layers 1 and 3 are shown in Figs. 6.2 (a) and (b). The true absolute permeability distribution for layer 2 is assumed to be uniform with a value of 0.3 Darcy.

The Chevron Oil Field Research Company Black Oil simulator, CLASS, is used to generate the observation data which include bottom hole pressure, water cut, rate of liquid production from individual layers and, in the three-phase problems, gas-oil ratio and the rate of gas production from individual layers. To generate noisy measured well data, a set of uniformly distributed pseudo-random numbers is added to the measured well data obtained from solving the reservoir simulator with the true permeability distribution.

In the two-phase (oil and water) case, the water injection rate is controlled using the voidage replacement option in which the volume rate of injection is determined to be the same as the volume of fluid produced in order to maintain the reservoir pressure. In the three-phase (oil, water and gas) case, two examples with different production scenarios are considered. In the first example, we assume that there is free gas in the reservoir initially. In this case, since gas is initially produced in large quantities causing a rapid decrease in reservoir pressure the injection rate slightly exceeds the production rate to ensure that the reservoir pressure does not

drop too low. In Example 2, no free gas exists in the reservoir initially, but evolves with time since the liquid production rate exceeds the water injection rate allowing the reservoir pressure to decrease. When the reservoir pressure falls below the bubble point pressure, gas is released from solution and percolates upward through the reservoir forming a gas cap at the top.

A total of 1413 pressure data are measured at the injection, production and observation wells, which represents 157 measurements per well at time intervals of 24 days over a ten-year period. In addition, 785 water cut and rate of liquid production measurements are made, and in the three-phase case, gas-oil ratio and the rate of gas production measurements are made at the five production wells.

A comparison is made between the estimation results using the zonation approach and those using the bicubic spline approximation. The effect of regularization on the final estimation results is investigated; the regularization parameter, β , is calculated automatically during the estimation procedure such that $\beta = 0.1W_p \frac{\bar{J}_{LS}}{\bar{J}_{ST}}$ for the two-phase cases and $\beta = 10W_p \frac{\bar{J}_{LS}}{\bar{J}_{ST}}$ for the three-phase cases. In general, the minimization scheme is run until $J_{SM_{final}} = 0.001J_{SM_{initial}}$. All computations are carried out using a CRAY X-MP/48.

TABLE 1 - PHYSICAL PROPERTIES OF THE RESERVOIR

(1) Fluid properties (ref. pres. 3600. psia)

	<u>Water</u>	<u>Oil</u>	<u>Gas</u>
Compressibility, psia^{-1}		1.0×10^{-5}	
Viscosity, CP	0.96	09.5	0.017
Surface specific gravity	1.015	0.72	0.89 (air = 1.0)
	$S_{iw} = 0.22$	$S_{ro} = 0.0$	
R_s , $\frac{\text{SCF}}{\text{STB}}$		1390.	

(2) Rock and reservoir properties

Porosity	0.3
Initial pressure, psia, at 3164.042 ft.	3600.
Rock compressibility, psia^{-1}	0.3×10^{-5}
Gas-oil contact, ft.	3100.
Water-oil contact, ft.	3400.
Top of Reservoir, ft.	3147.7

Two - phase case

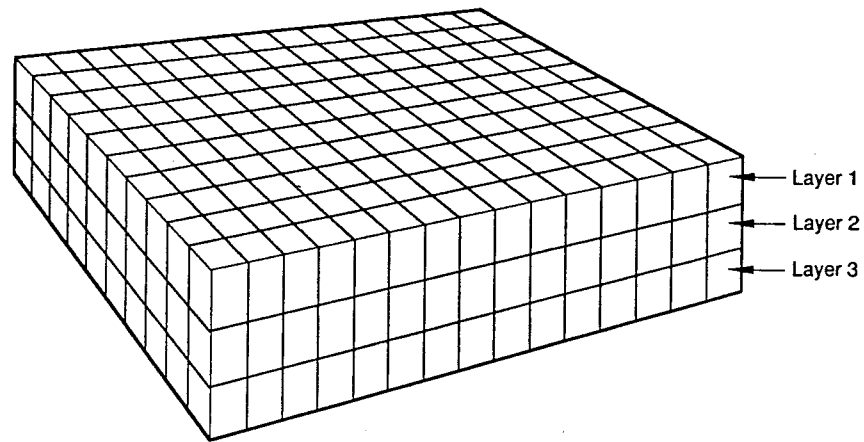
Production rate at all wells, $\frac{\text{STB}}{\text{DAY}}$	2000.
Injection rate (I1,I3,I4,I6), $\frac{\text{STB}}{\text{DAY}}$	1250.
Injection rate (I2,I5), $\frac{\text{STB}}{\text{DAY}}$	2500.
Bubble point pressure, psia	2000.

Three - phase case : Example1

Production rate at all wells, $\frac{\text{STB}}{\text{DAY}}$	1200.
Injection rate (I1,I3,I4,I6), $\frac{\text{STB}}{\text{DAY}}$	700.
Injection rate (I2,I5), $\frac{\text{STB}}{\text{DAY}}$	1200.
Bubble point pressure, psia	3600.

Three - phase case : Example2

Production rate at all wells, $\frac{\text{STB}}{\text{DAY}}$	1080.
Injection rate (I1,I3,I4,I6), $\frac{\text{STB}}{\text{DAY}}$	540.
Injection rate (I2,I5), $\frac{\text{STB}}{\text{DAY}}$	800.
Bubble point pressure, psia	3600.



	I			O			I			O		I	
	P			P			P			P		P	
	I			O			I			O		I	

I = Injection*

D = Observation

P = Production†

* Injection Wells Are Completed In Layer 3 Only

† Production Wells Are All Completed In Layers 1, 2 and 3

Fig. 6.1 - Reservoir shape and well locations

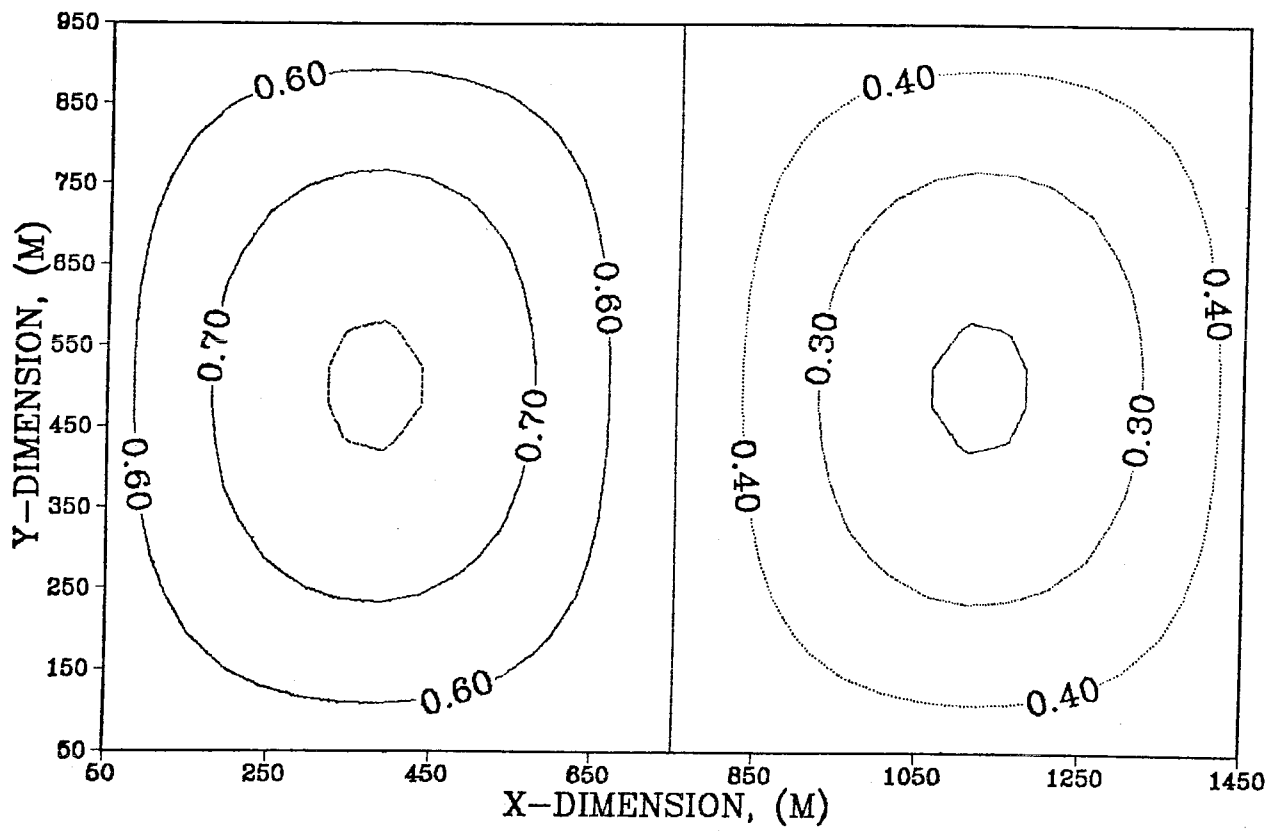


Fig. 6.2 (a) - True absolute permeability distribution
for layer 1

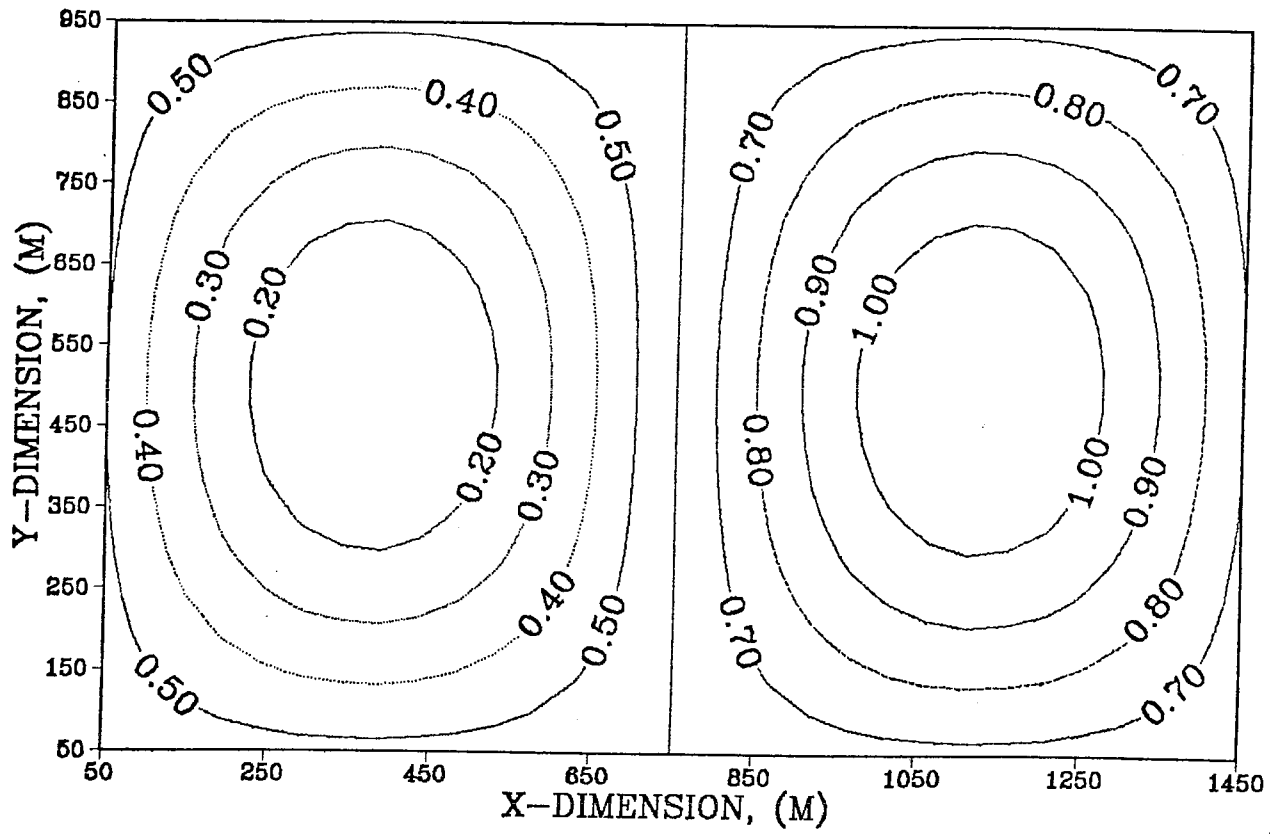


Fig. 6.2 (b) - True absolute permeability distribution
for layer 3

6.1 Generation of the Initial Guess

As discussed previously, a three-step minimization procedure is implemented to estimate the spatially-varying permeability distribution. Since the uniqueness of the solution of the parameter estimation problem is not guaranteed and since there may exist unidentifiable regions due to the configuration of the well measurements and time period over which the data are available, convergence of the algorithm may depend upon the initial guess. In the first step, the best uniform value for the absolute permeability is estimated for each layer to alleviate convergence difficulties associated with the choice of the initial guess in a multivariable minimization. In both the two- and three-phase cases, Step 1 of the minimization algorithm is begun with starting guesses of 0.05 Darcy for each layer.

In the two-phase case, as shown in Tables 2 and 3, the values of the uniform permeability that minimize J_{LS} in Step 1 are 0.336 Darcy for the top layer, 0.361 Darcy for the middle layer and 0.690 Darcy for the bottom layer. In Step 1, J_{LS} decreases from a value of 0.599×10^5 to a value of 0.521×10^4 which is 10.6 times the value of J_{LS} calculated based on the noisy observation data with the true permeability distribution. In Example 1 of the three-phase cases, as shown in Table 4, Step 1 of the algorithm converges to values of the permeability of 0.339 Darcy for the top layer, 0.234 Darcy for the middle layer and 0.514 Darcy for the bottom layer. In this case, the value of J_{LS} decreases from 0.734×10^6 to a value of 0.731×10^4 . In Example 2 of the three-phase cases, as shown in Table 5, Step 1 of the algorithm converges to values of the permeability of 0.139 Darcy for the top layer, 0.104 Darcy for the middle layer and 0.229 Darcy for the bottom layer. In this case, the value of J_{LS} decreases from a value of 0.540×10^7 to a value of 0.134×10^5 .

In all three cases, Step 1 was successful in decreasing the performance index by several orders of magnitude and estimating better starting guesses for each layer than 0.05 Darcy, for use as uniform initial guesses in Step 2, the first step of the multivariable minimization.

TABLE 2 - PERFORMANCE OF THE ESTIMATION FOR THE TWO-PHASE CASE USING BICUBIC SPLINE APPROXIMATION

	\bar{k} Darcy	β Darcy ⁻²	J_{LS}	J_{ST} Darcy ²	J_{SM}	CPU time ^a s	Number of Iterations ^b
Initial Guess ^c	0.05		59893				
Step 1			5210			1300	20
Layer 1	0.336						
Layer 2	0.361						
Layer 3	0.690						
Step 2		0.0	413	34.7	413	2600	40
Step 3		0.97	322	16.5	338	2600	40
True values			489				

a On Cray X-MP/48

b Number of solutions of the state and adjoint equations

c Same value for all three layers

TABLE 3 - PERFORMANCE OF THE ESTIMATION FOR THE TWO-PHASE CASE USING THE ZONATION APPROACH

	\bar{k} Darcy	β Darcy ⁻²	J_{LS}	J_{ST} Darcy ²	J_{SM}	CPU time ^a s	Number of Iterations ^b
Initial Guess ^c	0.05		59893				
Step 1			5210			1300	20
Layer 1	0.336						
Layer 2	0.361						
Layer 3	0.690						
Step 2		0.0	591	55.6	591	2600	40
Step 3		0.97	389	52.7	440	2470	38
True values			489				

a On Cray X-MP/48

b Number of solutions of the state and adjoint equations

c Same value for all three layers

TABLE 4 - PERFORMANCE OF THE ESTIMATION FOR THE THREE-PHASE CASE USING BICUBIC SPLINE APPROXIMATION: Example 1

	\bar{k} Darcy	β Darcy ⁻²	J_{LS}	J_{ST} Darcy ²	J_{SM}	CPU time ^a s	Number of Iterations ^b
Initial Guess ^c	0.05		7.34×10^5				
Step 1			7.31×10^3			5040	28
Layer 1	0.339						
Layer 2	0.234						
Layer 3	0.514						
Step 2		0.0	334	17.5	334	20,520	114
Step 3		29.2	175.4	5.9	363	14,400	80
True values			0^d				

a On Cray X-MP/48

b Number of solutions of the state and adjoint equations

c Same value for all three layers

d Noiseless observation data was used in the 3-phase examples

TABLE 5 - PERFORMANCE OF THE ESTIMATION FOR THE THREE-PHASE CASE USING BICUBIC SPLINE APPROXIMATION: Example 2

	\bar{k} Darcy	β Darcy ⁻²	J_{LS}	J_{ST} Darcy ²	J_{SM}	CPU time ^a s	Number of Iterations ^b
Initial Guess ^c	0.05		5.40×10^6				
Step 1			1.34×10^4			7200	40
Layer 1	0.139						
Layer 2	0.104						
Layer 3	0.229						
Step 2		0.0	3310	20.5	3310	12,600	70
Step 3		30.1	3310	20.5	3503	0	0
True values			0^d				

a On Cray X-MP/48

b Number of solutions of the state and adjoint equations

c Same value for all three layers

d Noiseless observation data was used in the 3-phase examples

6.2 The Types of Observation Data Needed to Estimate Permeabilities in Two- and Three-Phase, Three-Dimensional Reservoirs

The least-squares objective function used in the minimization algorithm consists of three types of measured well data in the two-phase case, which include bottom hole pressure, water cut and the rate of liquid production from individual completions, and five types in the three-phase case, which include those of the two-phase case and, in addition, the gas-oil ratio and the rate of gas production from individual completions. In a single-phase problem, only pressure data are required to estimate the absolute permeability distribution in an areal reservoir model. In a two-phase (oil and water) reservoir, both pressure and water cut information are necessary to predict the two-dimensional permeability distribution. In a three-dimensional reservoir, the change in the water cut with time generally depends more upon the permeability distribution in the bottommost layer than upon the distributions in the upper layers since most of the water migrates to the producing wells through the bottom layer. Thus, the permeabilities in the upper layers have little influence on the water breakthrough time. As a result, the rate of liquid production from the individual completions is necessary to estimate the permeability distribution in a reservoir with more than one layer since neither the pressure nor water cut data alone contain enough information about the varying permeability distributions in a multilayered system.

In three-phase reservoirs, the rate of gas production from individual completions and the gas-oil ratio are also needed for determination of the permeability distribution. The change in the gas-oil ratio with time generally depends more upon the permeability distribution in the topmost layer since gravity forces the gas to rise to the top of the reservoir and to migrate to the producing wells through the topmost layer. Thus, the permeabilities in the lower layers have little influence on the gas breakthrough time. In addition to the liquid flow rate from individual completions, the gas flow rate from each completion is needed to estimate the permeability distribution in three-phase reservoirs with more than one layer.

6.3 The Effects of the Spline Approximation Approach versus the Zonation Approach and Regularization on the Performance of the Matching History Matching Algorithm

Two criteria must be considered in evaluating the performance of the history matching algorithm. The first is how well the algorithm matches the observation data generated by solving the simulator with the true permeability distribution. The second is how well we can recover the true permeability distribution starting with some randomly chosen initial guess. In the following section, we will discuss the effects of spline representation versus zonation and regularization on these two criteria as they apply to the results of the estimation of permeabilities in two- and three-phase reservoirs.

6.3.1 Two-Phase Reservoirs

For the two-phase case, as shown in Figs. 6.3, 6.4 and 6.5 (a), (b) and (c), the calculated well data from the estimated permeability distributions match the actual observation well data more accurately when using the bicubic spline approach than when using the zonation approach. In using the zonation approach the absolute permeability values themselves at each grid cell are estimated during the minimization procedure, while using the bicubic spline approximation, the permeability is replaced with the coefficients of the spline function. In using the zonation approach, the calculated water cut and pressure data fit the observation data well as shown in Figs. 6.3 and 6.4; however, this method has difficulty matching the rate of liquid production from individual layers as accurately as the spline representation as can be seen in Fig. 6.5 (a), (b) and (c). When using the zonation approach, the objective function decreased from a value of 0.599×10^5 to a value of 440.0 in 98 iterations (see Table 3). When using the bicubic spline approach, the objective function decreased from a value of 0.599×10^5 to a value of 338.0 in 100 iterations (see Table 2). In spite of the relative closeness of 440 and 338, a comparison of Figs. 6.6 (a), (b) and (c) and Figs. 6.7 (a), (b) and (c) shows that the bicubic spline approach is clearly much more effective in representing the true permeability distribution even though both approaches led to a significant decrease in the performance index. In general, the effect of representing the permeability distribution with spline approximation is to impart a degree of smoothness and regularity to the estimated permeability distribution. The spline approximation both enhances the ability of the minimization algorithm to recover the true permeability distribution, and as a result, improves the overall match of the measured observation data generated by running the simulator with the true permeability distribution, particularly the

liquid flow rates from individual completions. A comparison of Figs. 6.6(a) and (b) with Fig. 6.6(c) illustrates that the permeability distribution in the bottom layer is estimated slightly more accurately than that in the top layer. This behavior is due in part to the fact that the water cut depends more on the permeability distribution in the bottom layer than that in the top and middle layers.

A further comparison of the two approaches can be made and the effect of regularization studied by considering the results after Step 2 of the algorithm which is the least-squares minimization with $\beta = 0$ as shown in Figs. 6.8 (a), (b) and (c) and 6.9 (a), (b) and (c) for the two-phase case. As can be seen, the bicubic spline function does not unduly constrain the possible values of the permeability while helping enormously in improving the results of the estimation by imparting a degree of smoothness on the estimated values even before the regularization step has been applied. In Step 2, when using the zonation approach, J_{LS} decreased from a value of 5210 to a value of 591, while with the bicubic spline approach, J_{LS} decreased from a value of 5210 to a value of 413.

In applying regularization to the results of Step 2 for the zonation approach, little improvement is made in the estimation of the permeability distribution as can be seen in a comparison of Figs. 6.7 (a), (b) and (c) and Figs. 6.8 (a), (b) and (c). The lack of improvement is due the fact that since the parameters are not represented by an analytic function as in the bicubic spline approach, the stabilizing functional, J_{ST} , must be calculated using a finite difference approximation, and thus, only its first derivative terms can be calculated with any accuracy. A comparison of Figs. 6.6 (a), (b) and (c) and Figs. 6.9 (a), (b) and (c) shows the improvement in the parameter estimation due to the application of regularization when using the bicubic spline approach. In particular, the contours are smoothed

in all three layers and the prediction of the peaks and valleys in layers 1 and 3 is enhanced.

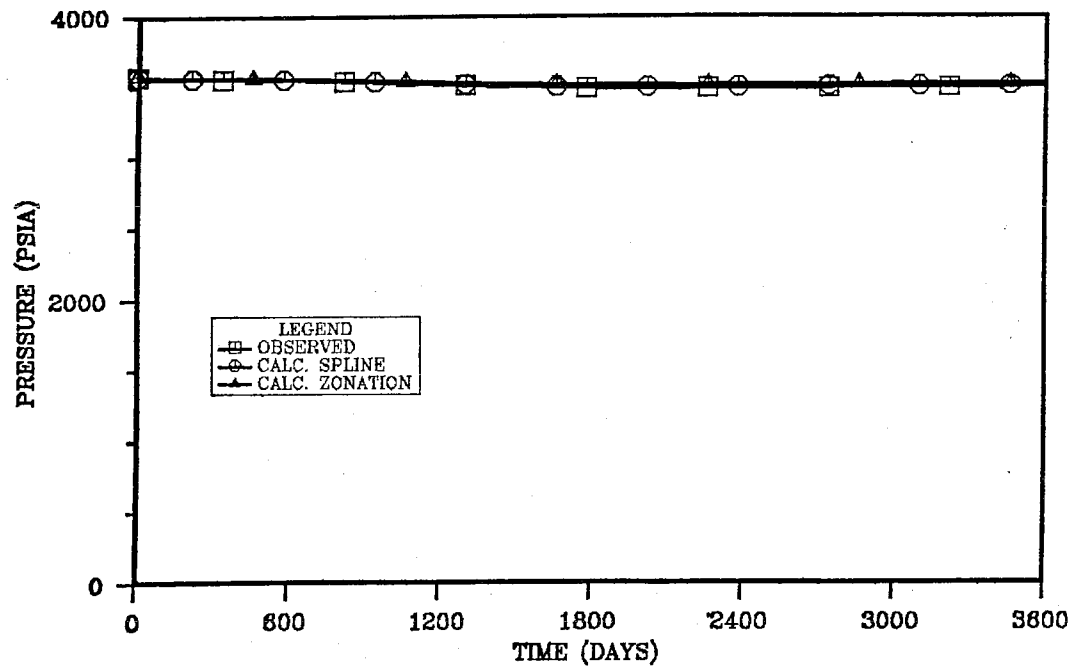


Fig. 6.3 - History match of bottomhole pressure from well P3
for 2-phases

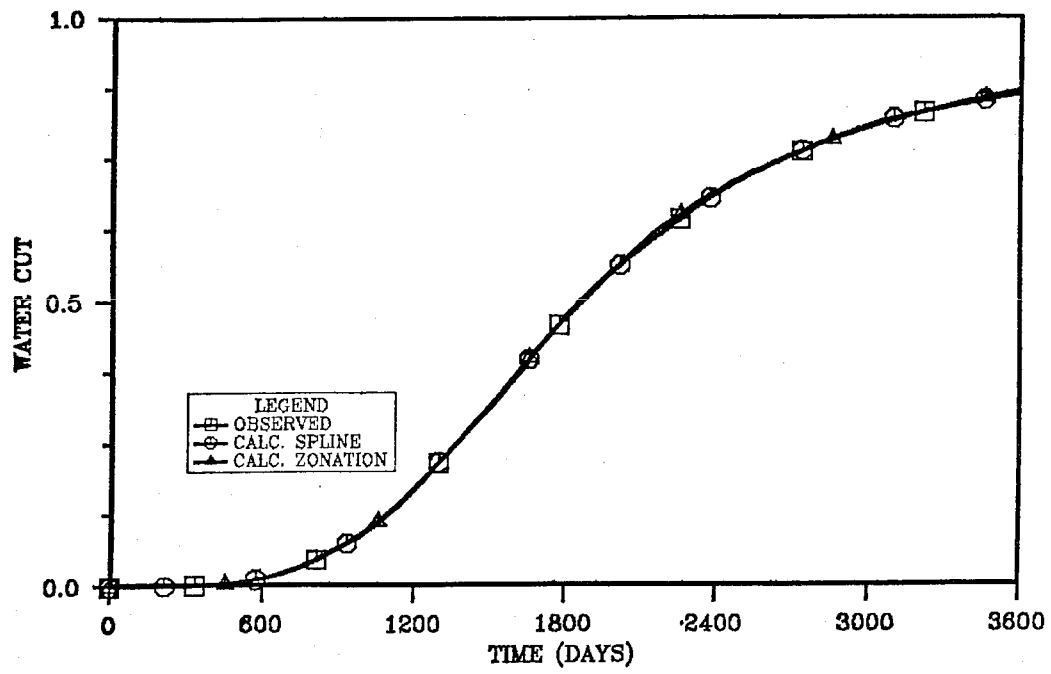


Fig. 6.4 - History match of water cut from well P3
for 2-phases

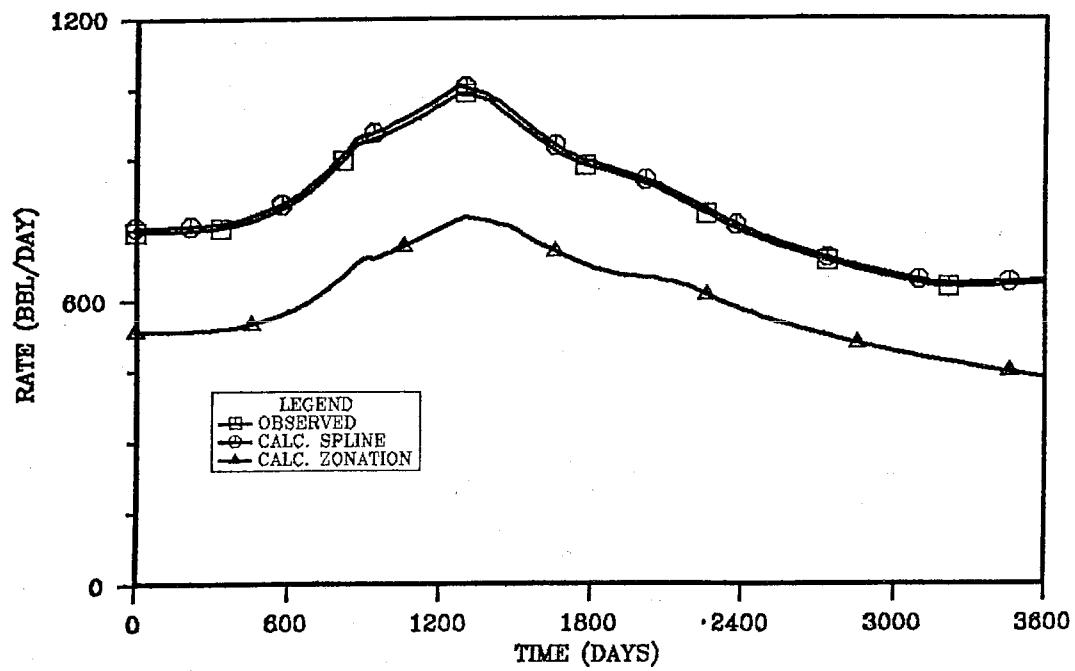


Fig. 6.5 (a) - History match of liquid flow rate from well P3 from completion 1 for 2-phases

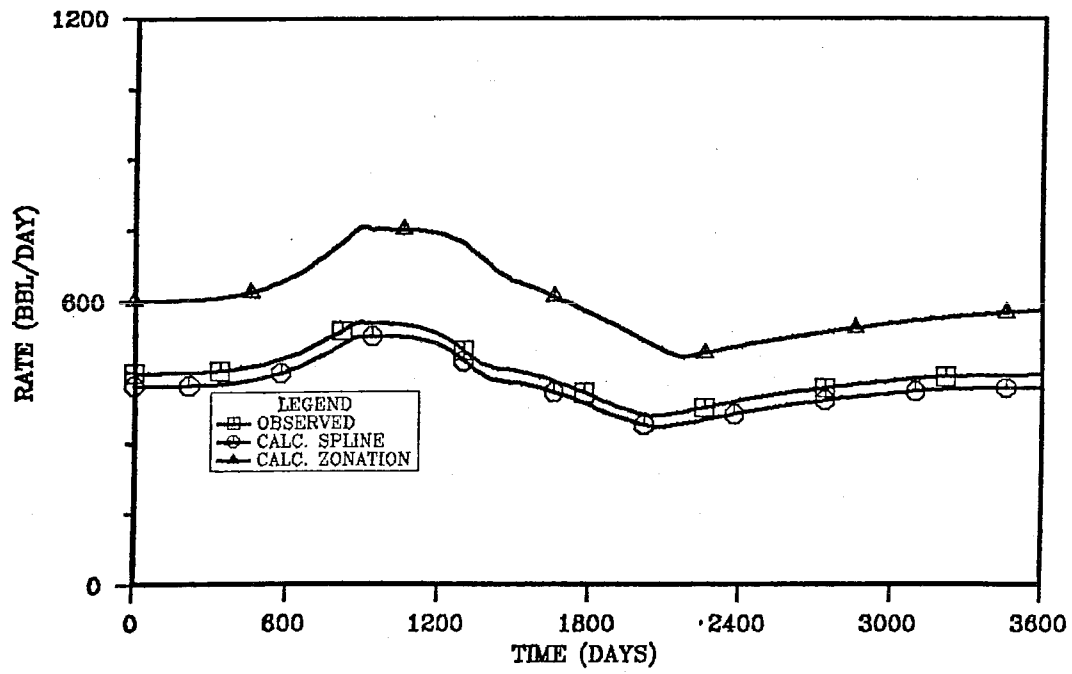


Fig. 6.5 (b) - History match of liquid flow rate from well P3
from completion 2 for 2-phases

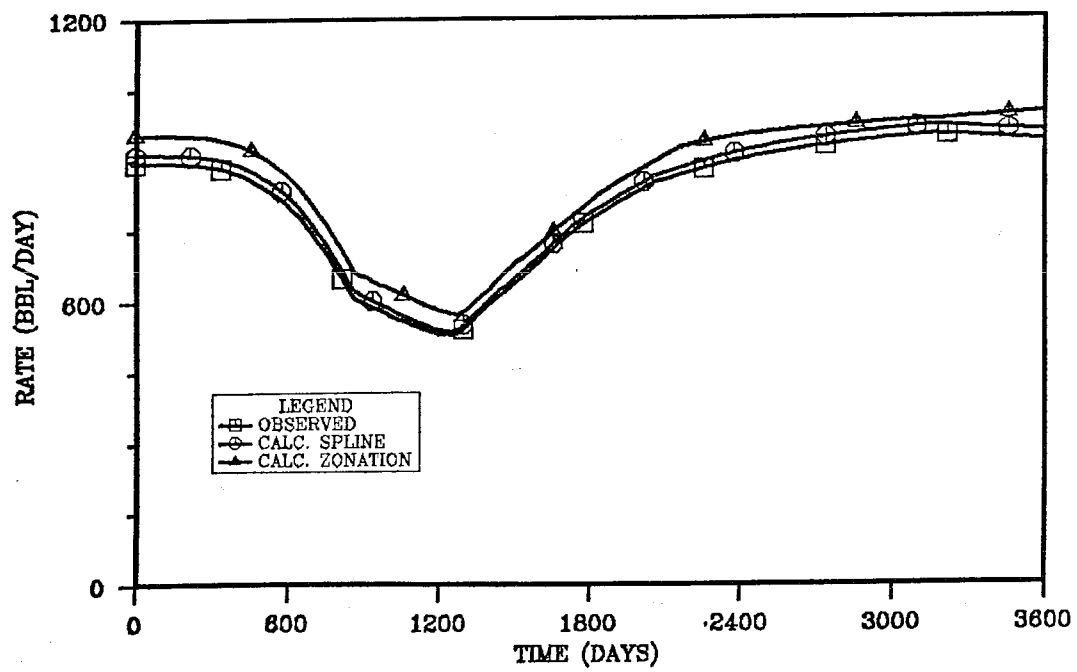


Fig. 6.5 (c) - History match of liquid flow rate from well P3
from completion 3 for 2-phases

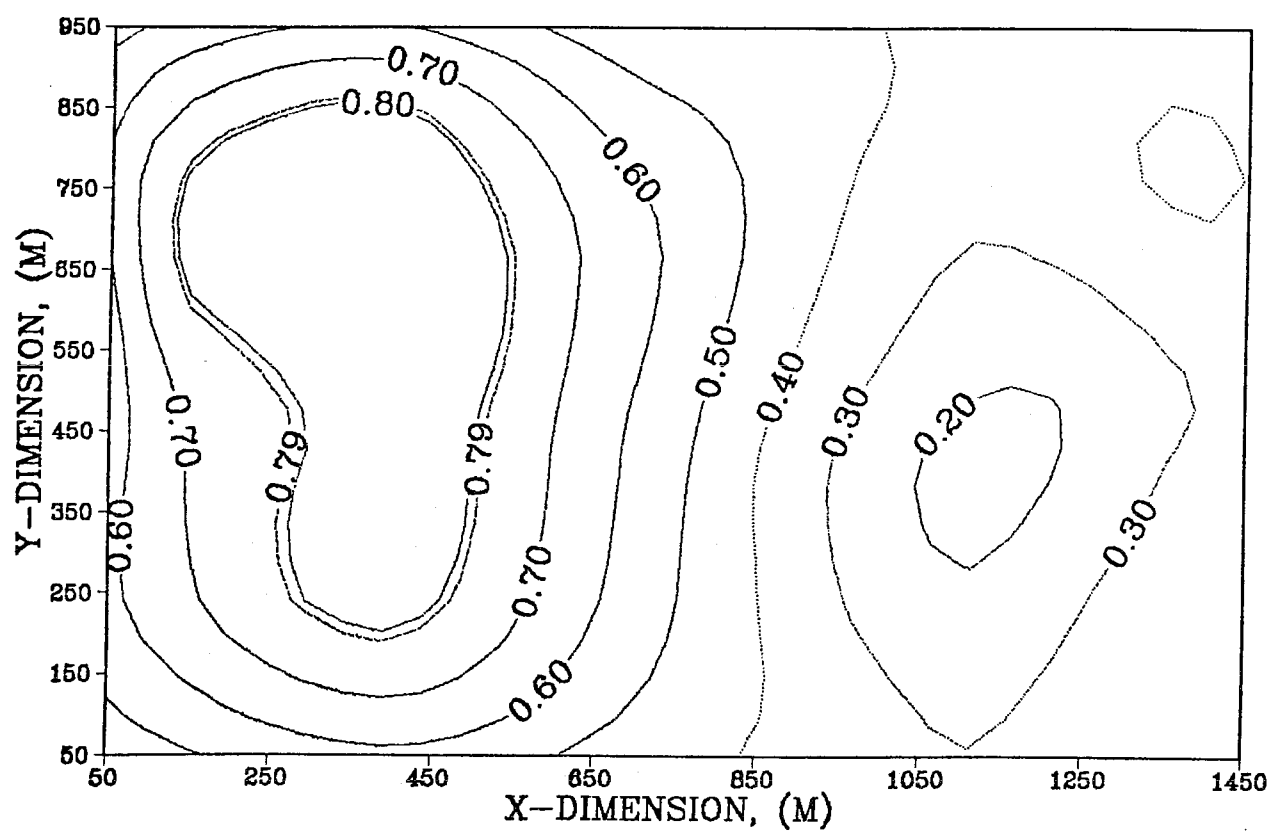


Fig. 6.6 (a) - Estimated permeability distribution of layer 1
for 2-phases after Step 3 using bicubic splines

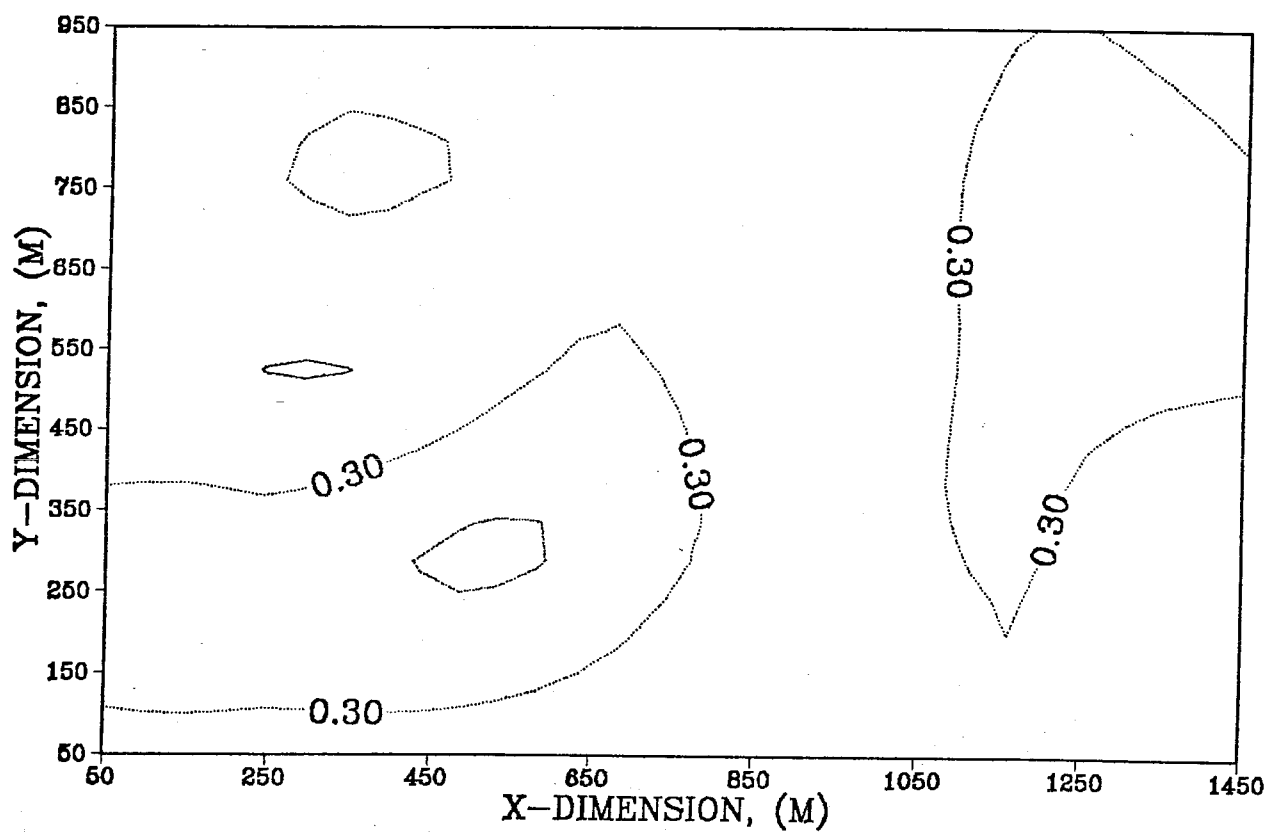


Fig. 6.6 (b) - Estimated permeability distribution of layer 2
for 2-phases after Step 3 using bicubic splines

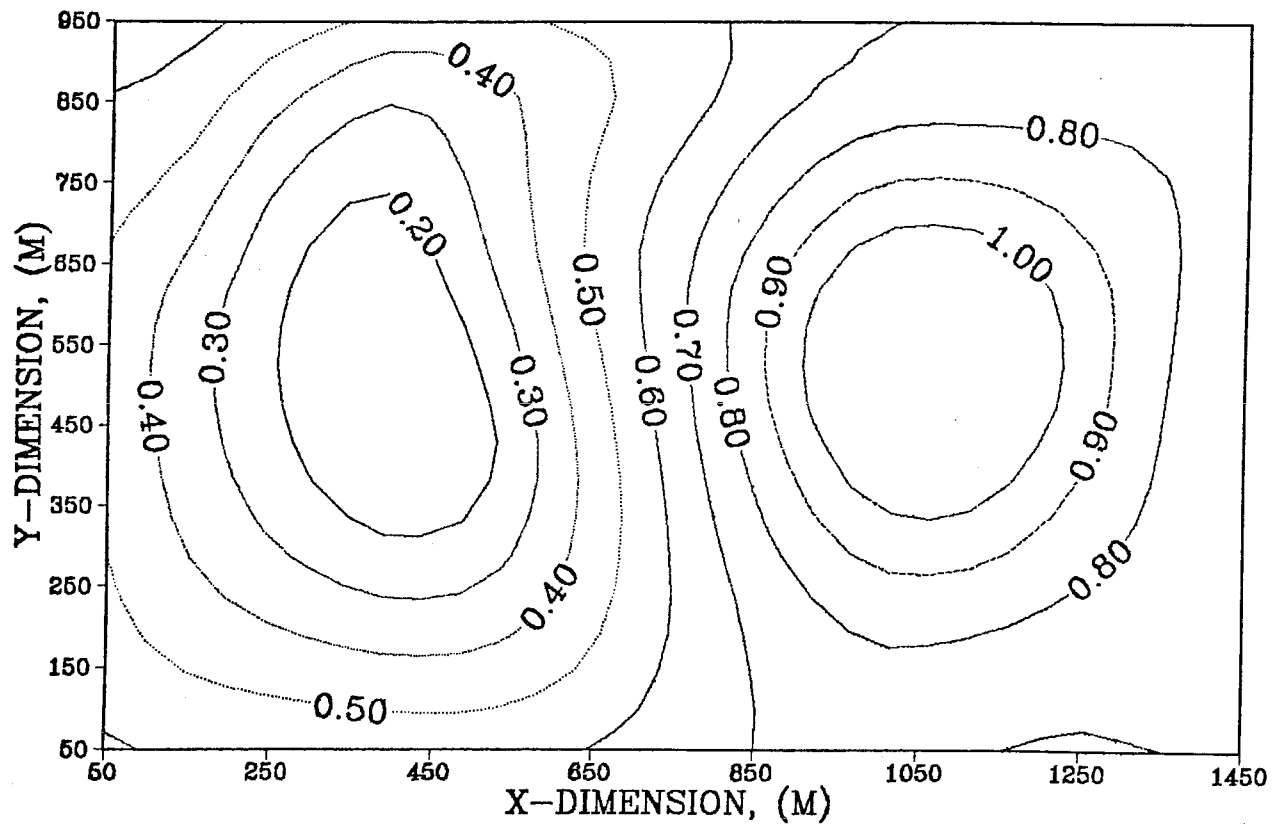


Fig. 6.6 (c) - Estimated permeability distribution of layer 3
for 2-phases after Step 3 using bicubic splines

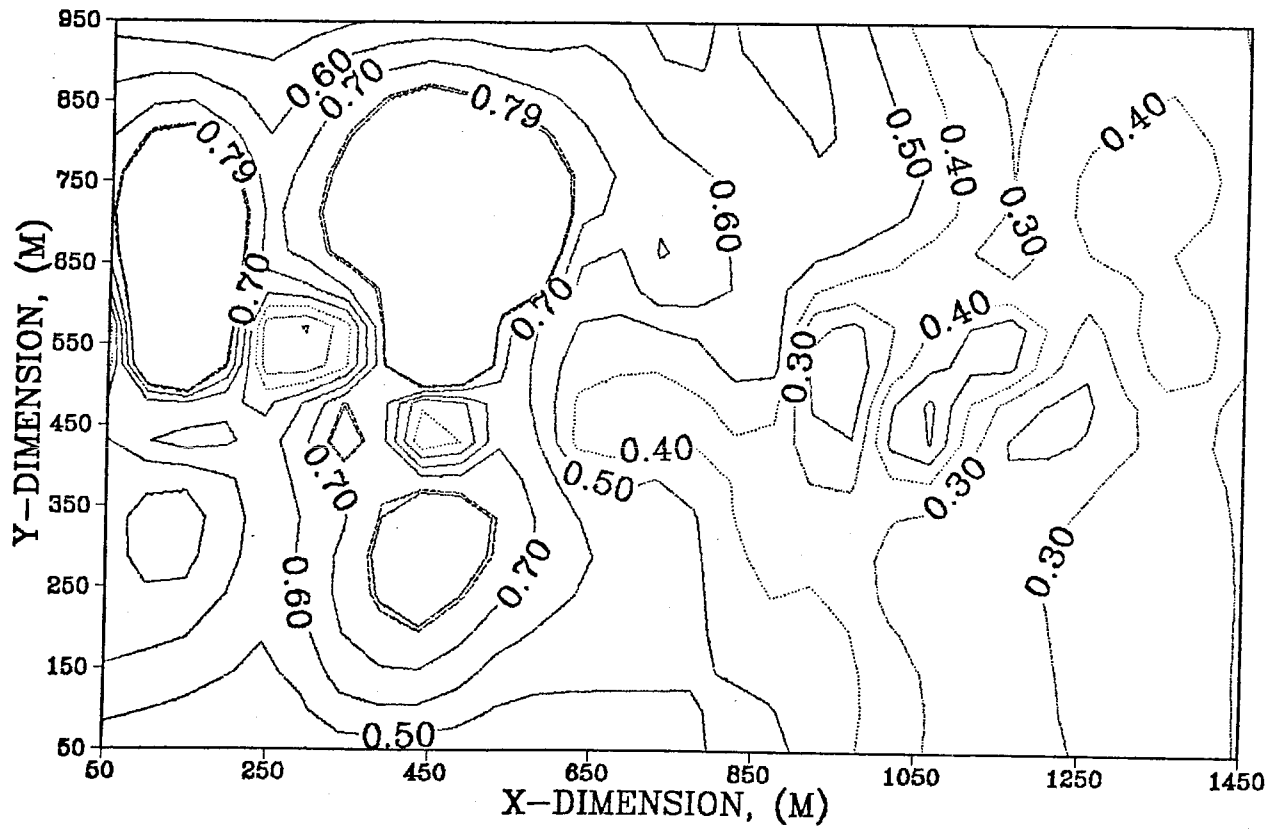


Fig. 6.7 (a) - Estimated permeability distribution of layer 1
for 2-phases after Step 3 using zonation

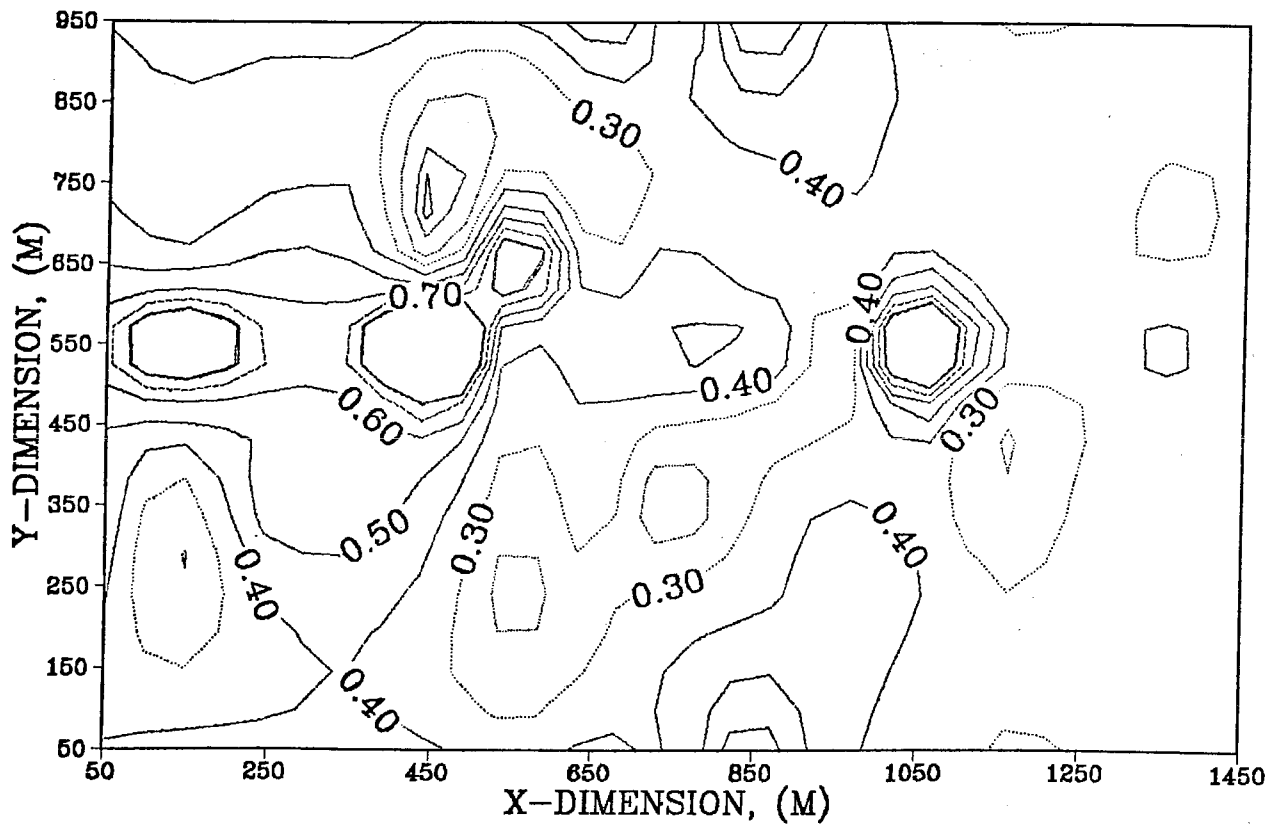


Fig. 6.7 (b) - Estimated permeability distribution of layer 2
for 2-phases after Step 3 using zonation

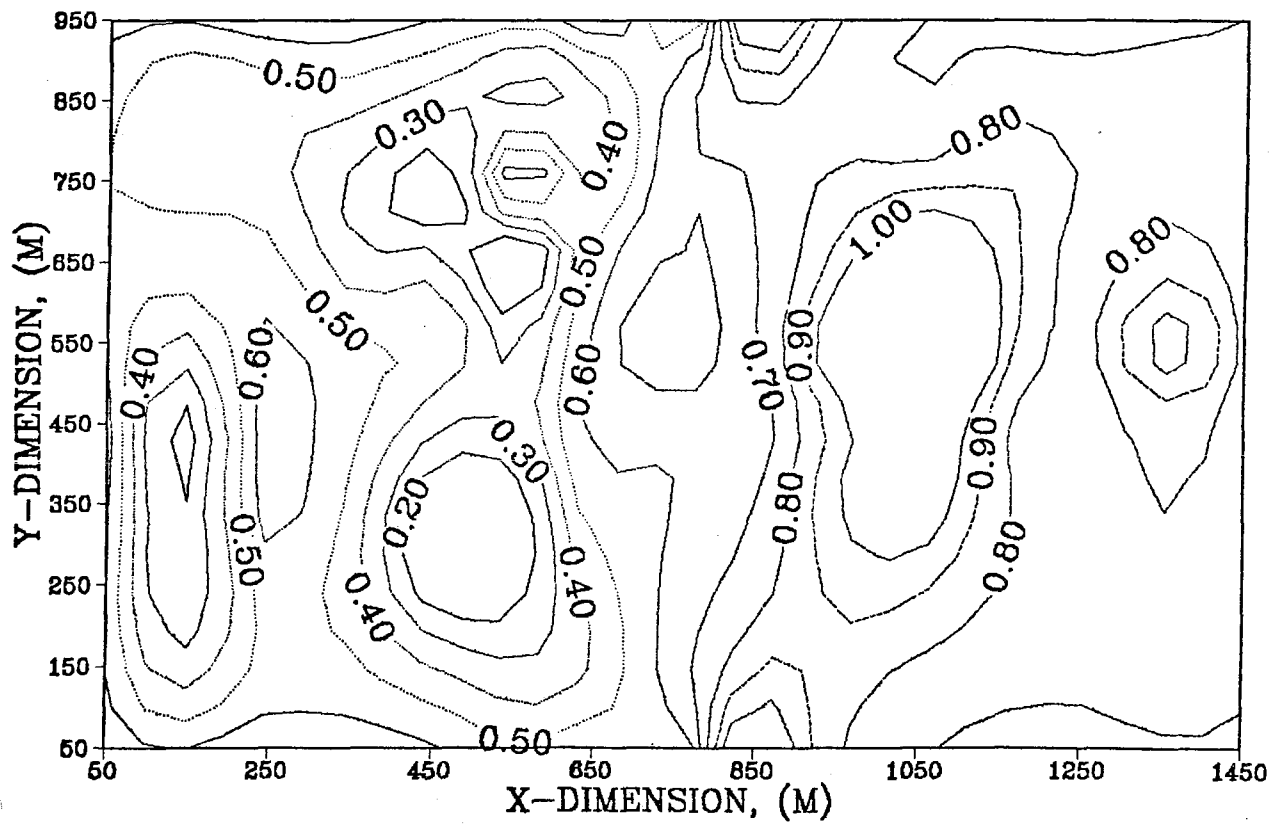


Fig. 6.7 (c) - Estimated permeability distribution of layer 3
for 2-phases after Step 3 using zonation

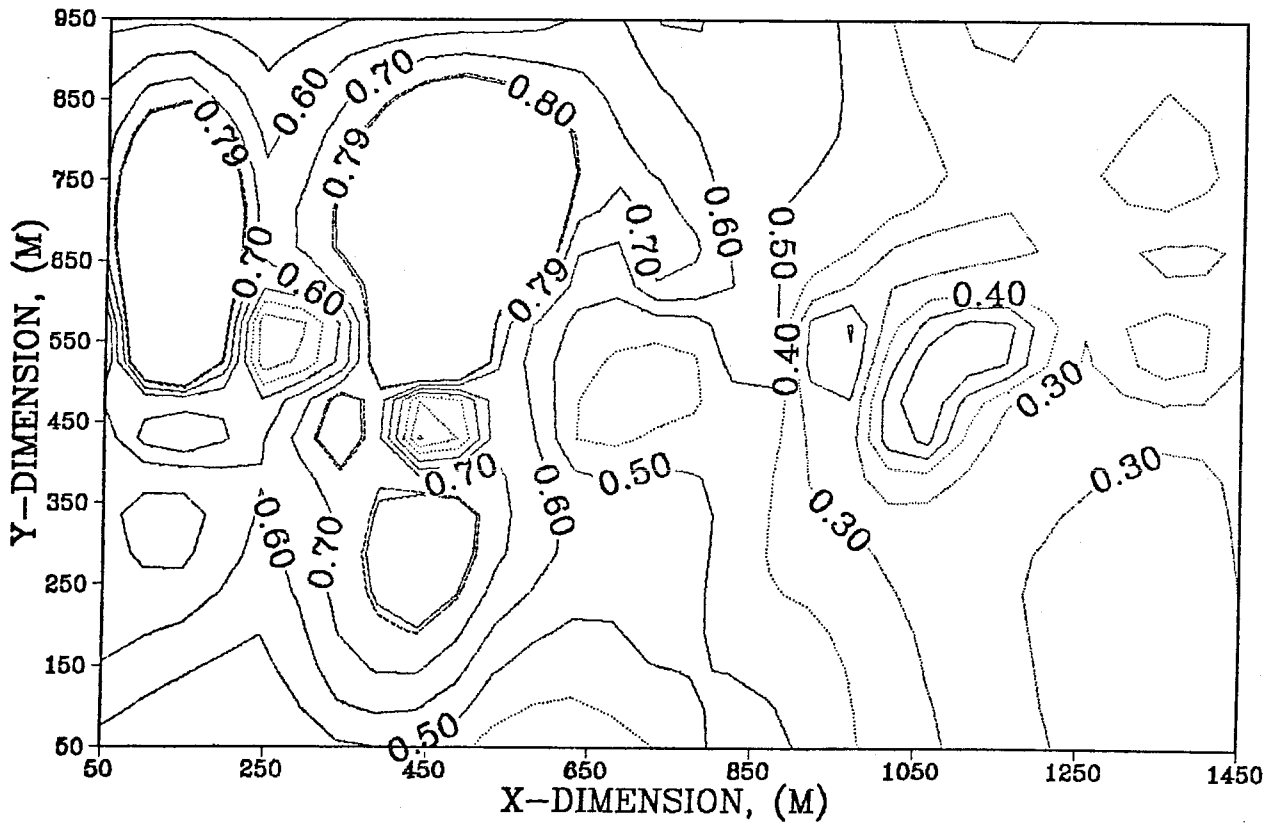


Fig. 6.8 (a) - Estimated permeability distribution of layer 1
for 2-phases after Step 2 using zonation

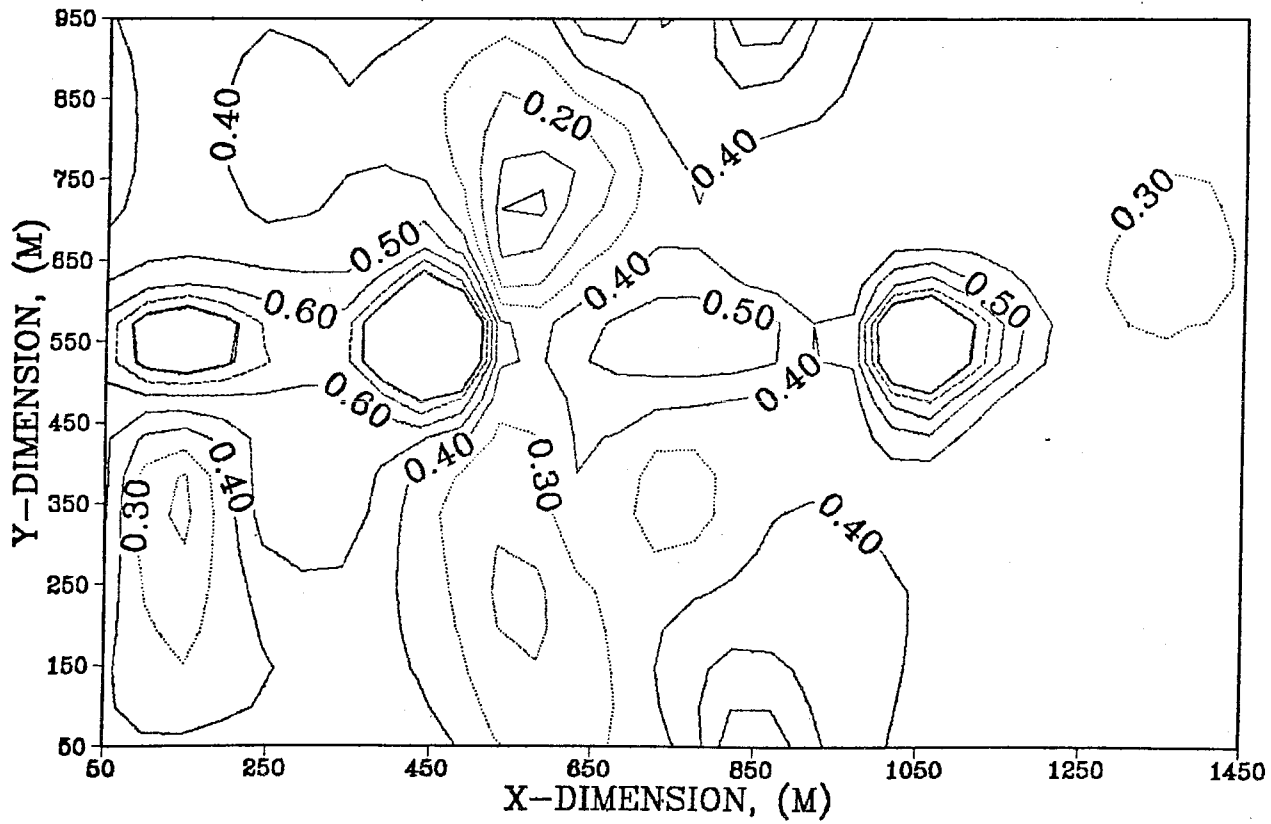


Fig. 6.8 (b) - Estimated permeability distribution of layer 2
for 2-phases after Step 2 using zonation

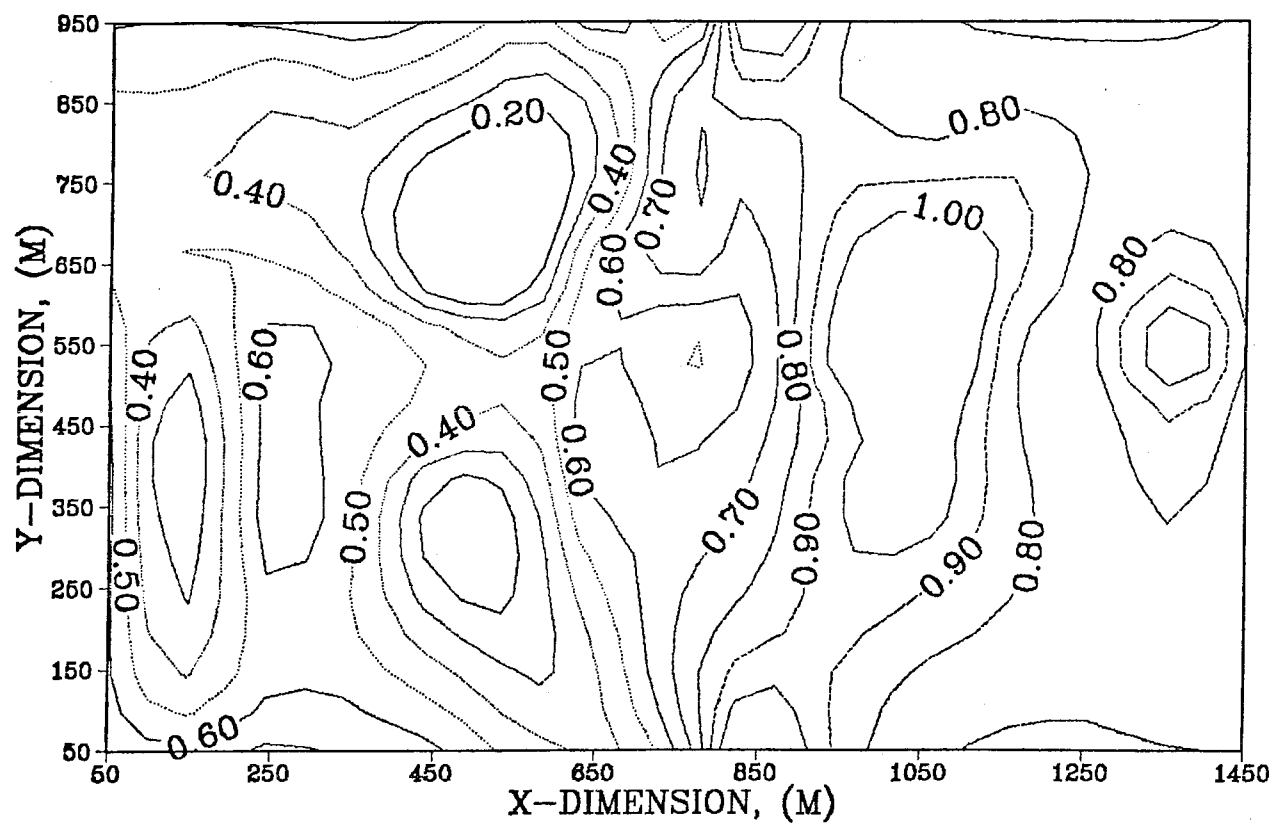


Fig. 6.8 (c) - Estimated permeability distribution of layer 3
for 2-phases after Step 2 using zonation

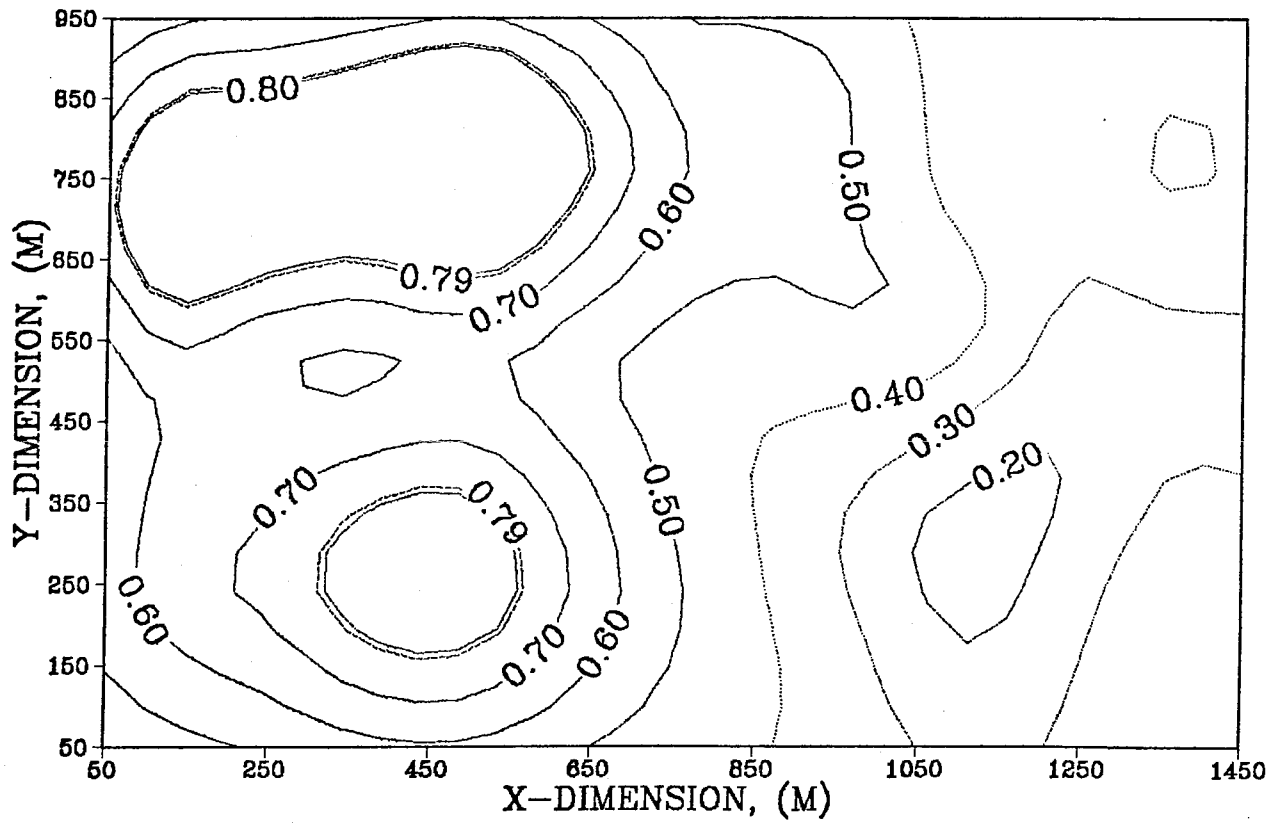


Fig. 6.9 (a) - Estimated permeability distribution of layer 1
for 2-phases after Step 2 using bicubic splines

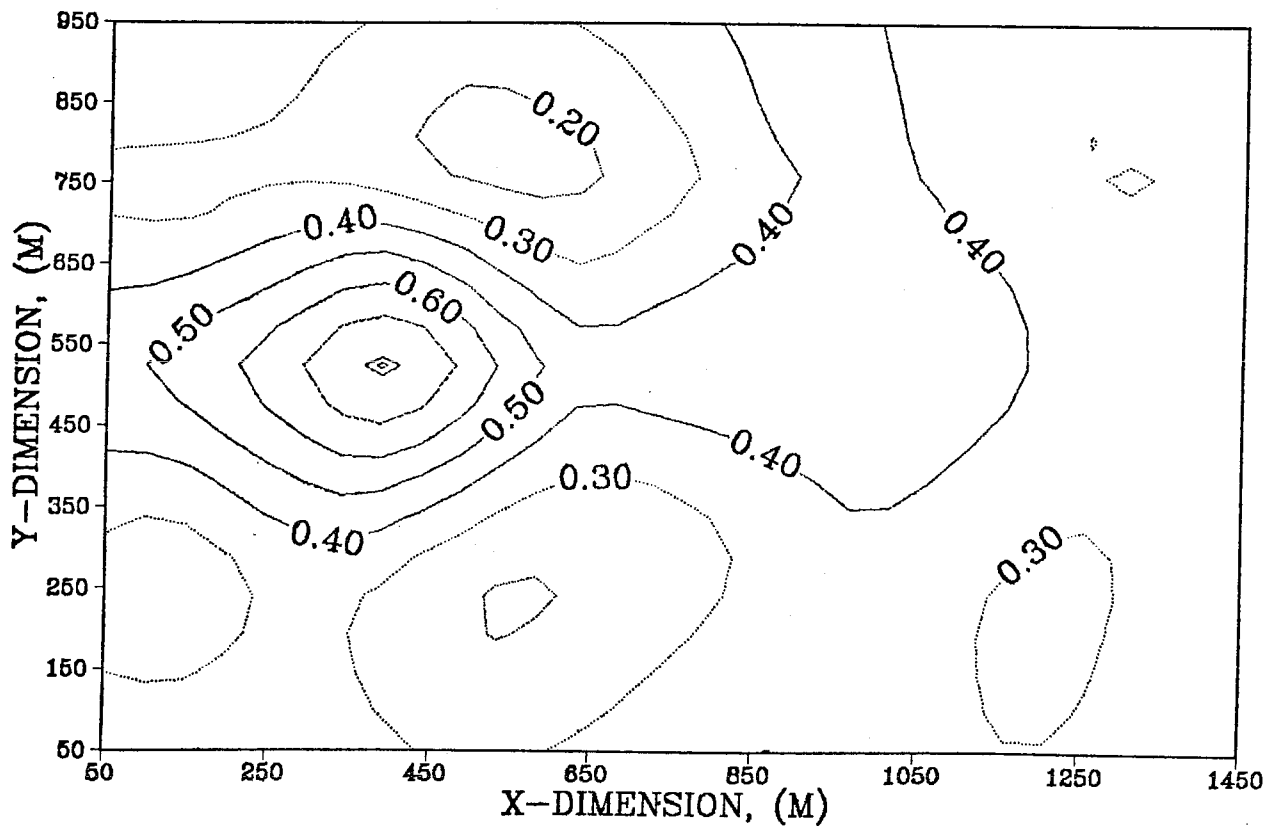


Fig. 6.9 (b) - Estimated permeability distribution of layer 2
for 2-phases after Step 2 using bicubic splines

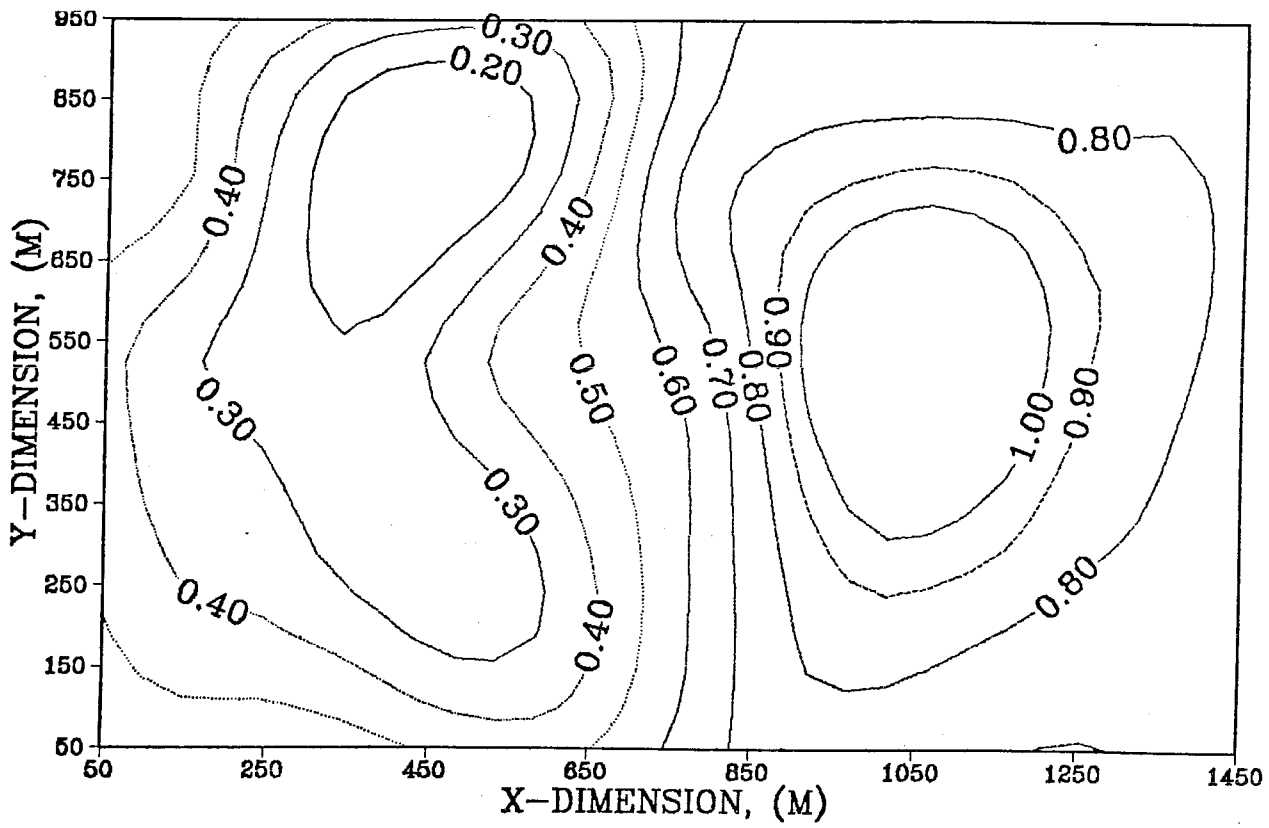


Fig. 6.9 (c) - Estimated permeability distribution of layer 3
for 2-phases after Step 2 using bicubic splines

6.3.2 Three-Phase Reservoirs

In the three-phase reservoir, the objective function includes the gas-oil ratio and the rate of gas production from individual layers as well as the other measured well data used in the two-phase case. In the three-phase case two situations with different physical behavior are considered. In Example 1, $S_g = 0.05$ initially everywhere in the reservoir. The existence of free gas in the system throughout the time period of the simulation ensures that the same simulator model is always used. In addition, the reservoir pressure is always at or below the bubble point causing the density of the oil-phase to always increase with decreasing reservoir pressure.

In Example 2, no free gas exists in the reservoir initially, but arises in the system from a reduction in the reservoir pressure to a pressure below the bubble point of the oil-phase. Before the appearance of free gas in a grid cell, that is, when the reservoir pressure in that grid cell is above the bubble point, the simulator solves the gas-phase material balance for R_s , the fraction of gas dissolved in the oil-phase. When the reservoir pressure in a particular grid cell falls below the bubble point and free gas is released from solution, R_s is calculated as a function of the saturation pressure and the simulator solves the gas-phase material balance for S_g , the saturation of the gas-phase. In addition to a change in the simulator equations due to the existence of free gas in the reservoir, the oil-phase physical properties, particularly the density, change behavior as a result of the reservoir pressure being above or below the bubble point. When the reservoir pressure is above the bubble point, a decrease in pressure causes a reduction in the oil-phase density. When the pressure is below the bubble point, a decrease in pressure causes more gas to be released from solution in the oil-phase and a corresponding increase in the density of the oil-phase.

The complex physical behavior in reservoirs exhibiting a transition between two- and three-phase behavior and the resulting change in the reservoir model used causes particular problems in the history match of the observation data. This can be understood by considering what occurs during the estimation procedure. First an initial guess is chosen. Not only does the production data generated by this guess of the true distribution not match the observation data calculated with the true permeabilities, but the production data were calculated using a different simulator model since with any estimate of the permeabilities the time and location at which gas is released from solution may vary from that with the true permeabilities. Since the existence of free gas in the system determines both which gas-phase material balance equation is used as well as the oil physical properties, a different physical model and hence possibly dramatically different physical behavior is observed in a reservoir with an estimated distribution other than that of the true permeability distribution. As a result of this complex behavior, convergence of the estimation problem is impeded.

A comparison of the history match of the measured data calculated with the estimated permeability distributions for three-phase Examples 1 and 2 to the observed data generated by the true permeability distribution is shown in Figs. 6.10.1, 6.10.2, 6.11.1, 6.11.2, 6.12.1 and 6.12.2 (a), (b) and (c), 6.13.1 and 6.13.2 (a), (b) and (c), 6.14.1 and 6.14.2. In Figs. 6.10.1 and 6.10.2, a comparison of the history match of the observed pressure data for Examples 1 and 2, shows that the pressures are matched more accurately in Example 1 where free gas exists in the system initially. Similarly, a comparison of the match of the water cut data for the two cases (see Figs. 6.11.1 and 6.11.2) shows that the water cut is also matched more accurately in Example 1. The flow rates of liquid and gas from individual completions are all matched more accurately in Example 1 than in Example 2. (see

Figs. 6.12.1 and 6.12.2 (a), (b) and (c) and 6.13.1 and 6.13.2 (a), (b) and (c).) The gas-oil ratio is matched accurately in both examples. The estimated permeability distribution for Example 1, as shown in Figs. 6.15 (a), (b) and (c), matches the true distribution more accurately than that in Example 2, shown in Figs. 6.16 (a), (b) and (c). In summary, the estimation of the permeability distribution in cases where there is a transition between two- and three-phase behavior is considerably more difficult than in cases where only two- or three-phase behavior exists.

In the first example of the three-phase cases, a comparison of Figs. 6.15 (a), (b) and (c) with Figs. 6.17 (a), (b) and (c) shows the smoothing effect of the application of regularization on the estimation of the permeability distribution. In layer 1, although there is improvement in the general shape of the permeability contours after regularization is applied, the 0.70 Darcy contour disappears during the regularization step. In layer 2, in which the true permeability distribution is uniform and has a value of 0.3 Darcy, regularization smoothes the estimate of the true permeability distribution. In layer 3, the effect of regularization on the estimate of the permeability distribution is the most dramatic. Not only does regularization help to smooth the estimated contours, but it also enhances the prediction of the peaks and the valleys. In Example 2, in which there is a transition between two- and three-phase behavior, regularization leads to no improvement in the permeability distribution, presumably because the transition in flow behavior exerts a much more profound influence on the performance of the minimization than does the smoothing provided by regularization.

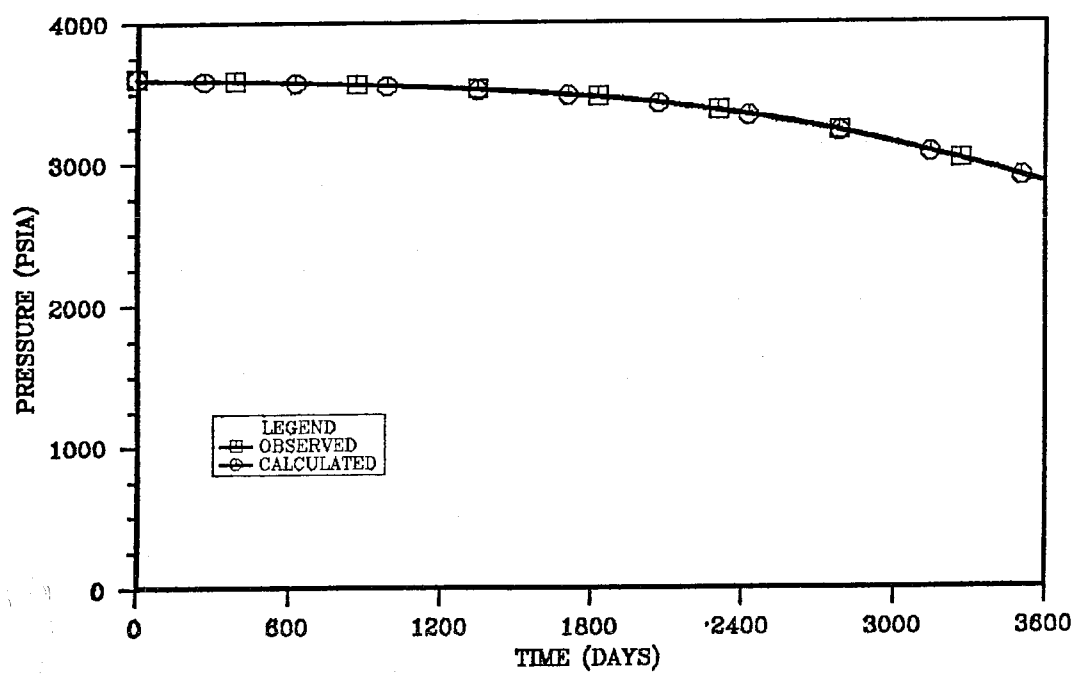


Fig. 6.10.1 - History match of bottomhole pressure from well P3
for 3-phases: Example 1

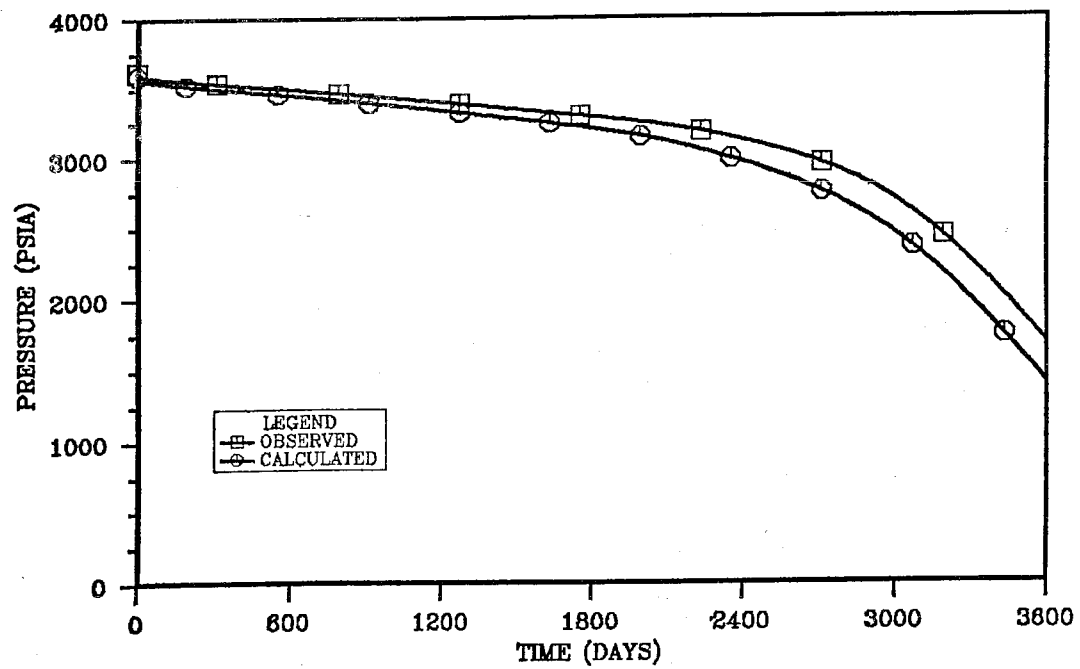


Fig. 6.10.2 - History match of bottomhole pressure from well P3
for 3-phases: Example 2

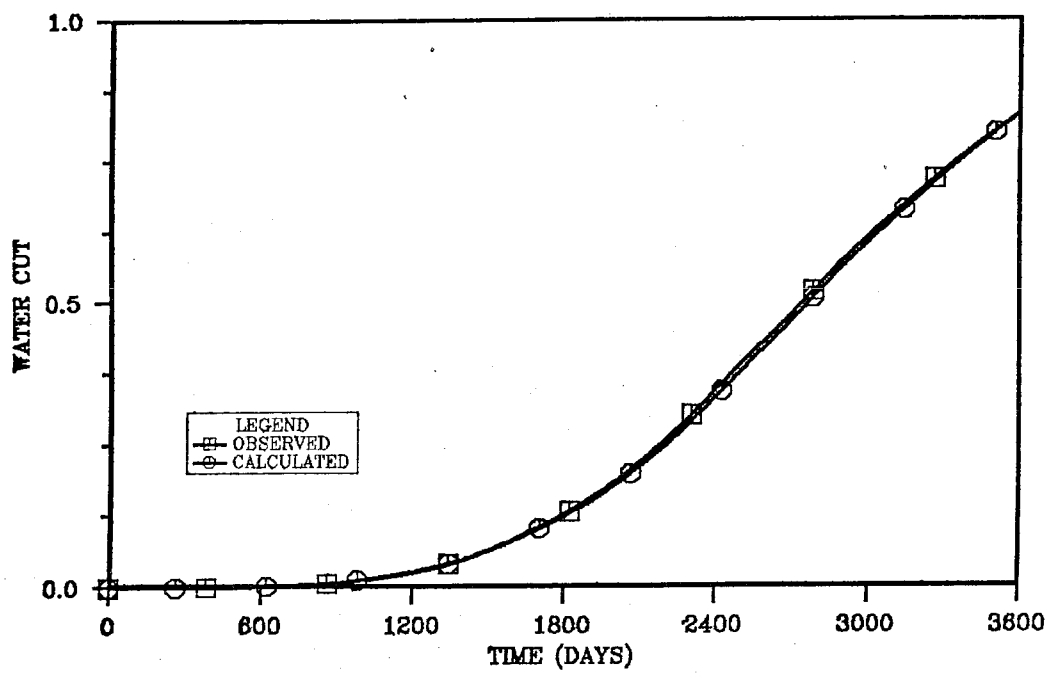


Fig. 6.11.1 - History match of water cut from well P3
for 3-phases: Example 1

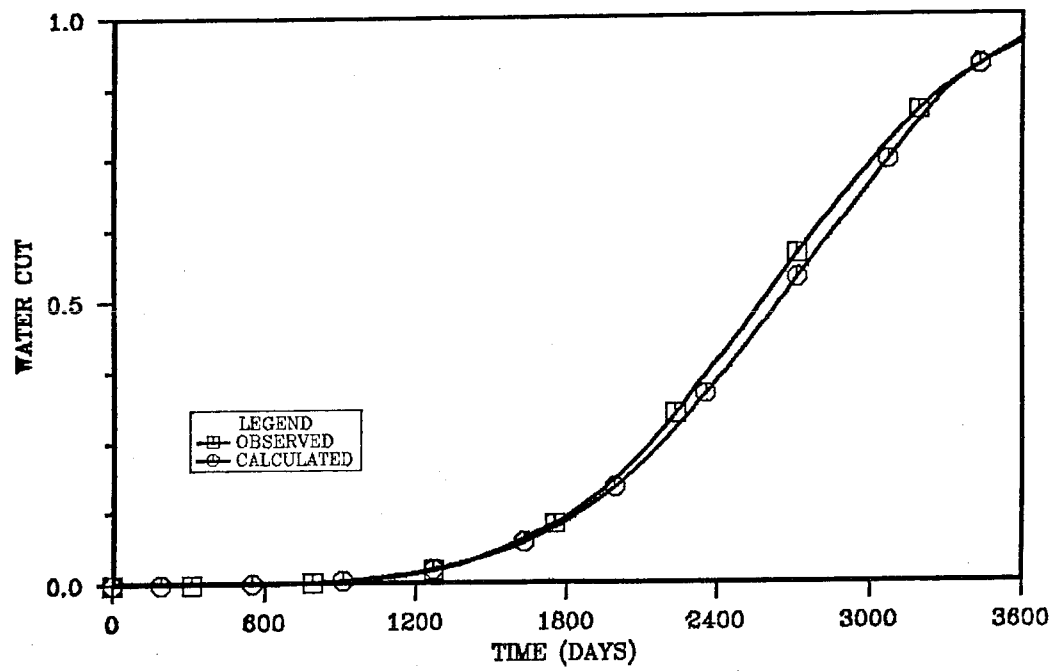


Fig. 6.11.2 - History match of water cut from well P3
for 3-phases: Example 2

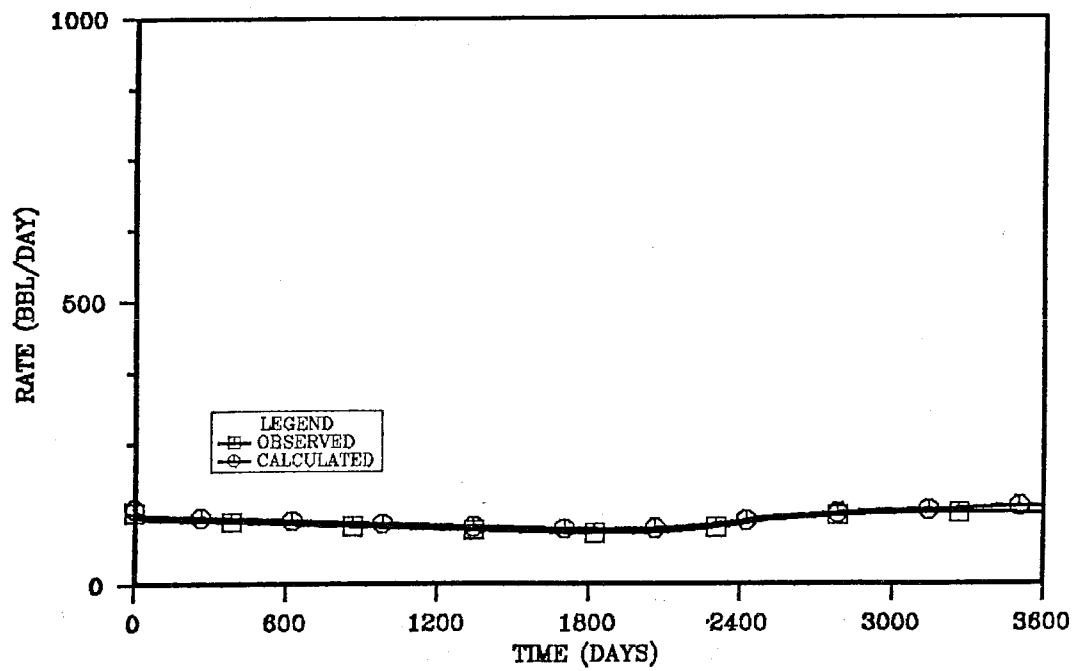


Fig. 6.12.1 (a) - History match of liquid flow rate from well P3
from completion 1 for 3-phases: Example 1

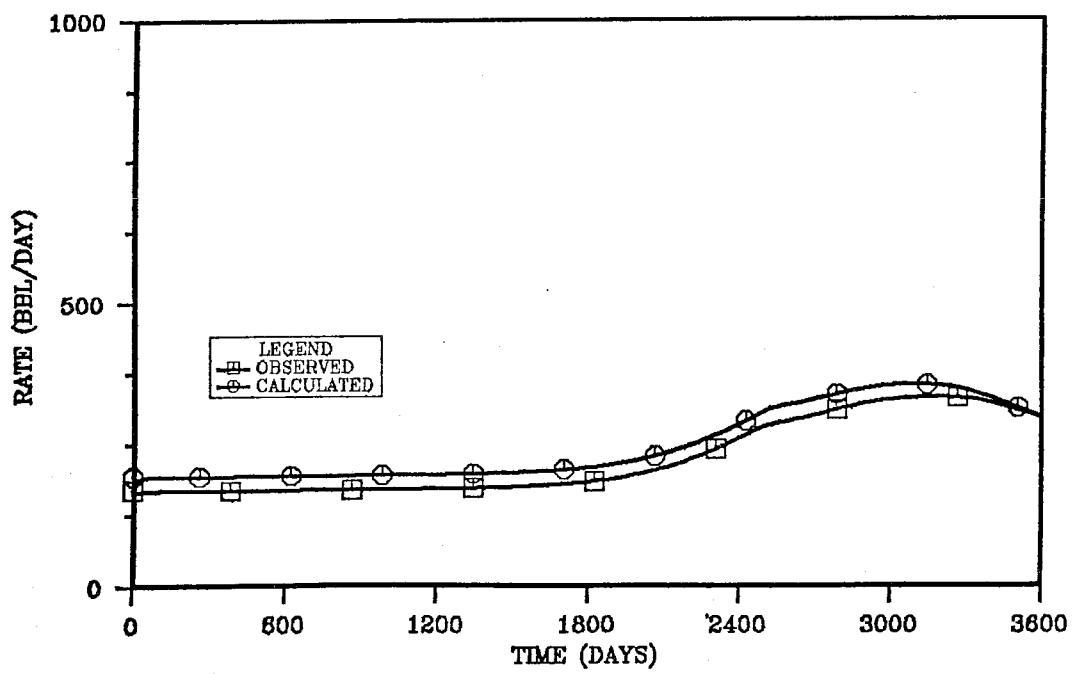


Fig. 6.12.1 (b) - History match of liquid flow rate from well P3
from completion 2 for 3-phases: Example 1

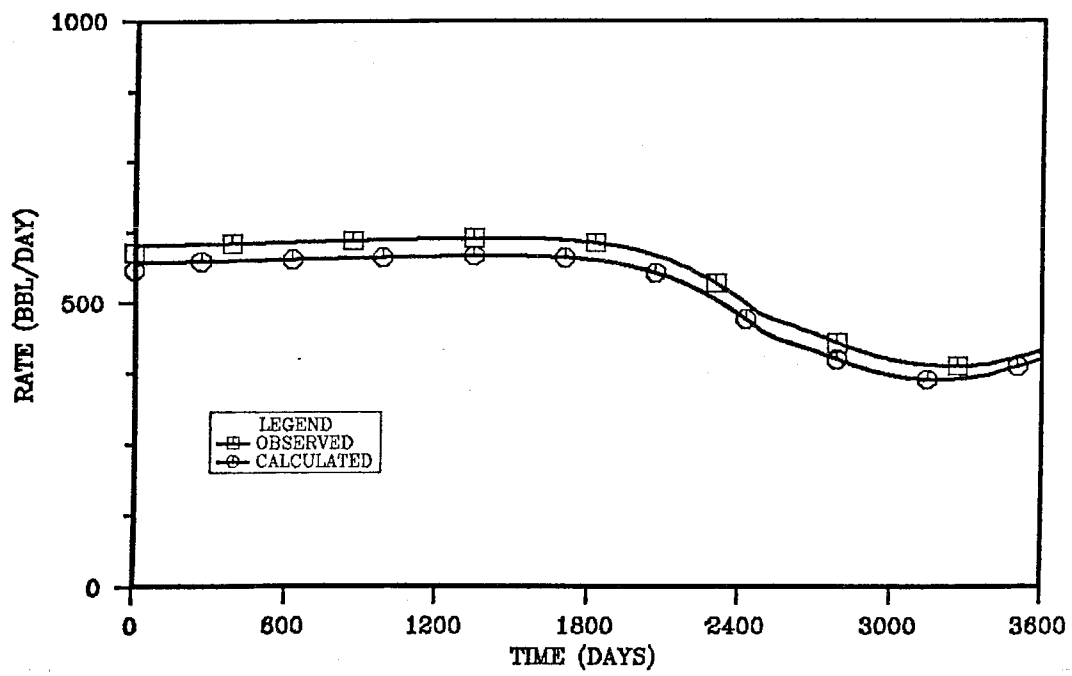


Fig. 6.12.1 (c) - History match of liquid flow rate from well P3
from completion 3 for 3-phases: Example 1

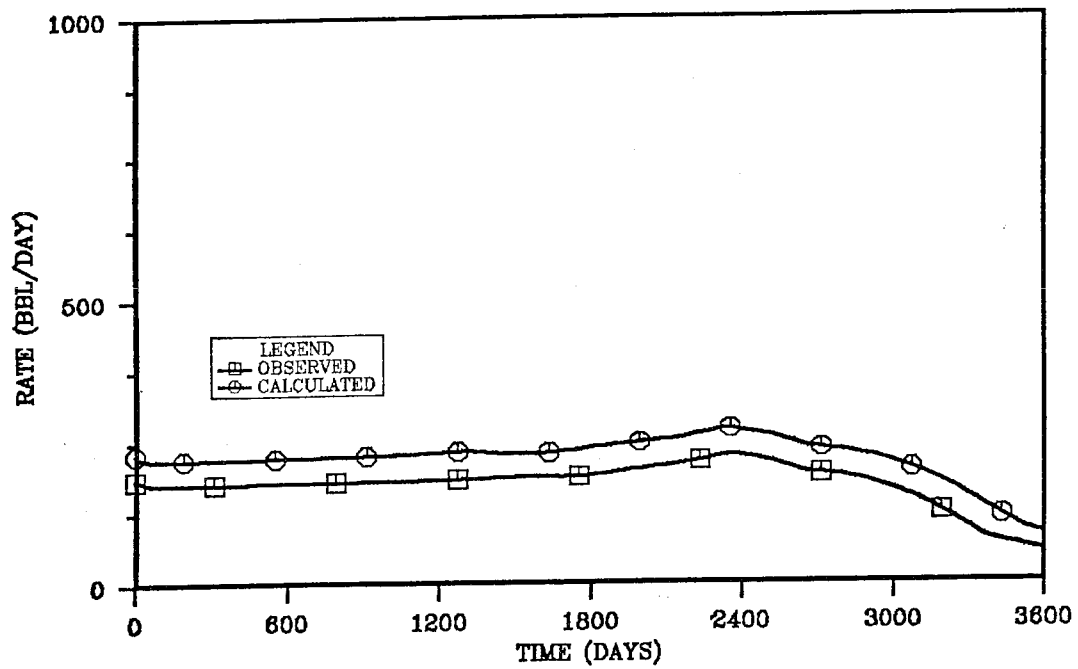


Fig. 6.12.2 (a) - History match of liquid flow rate from well P3
from completion 1 for 3-phases: Example 2

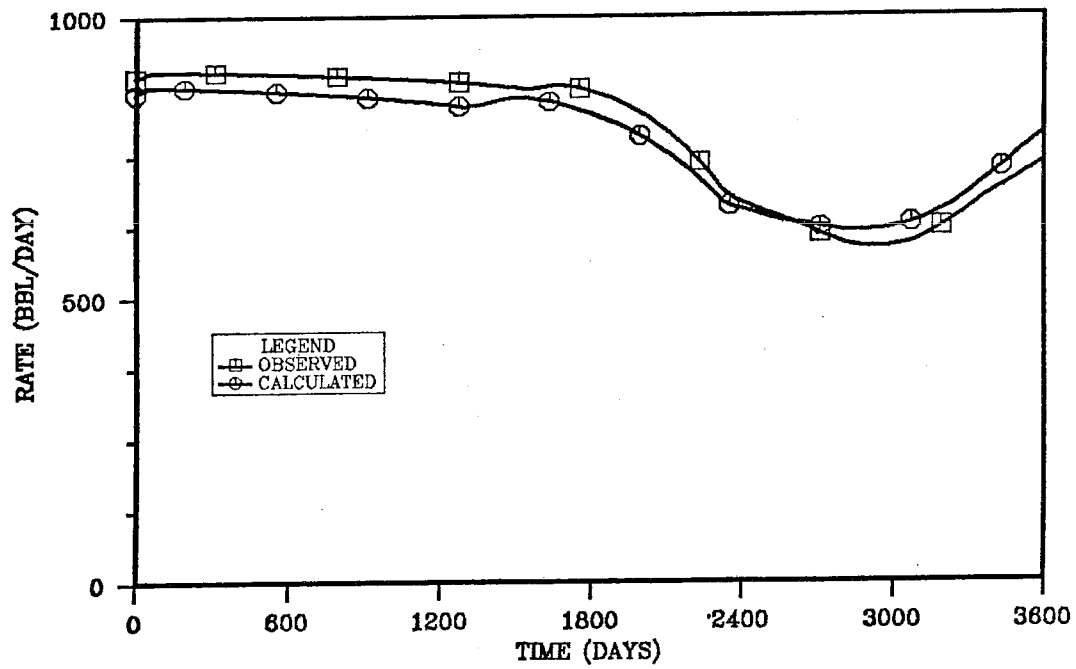


Fig. 6.12.2 (b) - History match of liquid flow rate from well P3
from completion 2 for 3-phases: Example 2

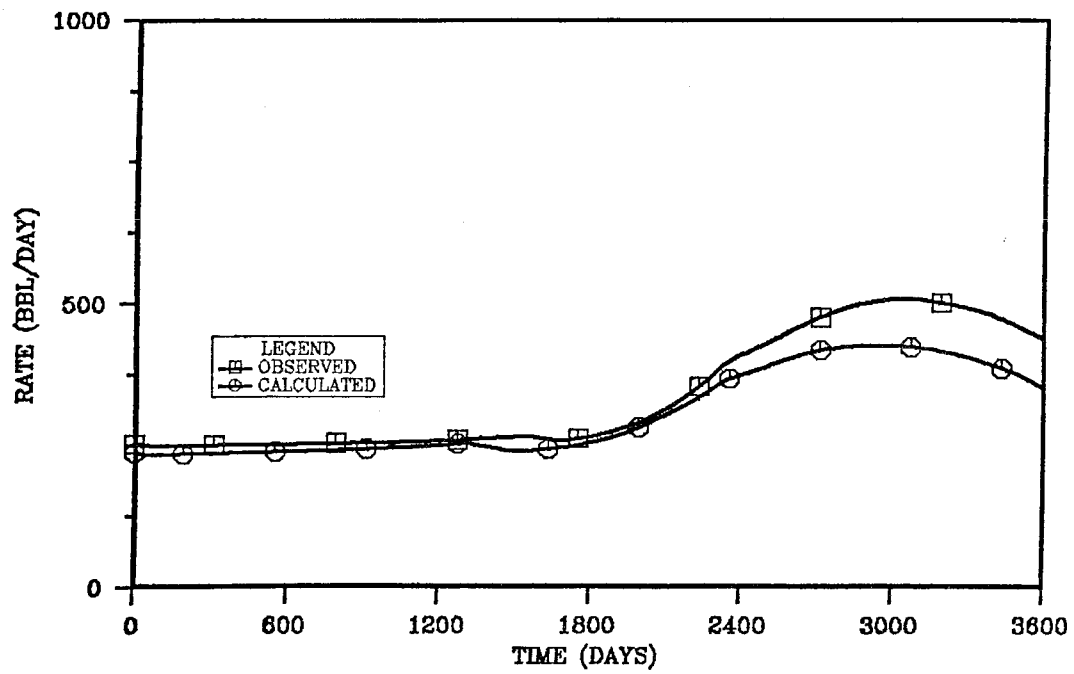


Fig. 6.12.2 (c) - History match of liquid flow rate from well P3
from completion 3 for 3-phases: Example 2

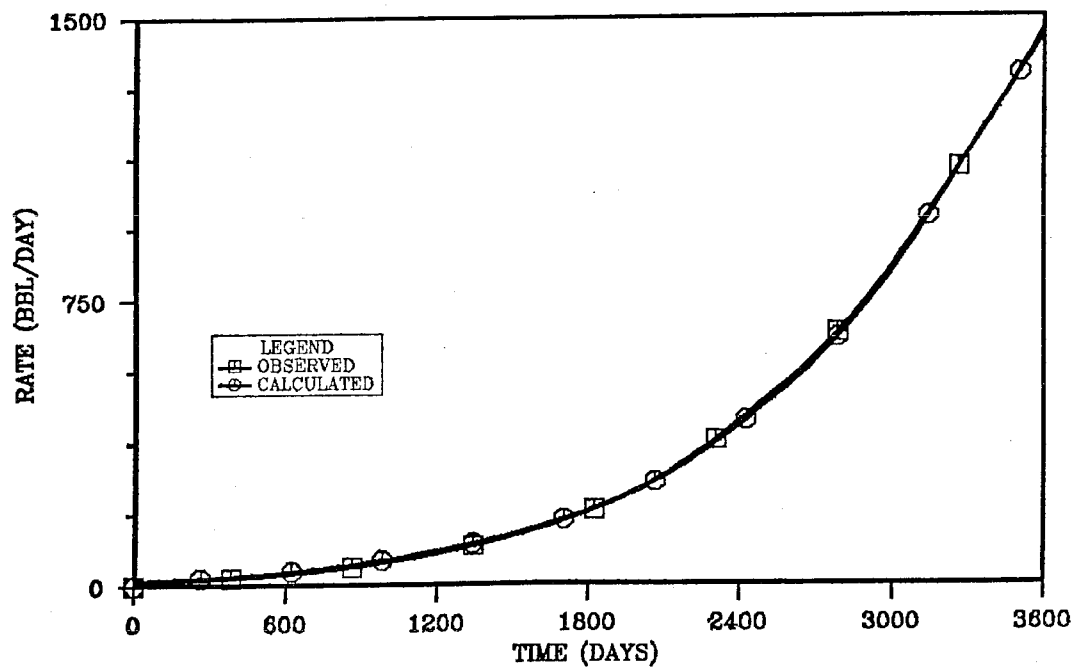


Fig. 6.13.1 (a) - History match of gas flow rate from well P3
from completion 1 for 3-phases: Example 1

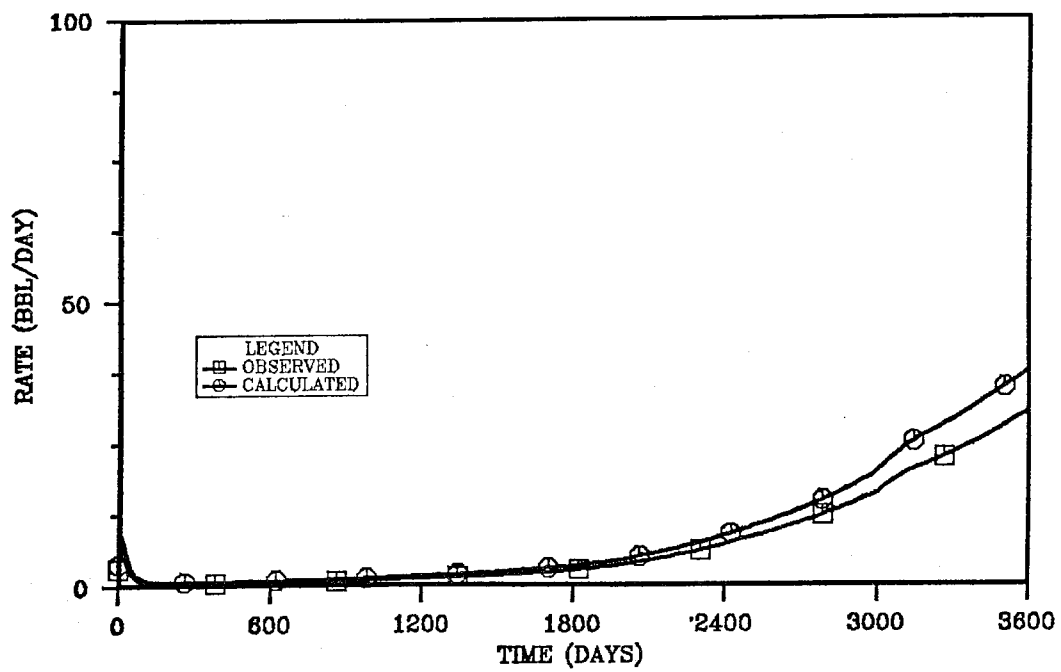


Fig. 6.13.1 (b) - History match of gas flow rate from well P3
from completion 2 for 3-phases: Example 1

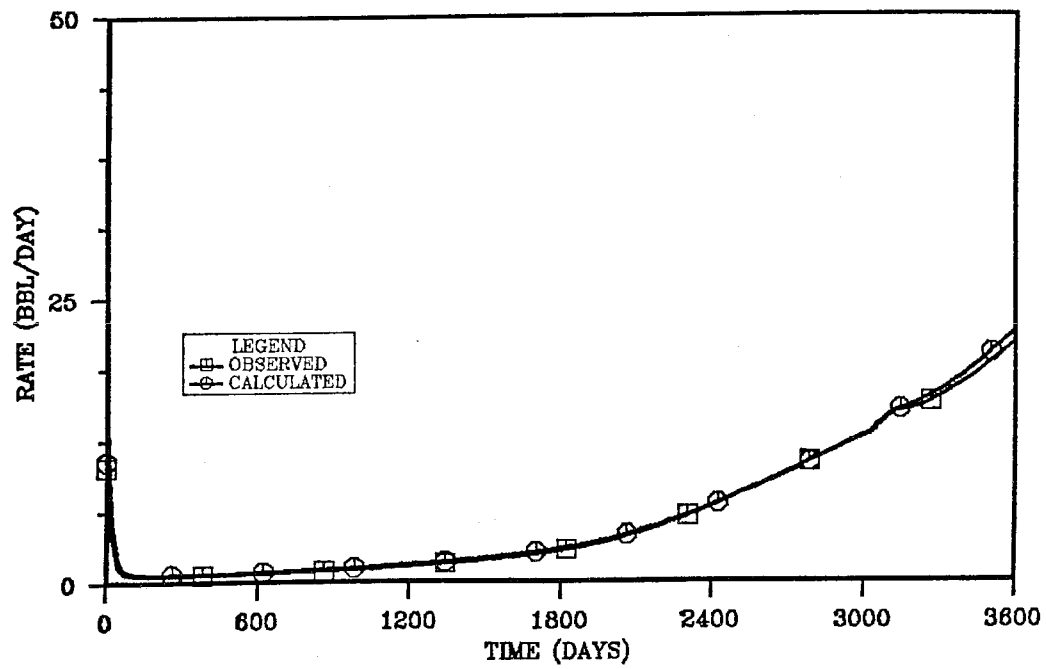


Fig. 6.13.1 (c) - History match of gas flow rate from well P3
from completion 3 for 3-phases: Example 1

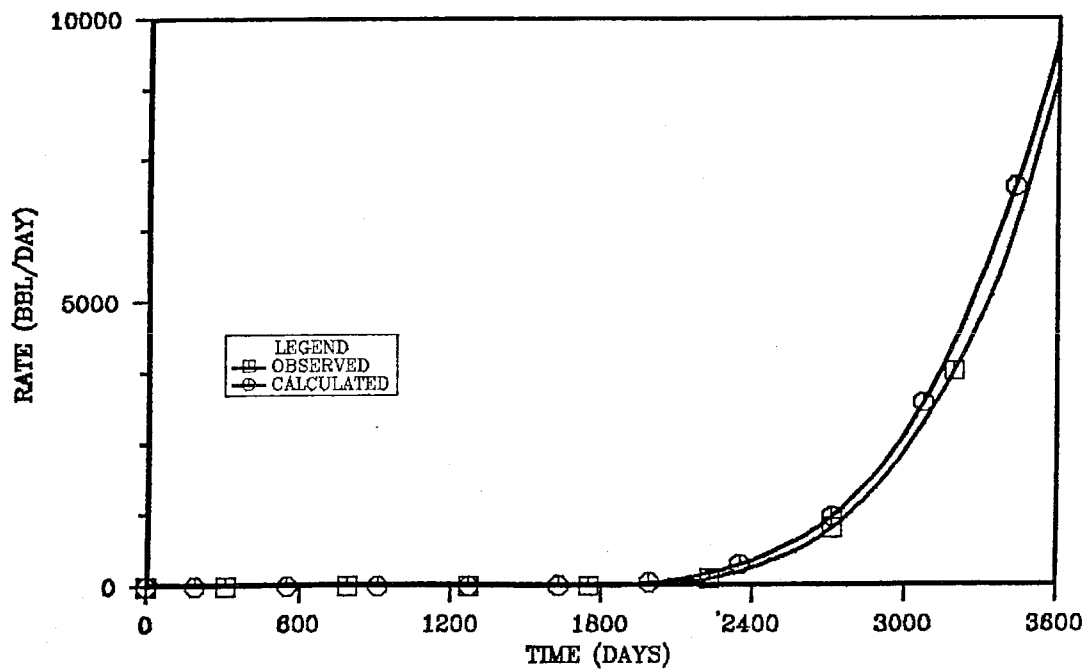


Fig. 6.13.2 (a) - History match of gas flow rate from well P3
from completion 1 for 3-phases: Example 2

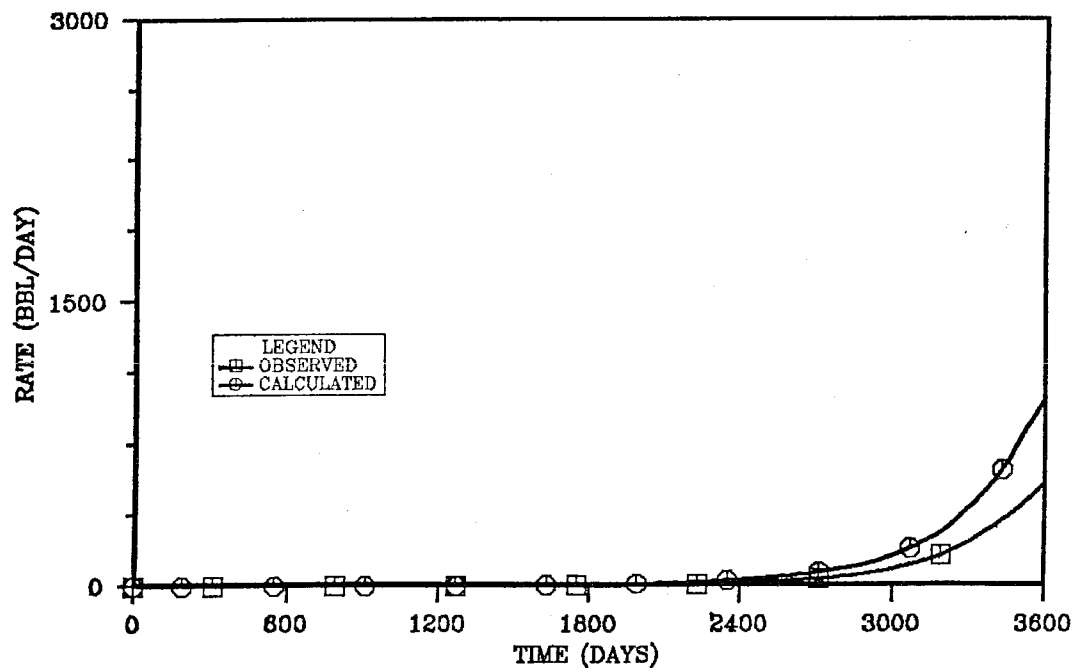


Fig. 6.13.2 (b) - History match of gas flow rate from well P3
from completion 2 for 3-phases: Example 2

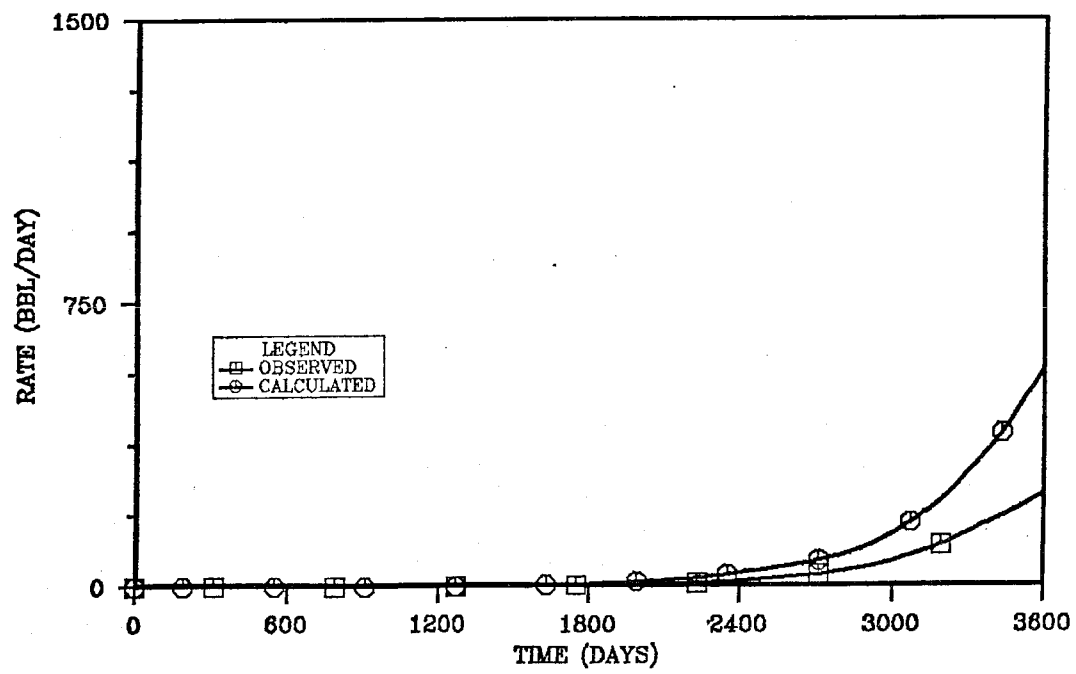


Fig. 6.13.2 (c) - History match of gas flow rate from well P3
from completion 3 for 3-phases: Example 2

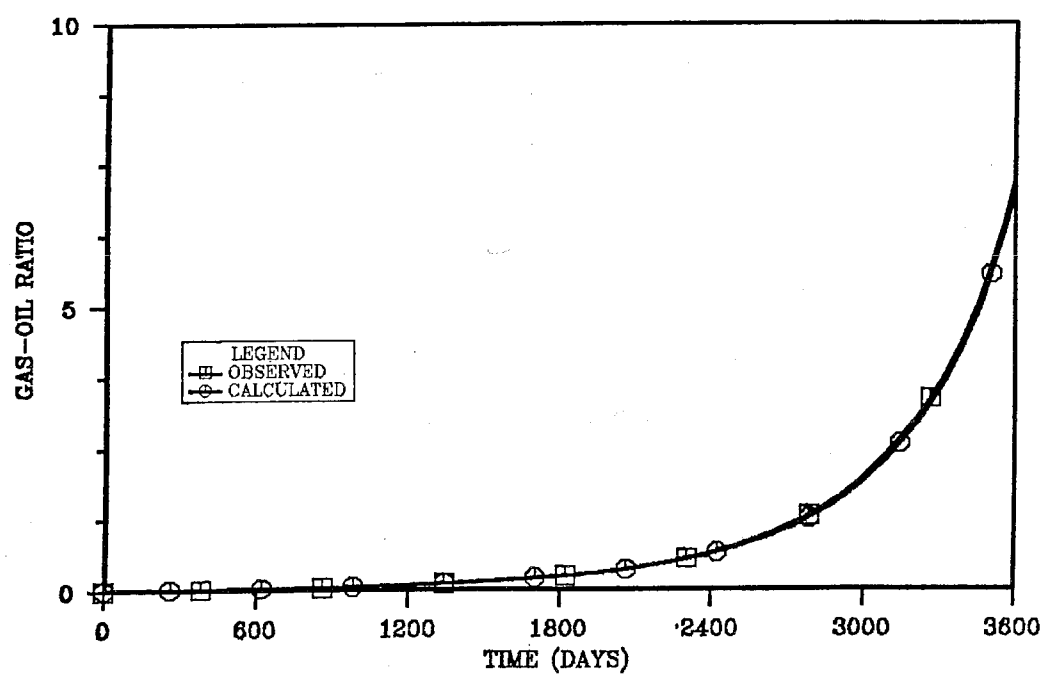


Fig. 6.14.1 - History match of gas-oil ratio from well P3
for 3-phases: Example 1

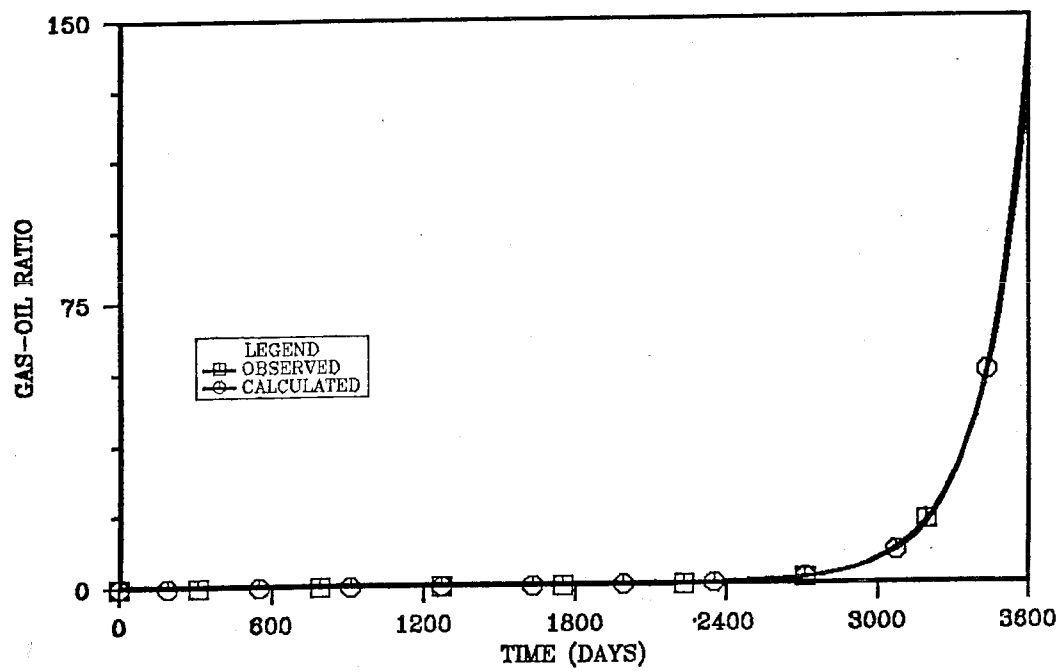


Fig. 6.14.2 - History match of gas-oil ratio from well P3
for 3-phases: Example 2

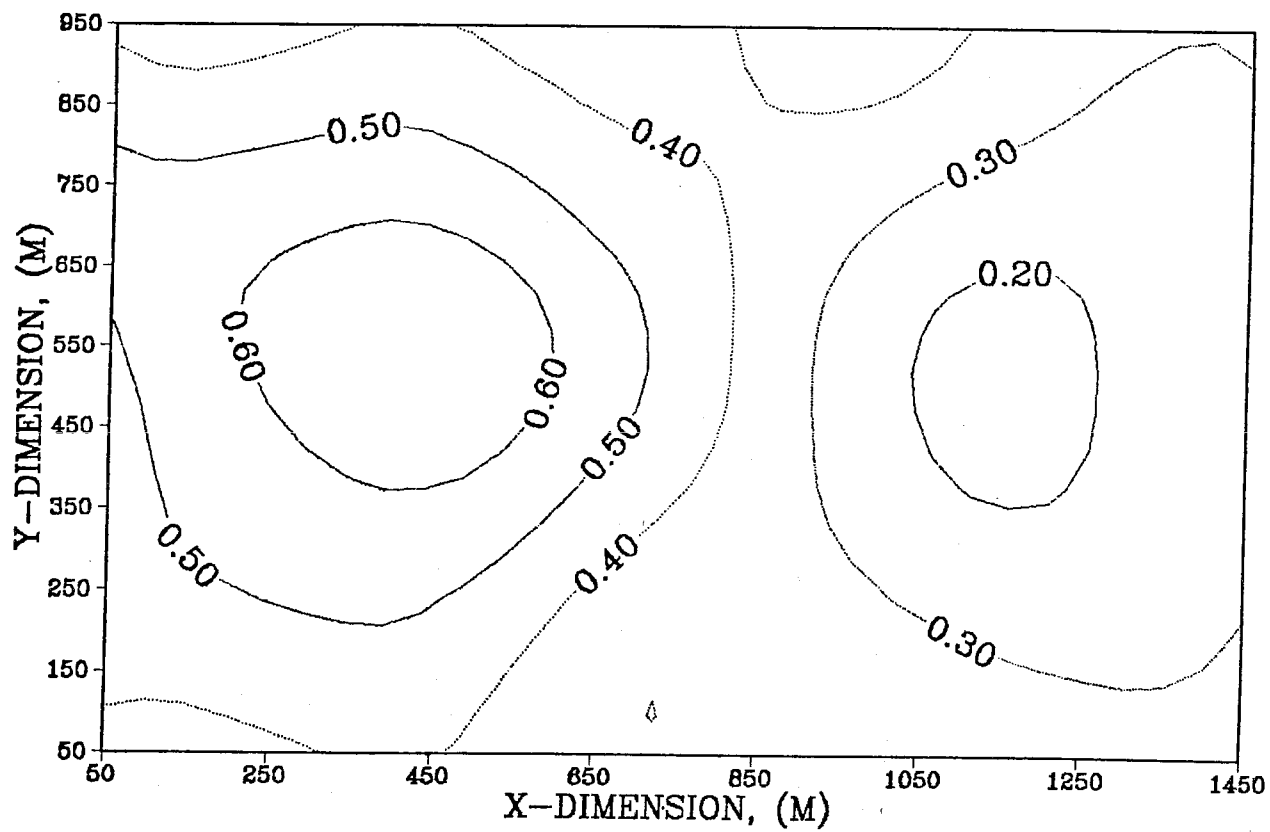


Fig. 6.15 (a) - Estimated permeability distribution of layer 1
for 3-phases after Step 3 using bicubic splines:
Example 2

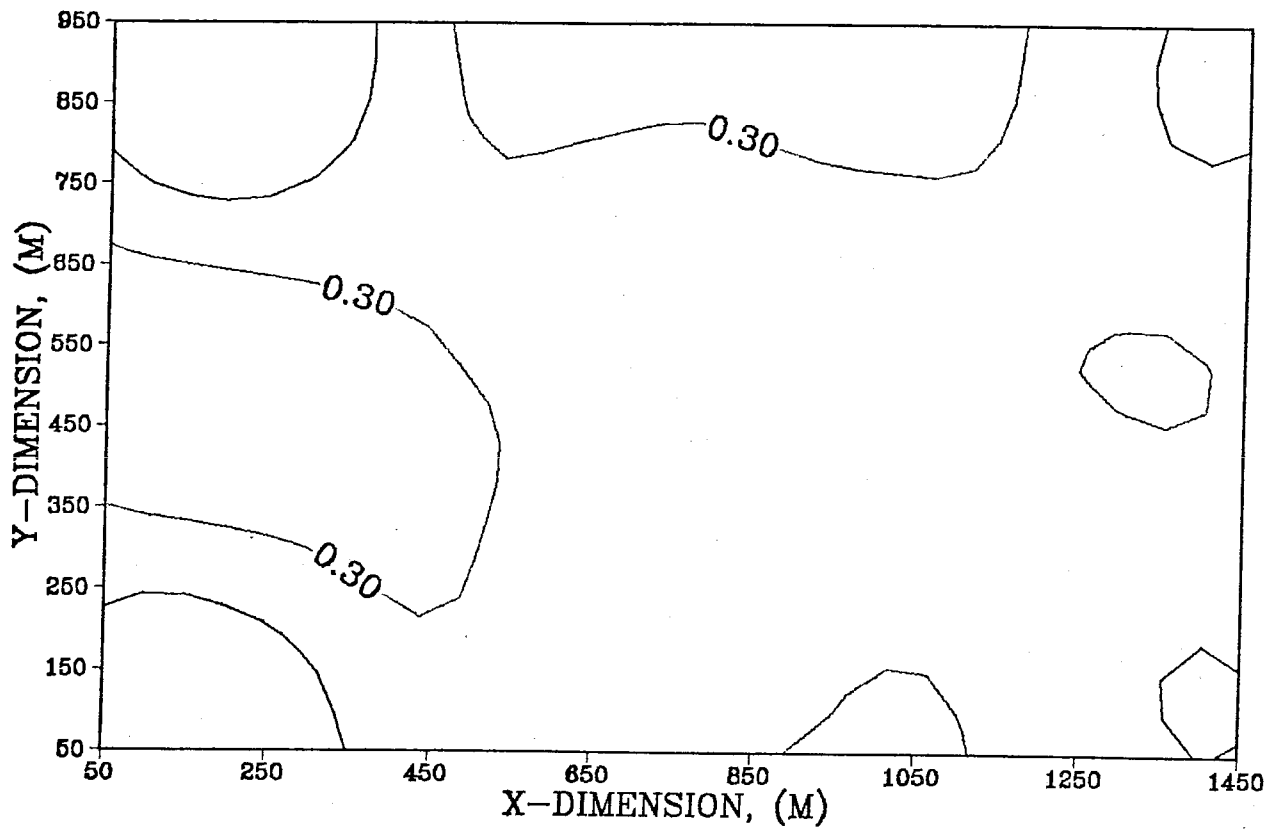


Fig. 6.15 (b) - Estimated permeability distribution of layer 2
for 3-phases after Step 3 using bicubic splines:
Example 2

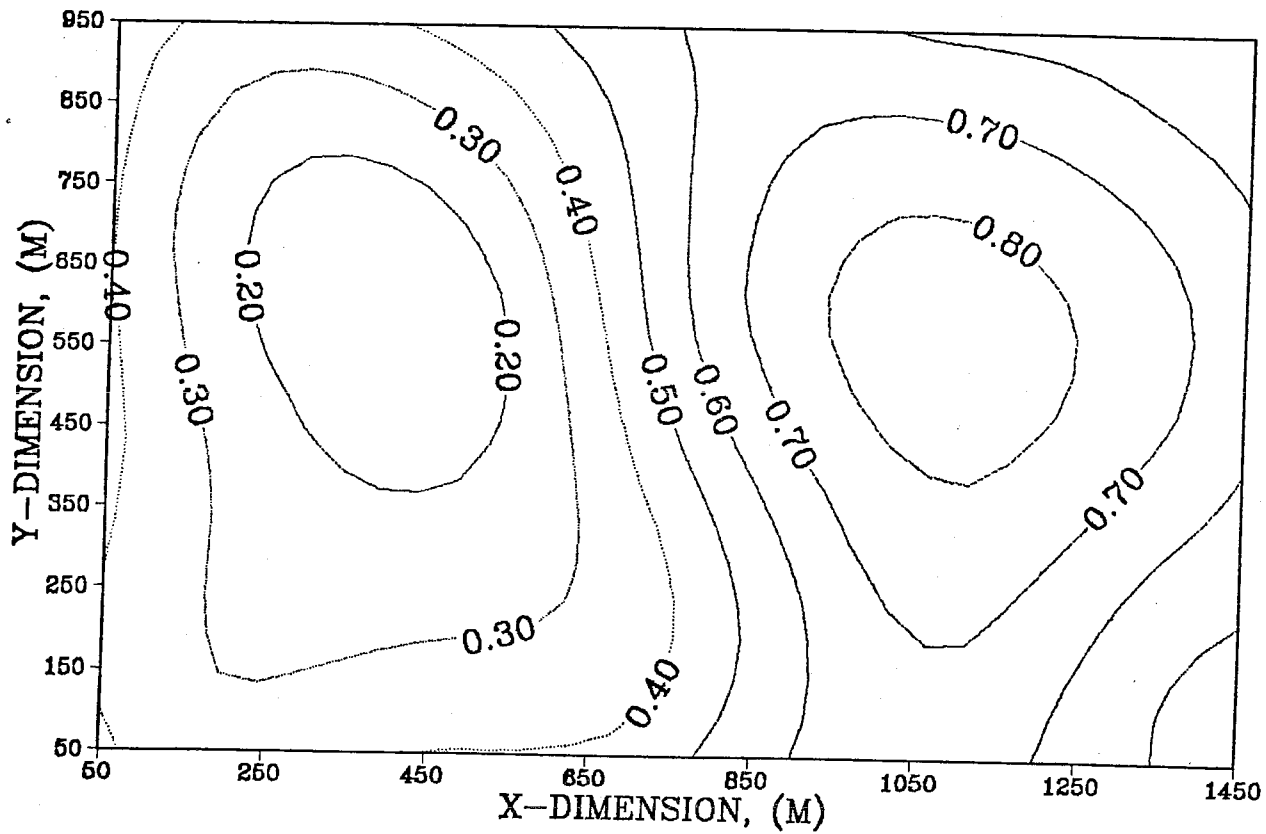


Fig. 6.15 (c) - Estimated permeability distribution of layer 3
for 3-phases after Step 3 using bicubic splines:
Example 2

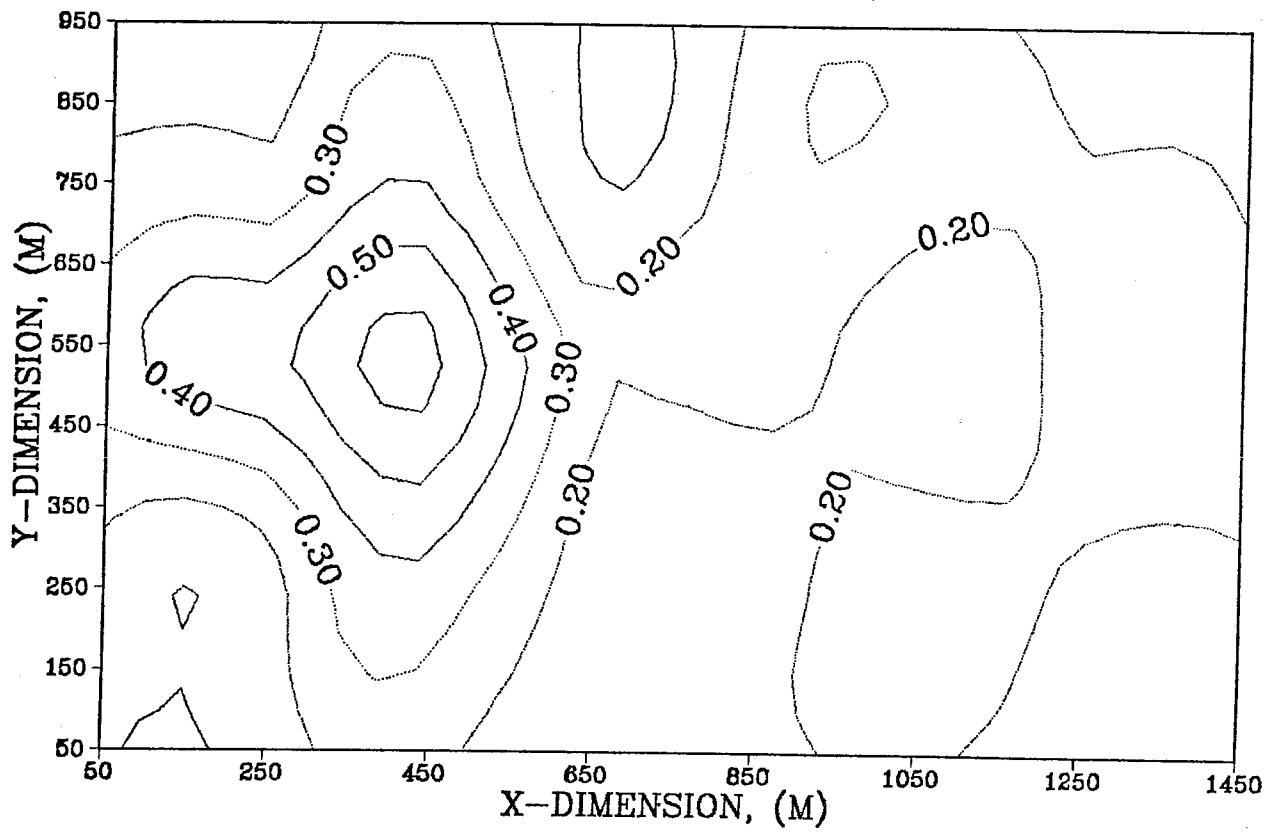


Fig. 6.16 (a) - Estimated permeability distribution of layer 1
for 3-phases after Step 2 using bicubic splines:
Example 1

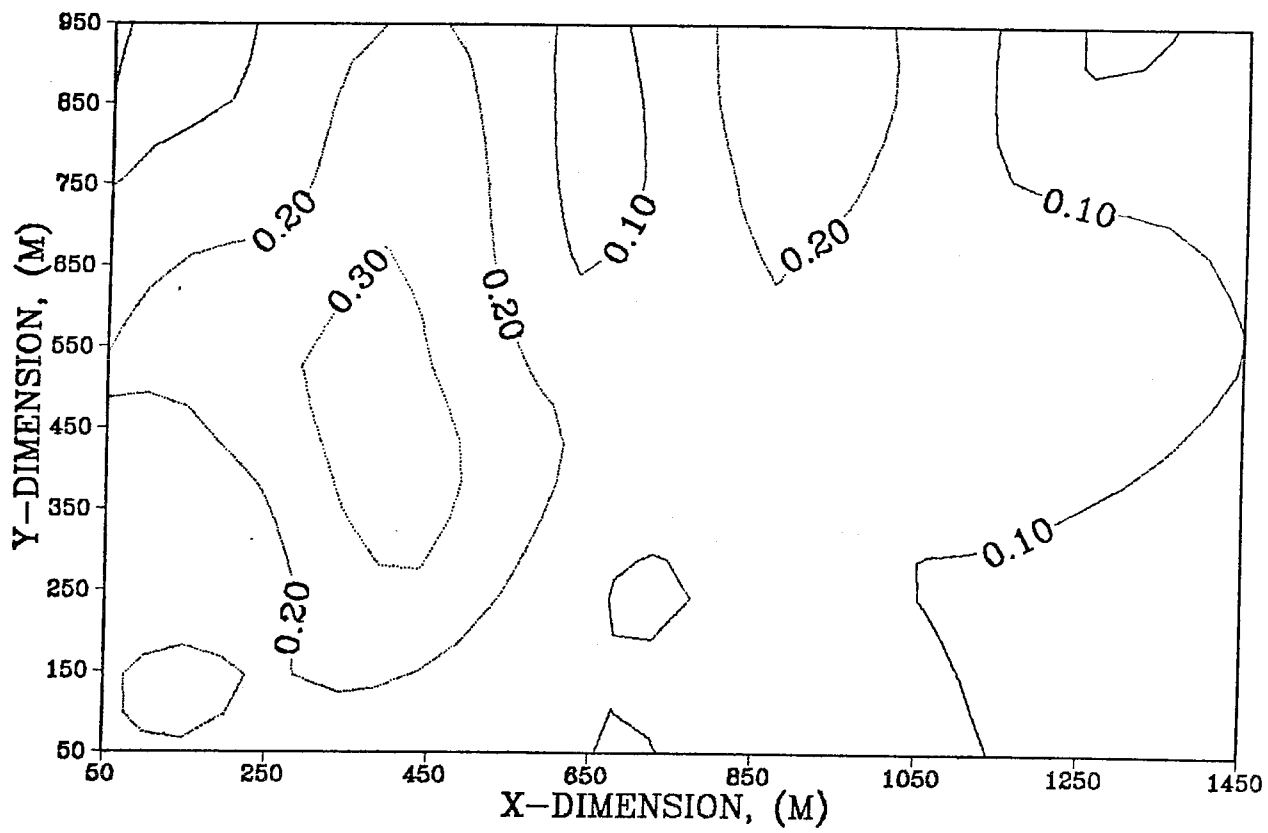


Fig. 6.16 (b) - Estimated permeability distribution of layer 2
for 3-phases after Step 2 using bicubic splines:
Example 1

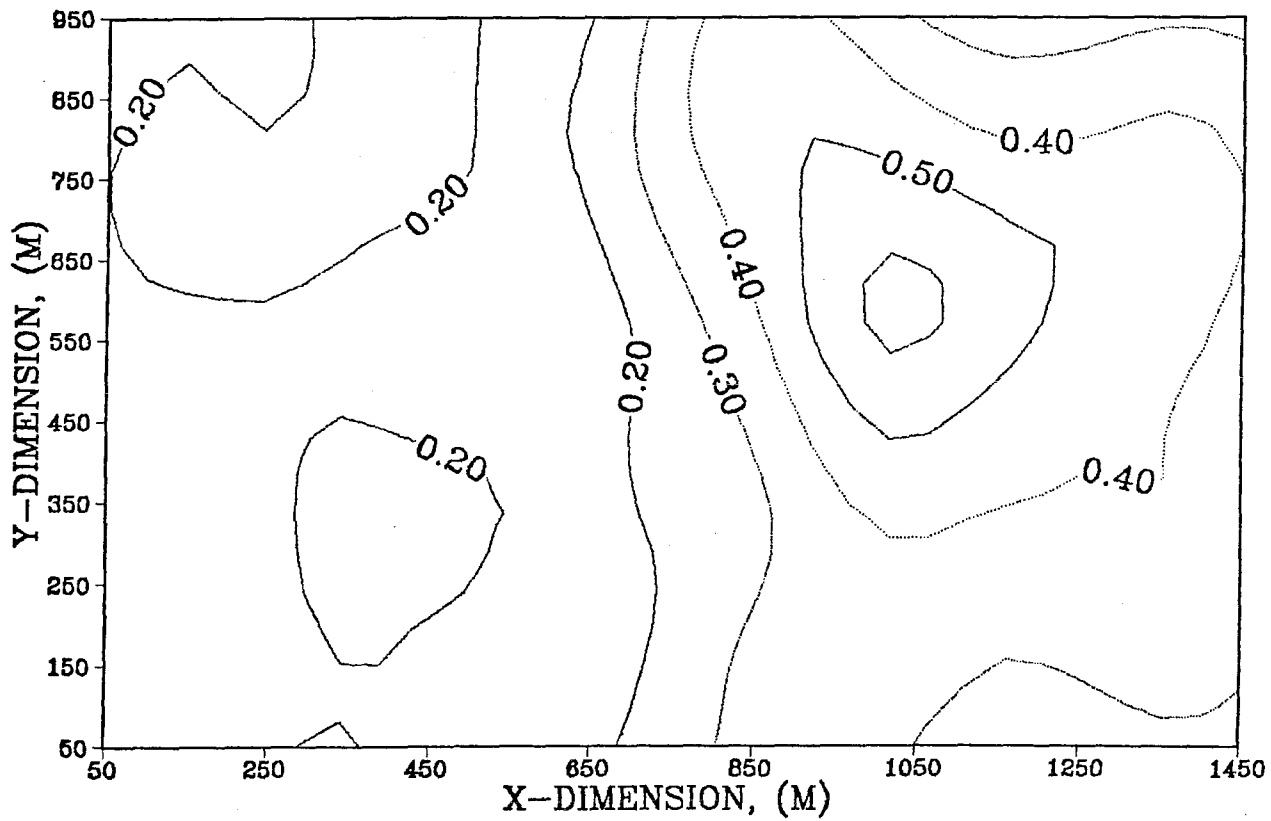


Fig. 6.16 (c) - Estimated permeability distribution of layer 3
for 3-phases after Step 2 using bicubic splines:
Example 1

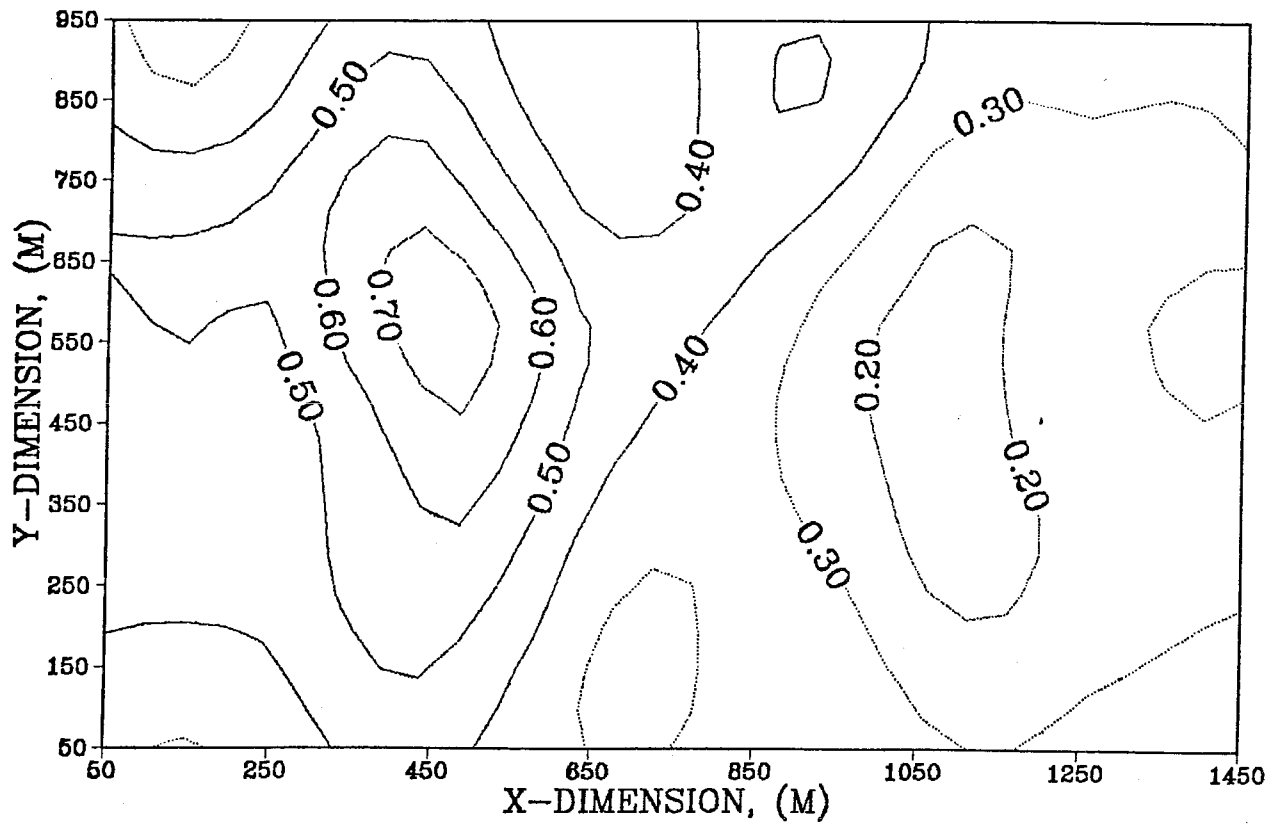


Fig. 6.17 (a) - Estimated permeability distribution of layer 1
for 3-phases after Step 2 using bicubic splines:
Example 2

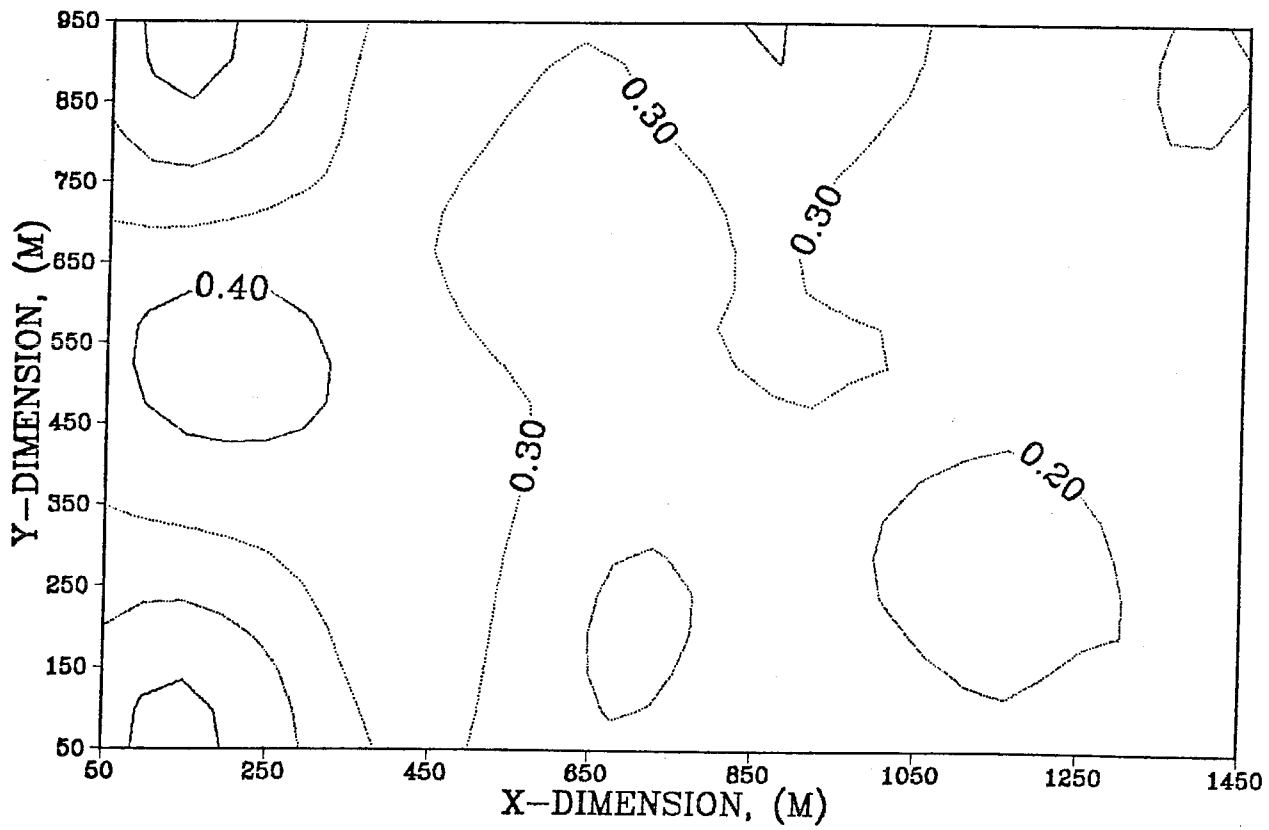


Fig. 6.17 (b) - Estimated permeability distribution of layer 2
for 3-phases after Step 2 using bicubic splines:
Example 2

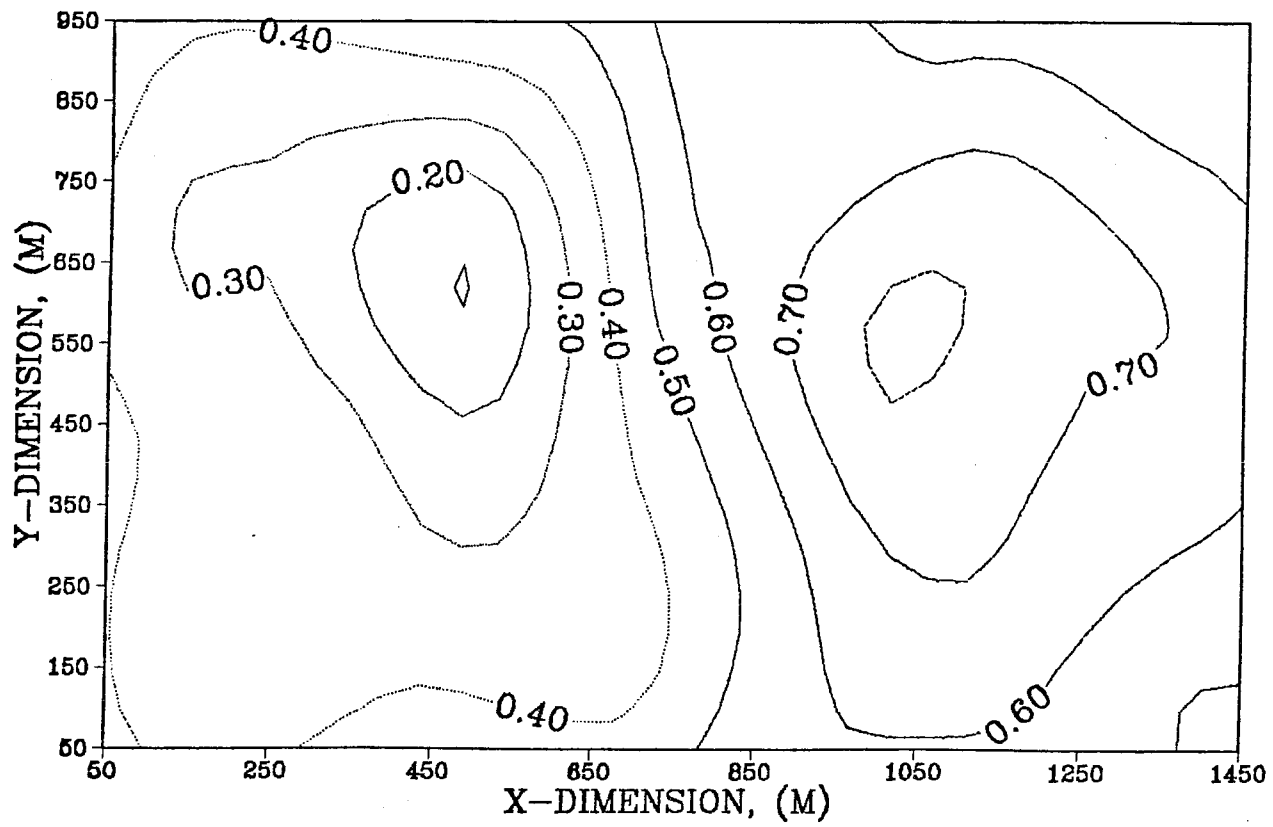


Fig. 6.17 (c) - Estimated permeability distribution of layer 3
for 3-phases after Step 2 using bicubic splines:
Example 2

6.3.3 Comparison of the Performance of the History Matching

Algorithm in Two- and Three-Phase Reservoirs

As can be seen by comparing Figs. 6.6 (a), (b) and (c) and Figs. 6.15 (a), (b) and (c), the permeability distribution is estimated more accurately in the two-phase case than in the three-phase cases. This behavior can be explained by considering the flow behavior in a single-phase reservoir as described in the following equation,

$$c\phi\frac{\partial p}{\partial t} = \nabla\left(\frac{k}{\mu}\nabla p\right) + \sum_{\nu=1}^{N_{well}} q_{\nu}\delta(x-x_{\nu})\delta(y-y_{\nu})\delta(z-z_{\nu}) \quad (31)$$

As the ratio of the permeability to the compressibility, $\frac{k}{c}$, decreases, the spatial variation of the permeability has a decreasing influence on the change in reservoir pressure with time. In multiphase reservoirs, the presence of gas makes the overall system more compressible. As a result, the spatial variation in the permeability distribution is more difficult to estimate in three-phase reservoirs than in two-phase reservoirs that contain only oil and water.

6.4 Computing Requirements

For the two-phase case, using the zonation approach, the entire algorithm, Steps 1, 2 and 3, required 98 iterations (solutions of the simulator and adjoint systems) corresponding to 6370 CPU seconds on a CRAY X-MP/48. The bicubic spline approach needed 100 iterations which corresponds to 6500 CPU seconds.

For Example 1 of the three-phase cases, the entire algorithm, Steps 1, 2 and 3, required 222 iterations corresponding to 666 CPU minutes on a CRAY X-MP/48. For Example 2 of the three-phase case, the entire algorithm, Steps 1, 2 and 3, required 110 iterations corresponding to 330 CPU minutes on a CRAY X-MP/48.

7 . CONCLUSIONS

The aim of this work has been to develop a three-dimensional, three-phase (gas, oil and water) history matching algorithm for use with an industrial Black Oil simulator, in which the absolute permeability distribution is estimated using measured well data, such as pressure, water cut, gas-oil ratio and flow rates of gas and liquid from individual completions. The algorithm which does not require any *a priori* information on the parameter to be estimated, employs a three-step procedure. In Step 1, the best uniform permeability distribution is estimated for each layer starting with a flat initial guess. This step helps to avoid convergence difficulties that may arise in estimating spatially-varying parameters from a poor initial guess. Usually this step converges in about 20 iterations for two-phase cases and 30 iterations for three-phase cases. In this work, an iteration refers to one iterative solution of the reservoir and adjoint equations. In Step 2, a conventional, non-regularized ($\beta = 0$) least-squares estimation is performed using spline approximation. The spline grid system is chosen so that the number of spline coefficients is the same as the number of grid cells for the solution of the reservoir PDE's. The parameter estimates from this step are usually ill-conditioned and dependent on the choice of spline grid. This step requires between 15-40 iterations for two-phase cases and 60-80 for three-phase cases to reduce the value of the performance index to 1/1000 of its starting value. In this step, approximate values of the upper bounds of J_{LS} , the traditional least-squares objective functional, and J_{ST} , the stabilizing functional, are calculated. In Step 3, parameter estimation by regularization and spline approximation is carried out to obtain the final solution. In this step, the regularization parameter is calculated to be $\frac{0.1W_p \overline{J_{LS}}}{J_{ST}}$ for two-phase problems and $\frac{10W_p \overline{J_{LS}}}{J_{ST}}$ for three-phase problems. This step of the algorithm converges after

approximately 40 iterations for two-phase problems and after approximately 80 iterations for three-phase problems. In general, the convergence rate for three-phase problems is slower than for two-phase ones which is due in part to the additional complexity of the physical behavior of three-phase reservoirs and to additional terms in least-squares objective function, in particular, the gas flow rate discrepancy term and the gas-oil ratio discrepancy term. Furthermore, an additional equation (gas material balance) must be solved in each grid cell for three-phase problems. Thus each iteration for a three-phase problem takes approximately 2.8 times as long as an iteration in a two-phase problem.

The algorithm has been applied to both two- and three-phase reservoirs cases. In the two-phase case, the permeability distribution is estimated by matching pressures, water-cuts, and liquid flow rates from individual completions. In two-dimensional reservoirs, only pressure and water cut data are needed to estimate the areal permeability distribution. In multilayered reservoirs, flow rate data from individual completions are necessary to predict the permeability distributions in the different layers. In three-phase reservoirs, gas-oil ratio and gas flow rate data are necessary to estimate the permeability distribution in a multilayered system.

Two examples of three-phase reservoir behavior have been considered. In the first, free gas is present in the reservoir initially. In the second, no free gas is present initially, but arises in the system from a reduction in reservoir pressure to a pressure below the bubble point of the oil-phase. Thus, in this case, a transition between two- and three-phase behavior occurs. The estimation of the permeability distribution in cases where there is a transition between two- and three-phase behavior is considerably more difficult than in cases where only two- or three-phase behavior exists. In three-phase reservoirs, the presence of gas makes the system more compressible. As a result, the spatial variation in the permeability distribution is more

difficult to estimate in three-phase reservoirs than in two-phase cases with only oil and water.

NOMENCLATURE

- b_{l_x} = B – spline function in the x – direction
 b_{l_y} = B – spline function in the y – direction
 g = gravitational acceleration
 h = height of the reservoir
 J_{LS} = least – squares objective function
 J_{PEN} = penalty function
 J_{SM} = smoothing functional
 J_{ST} = stabilizing functional
 $k(x, y, z)$ = absolute horizontal permeability
 $k_{r,l}$ = relative permeability of phase l
 k_v = absolute vertical permeability
 N_o = total number of observation wells
 N_s = total number of spline grid blocks
 N_t = total number of observation times
 N_{well} = total number of wells
 N_x = total number of grid blocks in the x – direction
 N_{x_s} = total number of spline grid blocks in the x – direction
 N_y = total number of grid blocks in the y – direction
 N_{y_s} = total number of spline grid blocks in the y – direction
 N_z = total number of grid blocks in the z – direction
 p = reservoir pressure
 p_0 = initial reservoir pressure
 p_l = pressure of phase l
 $p_{wb_{\nu_w}}$ = wellbore pressure of well ν
 P_{cwo} = capillary pressure water – oil
 P_{cog} = capillary pressure oil – gas
 q_g = mass rate per unit volume of gas production
 q_o = mass rate per unit volume of oil production
 q_w = mass rate per unit volume of water production

- q_ν = rate per unit mass per unit volume from well ν
- Q_g = gas flow rate
- Q_o = oil flow rate
- Q_w = water flow rate
- Q_l = liquid flow rate
- $Q_{g,\nu,k}^{INJ}$ = gas flow rate from well ν and layer k
- $Q_{l,\nu,k}^{INJ}$ = liquid flow rate from well ν and layer k
- R_l = material balance equation of phase l
- R_{p_i} = adjoint equation associated with p_i
- $R_{R_{s_i}}$ = adjoint equation associated with R_{s_i}
- R_s = fraction of gas dissolved in the oil phase
- $R_{S_{g_i}}$ = adjoint equation associated with S_{g_i}
- $R_{S_{o_i}}$ = adjoint equation associated with S_{o_i}
- $R_{w_{\nu w}}$ = adjoint equation associated with $p_{wb_{\nu w}}$
- S_l = saturation of phase l
- S_{iw} = irreducible water saturation
- S_{io} = initial oil saturation
- t = time
- v_l = velocity of phase l
- V_i = volume of grid block i
- $W_{l,k}$ = bicubic spline coefficients for spline grid layer k
- W_k = weighting factor for the penalty function
- W_G = weighting factor for the gas – oil ratio discrepancy term
- W_p = weighting factor for the pressure discrepancy term
- W_{Q_g} = weighting factor for the gas flow rate discrepancy term
- W_{Q_l} = weighting factor for the liquid flow rate discrepancy term
- W_W = weighting factor for the water – cut discrepancy term
- x = spatial variable
- y = spatial variable
- z = spatial variable

GREEK

- β = regularization parameter
- β_l = formation volume factor of phase l
- δ = Dirac delta function
- Δt^n = time step size of time step n
- Δx = grid block length in the x – direction
- Δy = grid block length in the y – direction
- Δx_s = spline grid block length in the x – direction
- Δy_s = spline grid block length in the y – direction
- Δz = grid block height
- ζ_m = coefficient of the stabilizing functional, $m = 0, 1, 2, 3$
- η = dimensionless spatial variable in the y – direction
- μ_l = viscosity of phase l
- ξ = dimensionless spatial variable in the x – direction
- ρ_l = density of phase l
- σ_G^2 = gas – oil ratio discrepancy term
- σ_p^2 = pressure discrepancy term
- $\sigma_{Q_g}^2$ = gas flow rate discrepancy term
- $\sigma_{Q_l}^2$ = liquid flow rate discrepancy term
- σ_W^2 = water cut discrepancy term
- $\overline{\sigma^2}$ = upper bound of the discrepancy term
- ϕ = porosity
- Ψ_{p_i} = adjoint variable associated with p_i
- $\Psi_{R_{s_i}}$ = adjoint variable associated with R_{s_i}
- $\Psi_{S_{g_i}}$ = adjoint variable associated with S_{g_i}
- $\Psi_{S_{o_i}}$ = adjoint variable associated with S_{o_i}

SUBSCRIPTS

g = gas phase

G = gas – oil ratio

i = i^{th} grid cell

k = index of layers

l = liquid

LAY = layer

o = oil phase

w = water phase

W = water cut

SUPERSCRIPTS

n = time step index

REFERENCES

- (1) Wasserman, M. L., Emanuel, A. S., and Seinfeld, J. H.: *SPEJ*, **15**, 347 (1975).
- (2) Chavent, G., Dupuy, M., and Lemonnier, P.: "History Matching by Use of Optimal Control Theory," *SPEJ*, (Feb. 1975) 74-86; *Trans.*, AIME, **259**.
- (3) Yakowitz, S., and Duckstein, L.: "Instability in Aquifer Identification: Theory and Case Studies," *Water Resources Research*, **16**, No. 198, 1054-64.
- (4) Lee, T., Kravaris, C., and Seinfeld, J. H.: "History Matching by Spline Approximation and Regularization in Single-Phase Areal Reservoirs," *SPE Reservoir Engineering*, **1**, 521 (1986).
- (5) Banks, H. T.: "Distributed System Optimal Control and Parameter Estimation: Computational Techniques Using Spline Approximation," *Proc.*, 3rd IFAC Symposium on Control of Distributed Parameter Systems, Toulouse, (June 29 - July 2, 1982).
- (6) Banks, H. T., and Crowley, J. M.: "Parameter Identification in Continuum Models," *Proc.*, American Control Conference, San Francisco (June 1983).
- (7) Banks, H. T., and Murphy, K. A.: "Estimation of Coefficients and Boundary Parameters in Hyperbolic Systems," Div. of Applied Mathematics, Brown U., Providence, RI, report LCDS No. 84-5 (Feb. 1984).
- (8) Banks, H. T., and Lamm, P. D.: "Estimation of Variable Coefficients in Parabolic Distributed Systems," *I.E.E.E. Trans. Auto. Control*, **30**, No. 4, 386-98.
- (9) Trummer, M. R.: *SIAM J. Numer. Anal.*, **21**, 729 (1984).

- (10) Locker, J., and Prenter, P. M.: *J. Math. Anal. Appl.*, **74**, 504, (1980).
- (11) Lee, T., and Seinfeld, J. H.: "Estimation of Two-Phase Petroleum Reservoir Properties by Regularization," *J. Computational Physics*.
- (12) Craven, P., and Wahba, G.: *Numer. Math.*, **31**, 377 (1979).
- (13) Tikhonov, A. N., and Arsenin, V. Y.: *Solutions of Ill-Posed Problems*, H. Winston and Sons, Washington, DC (1977).
- (14) Miller, K.: *SIAM J. Math. Anal. Appl.*, **1**, 52 (1970).
- (15) Shah, P. C., Gavalas, G. R., and Seinfeld, J. H.: "Error Analysis in History Matching: The Optimum Level of Parameterization," *SPEJ* (June 1978) 219-28.
- (16) Chen, W. H. *et al.*: "A New Algorithm for Automatic History Matching," *SPEJ*, **14**, (Dec. 1974) 593 - 608.
- (17) Van den Bosch, B., and Seinfeld, J. H.: *SPEJ*, **17**, 398 (1977).
- (18) Kravaris, C., and Seinfeld, J. H.: "Identification of Spatially-Varying Parameters in Distributed Parameter Systems by Discrete Regularization," *J. Mathematical Analysis and Appl.*, (1986) **118**, No. 9.
- (19) Scales, L. E.: *Introduction to Non-Linear Optimization*, (Springer-Verlag, New York, 1985) p. 106.
- (20) Lee, T., and Seinfeld, J. H.: "Estimation of Absolute and Relative Permeabilities in Petroleum Reservoirs," *Inverse Problems*.

- (21) Nazareth, L.: "A Conjugate Direction Algorithm Without Line Searchers," *J. Optimization Theory and Application* (Nov. 1977) 373-87.
- (22) Lake, L.: "The Origins of Anisotropy," *JPT* (April 1988) 395-396.
- (23) Prats, M.: "The Influence of Oriented Arrays of Thin Impermeable Shale Lenses or of Highly Conductive Natural Fractures on Apparent Permeability Anisotropy," *JPT* (Oct. 1972) 1219-21.

Appendix A. Finite Difference Reservoir Equations

Consider the three-dimensional, unsteady flow of oil, water and gas in a petroleum reservoir. If the three phases are immiscible, then the mass conservation equations for the water, oil and gas phases are given by Eqs. (1)-(13). In this work, CLASS (Chevron Limited Applications Simulation System) is used as the basic reservoir model. Using a finite difference approximation, a nonlinear system of algebraic equations is generated as shown

$$\begin{aligned}
 R_{w_i} \equiv & - \sum_{j \in J_i} k h_{i,j} \left(\frac{k_{rw}}{\mu_w \beta_w} \right)_{i,j}^n (p_i - p_j - g \rho_{w,i,j} (z_i - z_j) - P_{cwo_i} + P_{cwo_j})^n \\
 & - Q_{w_i}^n - \frac{V_i}{\Delta t^n} \left[\left(\frac{S_w \phi}{\beta_w} \right)_i^n - \left(\frac{S_w \phi}{\beta_w} \right)_i^{n-1} \right] = 0
 \end{aligned} \tag{A.1}$$

$$\begin{aligned}
 R_{o_i} \equiv & - \sum_{j \in J_i} k h_{i,j} \left(\frac{k_{ro}}{\mu_o \beta_o} \right)_{i,j}^n (p_i - p_j - g \rho_{o,i,j} (z_i - z_j))^n \\
 & - Q_{o_i}^n - \frac{V_i}{\Delta t^n} \left[\left(\frac{S_o \phi}{\beta_o} \right)_i^n - \left(\frac{S_o \phi}{\beta_o} \right)_i^{n-1} \right] = 0
 \end{aligned} \tag{A.2}$$

$$\begin{aligned}
 R_{g_i} \equiv & - \sum_{j \in J_i} k h_{i,j} \left[\left(\frac{R_s k_{ro}}{\mu_o \beta_o} \right)_{i,j}^n (p_i - p_j - g \rho_{o,i,j} (z_i - z_j))^n \right. \\
 & + \left. \left(\frac{k_{rg}}{\mu_g \beta_g} \right)_{i,j}^n (p_i - p_j - g \rho_{g,i,j} (z_i - z_j) + P_{cog_i} - P_{cog_j})^n \right] - Q_{g_i}^n \\
 & - \frac{V_i}{\Delta t^n} \left[\left(\frac{R_s S_o \phi}{\beta_o} \right)_i^n - \left(\frac{R_s S_o \phi}{\beta_o} \right)_i^{n-1} + \left(\frac{S_g \phi}{\beta_g} \right)_i^n - \left(\frac{S_g \phi}{\beta_g} \right)_i^{n-1} \right] = 0
 \end{aligned} \tag{A.3}$$

for $n = 1, \dots, N_t$ and $i \in \bar{N}$ defined by

$$\begin{aligned}
\overline{N} &\equiv \{i \mid i = i_x + N_x(i_y - 1) + N_x N_y(i_z - 1), \\
&\quad i_x = 1, \dots, N_x, \ i_y = 1, \dots, N_y, \ i_z = 1, \dots, N_z\} \\
&= \{1, \dots, N\}
\end{aligned} \tag{A.4}$$

where $N = N_x N_y N_z$ and i_x , i_y and i_z denote the PDE grid blocks along the x -, y - and z -directions, and the index set J_i , defined for each $i \in \overline{N}$ by

$$J_i = \{j \mid j = i - N_x N_y, i - N_x, i - 1, i + 1, i + N_x, i + N_x N_y\} \cap \overline{N}, \tag{A.5}$$

is introduced for simplicity, with initial conditions

$$p_i^0 = p_0 \tag{A.6}$$

$$S_{w_i}^0 = S_{iw}. \tag{A.7}$$

An harmonic average is used for the absolute permeability

$$kh_{i,j} = \frac{2.0 \text{ UFAC} X_{i,j}}{\frac{\Delta x_j}{UX_j k_j} + \frac{\Delta x_i}{UX_i k_i}} \tag{A.8}$$

for $j = i - 1, i + 1$, where

$$\text{UFAC} X_{i,j} = \frac{\frac{1}{4}(\Delta x_i + \Delta x_j)^2}{\frac{1}{4}(\Delta x_i + \Delta x_j)^2 + (\Delta z_i + \Delta z_j)^2} \tag{A.9}$$

and

$$UX_i = \Delta y_i \Delta z_i, \tag{A.10}$$

$$kh_{i,j} = \frac{2.0 UFACY_{i,j}}{\frac{\Delta y_j}{UY_j k_j} + \frac{\Delta y_i}{UY_i k_i}} \quad (\text{A.11})$$

for $j = i - N_x, i + N_x$, where

$$UFACY_{i,j} = \frac{\frac{1}{4}(\Delta y_i + \Delta y_j)^2}{\frac{1}{4}(\Delta y_i + \Delta y_j)^2 + (\Delta z_i + \Delta z_j)^2} \quad (\text{A.12})$$

and

$$UY_i = \Delta x_i \Delta z_i, \quad (\text{A.13})$$

and

$$kh_{i,j} = \frac{2.0}{\frac{\Delta z_j}{0.1 UZ_j k_j} + \frac{\Delta z_i}{0.1 UZ_i k_i}} \quad (\text{A.14})$$

for $j = i - N_x N_y, i + N_x N_y$, where

$$UZ_i = \Delta x_i \Delta y_i. \quad (\text{A.15})$$

Furthermore, upstream weighting is used for the relative permeabilities for the stability of the numerical integration given by

$$\begin{aligned} k_{r,oi,j}^n &= k_{ro}(S_{w_i}^n, S_{g_i}^n) \text{ if } p_{o_i}^n \geq p_{o_j}^n \\ k_{r,oi,j}^n &= k_{ro}(S_{w_j}^n, S_{g_j}^n) \text{ otherwise} \end{aligned} \quad (\text{A.16})$$

$$\begin{aligned} k_{r,wi,j}^n &= k_{rw}(S_{w_i}^n) \text{ if } p_{w_i}^n \geq p_{w_j}^n \\ k_{r,wi,j}^n &= k_{rw}(S_{w_j}^n) \text{ otherwise} \end{aligned} \quad (\text{A.17})$$

$$\begin{aligned} k_{r,gi,j}^n &= k_{rg}(S_{g_i}^n) \text{ if } p_{g_i}^n \geq p_{g_j}^n \\ k_{r,gi,j}^n &= k_{rg}(S_{g_j}^n) \text{ otherwise} \end{aligned} \quad (\text{A.18})$$

The viscosity, formation volume factor and fraction of gas dissolved in the oil-phase are treated similarly.

Several equation solver options are available for use with the CLASS simulator. Since convergence difficulties are encountered when using iterative techniques to solve the adjoint system of equations, a direct method is employed in this work.

Appendix B. Functional Derivative of J_{LS}

The finite difference version of the first-order necessary condition of the least squares discrepancy function is defined by Eqs. (15) - (20). The corresponding Hamiltonian of the conventional least-squares problem is

$$\begin{aligned} \widetilde{J}_{LS} = J_{LS} &+ \sum_{n=1}^{N_t} \left[\sum_{i=1}^N (\Psi_{p_i}^n R_{w_i}^n + \Psi_{S_{o_i}}^n R_{o_i}^n + \Psi_{S_{g_i}}^n R_{g_i}^n) \right. \\ &\left. + \sum_{\nu=1}^{N_{wells}} \Psi_{wells_\nu}^n R_{wells_\nu}^n \right]. \end{aligned} \quad (B.1)$$

From the first variation of Eq. (B.1), the adjoint equations are given by the following, where the terms that include δp_i^n yield

$$\begin{aligned} R_{p_i}^n = & - \sum_{j \in J_i} (\Psi_{p_i} - \Psi_{p_j})^n \left[\left(\frac{k k_{rw}}{\mu_w \beta_w} \right)_{i,j} \left(1 - g \frac{\partial \rho_{w,i,j}}{\partial p} (z_i - z_j) \right) \right. \\ & + u_{w,i,j} (k k_{rw})_{i,j} \frac{\partial}{\partial p} \left(\frac{1}{\mu_w \beta_w} \right)_{i,j} (p_i - p_j - g \rho_{w,i,j} (z_i - z_j) - P_{cwo_i} + P_{cwo_j}) \left. \right]^n \\ & - \sum_{j \in J_i} (\Psi_{S_{o_i}} - \Psi_{S_{o_j}})^n \left[\left(\frac{k k_{ro}}{\mu_o \beta_o} \right)_{i,j} \left(1 - g \frac{\partial \rho_{o,i,j}}{\partial p} (z_i - z_j) \right) \right. \\ & + u_{o,i,j} (k k_{ro})_{i,j} \frac{\partial}{\partial p} \left(\frac{1}{\mu_o \beta_o} \right)_{i,j} (p_i - p_j - g \rho_{o,i,j} (z_i - z_j)) \left. \right]^n \\ & - \sum_{j \in J_i} (\Psi_{S_{g_i}} - \Psi_{S_{g_j}})^n \left[\left(\frac{k k_{ro} R_s}{\mu_o \beta_o} \right)_{i,j} \left(1 - g \frac{\partial \rho_{o,i,j}}{\partial p} (z_i - z_j) \right) \right. \\ & + u_{o,i,j} (k k_{ro})_{i,j} \frac{\partial}{\partial p} \left(\frac{R_s}{\mu_o \beta_o} \right)_{i,j} (p_i - p_j - g \rho_{o,i,j} (z_i - z_j)) \left. \right]^n \\ & - \sum_{j \in J_i} (\Psi_{S_{g_i}} - \Psi_{S_{g_j}})^n \left[\left(\frac{k k_{rg}}{\mu_g \beta_g} \right)_{i,j} \left(1 - g \frac{\partial \rho_{g,i,j}}{\partial p} (z_i - z_j) \right) \right. \\ & + u_{g,i,j} (k k_{rg})_{i,j} \frac{\partial}{\partial p} \left(\frac{1}{\mu_g \beta_g} \right)_{i,j} (p_i - p_j - g \rho_{g,i,j} (z_i - z_j) + P_{cogi} - P_{cog_j}) \left. \right]^n \end{aligned}$$

$$\begin{aligned}
& - \Psi_{pi}^n \frac{\partial Q_{wi}^n}{\partial p} - \Psi_{S_{oi}}^n \frac{\partial Q_{oi}^n}{\partial p} - \Psi_{S_{gi}}^n \frac{\partial Q_{gi}^n}{\partial p} \\
& + V_i S_{wi} \frac{\partial}{\partial p} \left(\frac{\phi}{\beta_w} \right)_i^n \left(\frac{\Psi_{pi}^{n+1}}{\delta t^{n+1}} - \frac{\Psi_{pi}^n}{\delta t^n} \right) + V_i S_{oi} \frac{\partial}{\partial p} \left(\frac{\phi}{\beta_o} \right)_i^n \left(\frac{\Psi_{S_{oi}}^{n+1}}{\delta t^{n+1}} - \frac{\Psi_{S_{oi}}^n}{\delta t^n} \right) \\
& + V_i [S_{oi} \frac{\partial}{\partial p} \left(\frac{\phi R_s}{\beta_o} \right)_i^n + S_{gi} \frac{\partial}{\partial p} \left(\frac{\phi}{\beta_g} \right)_i^n] \left(\frac{\Psi_{S_{gi}}^{n+1}}{\delta t^{n+1}} - \frac{\Psi_{S_{gi}}^n}{\delta t^n} \right) \\
& + \sum_{n=1}^{N_t} \sum_{i=1}^N \sum_{\nu_o=1}^{N_{\nu_o}} \frac{\partial G}{\partial p_i^n} \delta_{i,i_{\nu_o}} + \frac{\partial}{\partial p_i^n} \sum_{n=1}^{N_t} \sum_{i=1}^N \sum_{\nu_w=1}^{N_{\nu_w}} \Psi_{\nu_w}^n R_{w\nu_w}^n \delta_{i,i_{\nu_w}} = 0, \quad (B.2)
\end{aligned}$$

where the terms that include δS_{oi}^n yield

$$\begin{aligned}
R_{S_{oi}}^n = & - \sum_{j \in J_i} (\Psi_{pi} - \Psi_{pj})^n \left[\left(\frac{k k_{rw}}{\mu_w \beta_w} \right)_{i,j} \frac{\partial P_{cwoi}}{\partial S_w} \right. \\
& - u_{wi,j} \left(\frac{k}{\mu_w \beta_w} \right)_{i,j} \frac{\partial k_{rw,i,j}}{\partial S_w} (p_i - p_j - g \rho_{wi,j} (z_i - z_j) - P_{cwoi} + P_{cwoj}) \Big]^n \\
& + \sum_{j \in J_i} (\Psi_{S_{oi}} - \Psi_{S_{oj}} + R_{si,j} (\Psi_{S_{gi}} - \Psi_{S_{gj}}))^n \\
& \times [u_{oi,j} \left(\frac{k}{\mu_o \beta_o} \right)_{i,j} \left(\frac{\partial k_{ro}}{\partial S_w} + \frac{\partial k_{ro}}{\partial S_g} \right)_{i,j} (p_i - p_j - g \rho_{oi,j} (z_i - z_j))]^n \\
& + \sum_{j \in J_i} (\Psi_{S_{gi}} - \Psi_{S_{gj}})^n \left[\left(\frac{k k_{rg}}{\mu_g \beta_g} \right)_{i,j} \frac{\partial P_{cogi}}{\partial S_g} \right. \\
& - u_{gi,j} \left(\frac{k}{\mu_g \beta_g} \right)_{i,j} \frac{\partial k_{rg,i,j}}{\partial S_g} (p_i - p_j - g \rho_{gi,j} (z_i - z_j) + P_{cogi} - P_{cogj}) \Big]^n \\
& + \Psi_{pi}^n \frac{\partial Q_{wi}^n}{\partial S_w} + \Psi_{S_{oi}}^n \frac{\partial Q_{oi}^n}{\partial S_w} + \Psi_{S_{gi}}^n \frac{\partial Q_{gi}^n}{\partial S_g} \\
& - V_i \left(\frac{\phi}{\beta_w} \right)_i^n \left(\frac{\Psi_{pi}^{n+1}}{\delta t^{n+1}} - \frac{\Psi_{pi}^n}{\delta t^n} \right) + V_i \left(\frac{\phi}{\beta_o} \right)_i^n \left(\frac{\Psi_{S_{oi}}^{n+1}}{\delta t^{n+1}} - \frac{\Psi_{S_{oi}}^n}{\delta t^n} \right) \\
& + V_i \left[\left(\frac{\phi R_s}{\beta_o} \right)_i^n - \left(\frac{\phi}{\beta_g} \right)_i^n \right] \left(\frac{\Psi_{S_{gi}}^{n+1}}{\delta t^{n+1}} - \frac{\Psi_{S_{gi}}^n}{\delta t^n} \right) \\
& + \sum_{n=1}^{N_t} \sum_{i=1}^N \sum_{\nu_o=1}^{N_{\nu_o}} \frac{\partial G}{\partial S_{oi}^n} \delta_{i,i_{\nu_o}} + \frac{\partial}{\partial S_{oi}^n} \sum_{n=1}^{N_t} \sum_{i=1}^N \sum_{\nu_w=1}^{N_{\nu_w}} \Psi_{\nu_w}^n R_{w\nu_w}^n \delta_{i,i_{\nu_w}} = 0, \quad (B.3)
\end{aligned}$$

where for an unsaturated reservoir, the terms that include δR_{s_i} yield

$$\begin{aligned}
R_{R_{s_i}}^n = & \sum_{j \in J-i} [\Psi_{S_{o_i}} - \Psi_{S_{o_j}} + R_{s_{i,j}}(\Psi_{R_{s_i}} - \Psi_{R_{s_j}})]^n [g(\frac{k k_{ro}}{\mu_o \beta_o} \frac{\partial \rho_o}{\partial R_s})_{i,j}^n (z_i - z_j) \\
& - u_{o_{i,j}}(k k_{ro} \frac{\partial}{\partial R_s} (\frac{1}{\mu_o \beta_o}))_{i,j}^n (p_i - p_j - g \rho_{o_{i,j}}(z_i - z_j))^n] \\
& - \sum_{j \in J_i} (\Psi_{R_{s_i}} - \Psi_{R_{s_j}})^n [u_{o_{i,j}}(\frac{k k_{ro}}{\mu_o \beta_o})_{i,j}^n (p_i - p_j - g \rho_{o_{i,j}}(z_i - z_j))^n] \\
& - \Psi_{S_{o_i}}^n \frac{\partial Q_{o_i}}{\partial R_s}^n - \Psi_{S_{g_i}}^n \frac{\partial Q_{g_i}}{\partial R_s}^n + V_i S_{o_i} (\frac{\phi}{\beta_o})_i^n (\frac{\Psi_{R_{s_i}}^{n+1}}{\delta t^{n+1}} - \frac{\Psi_{R_{s_i}}^n}{\delta t^n}) \\
& + V_i S_{o_i} \frac{\partial}{\partial R_s} (\frac{\phi}{\beta_o})_i^n [\frac{\Psi_{S_{o_i}}^{n+1}}{\delta t^{n+1}} - \frac{\Psi_{S_{o_i}}^n}{\delta t^n} + R_{s_i}^n (\frac{\Psi_{R_{s_i}}^{n+1}}{\delta t^{n+1}} - \frac{\Psi_{R_{s_i}}^n}{\delta t^n})] \\
& + \sum_{n=1}^{N_t} \sum_{i=1}^N \sum_{\nu_o=1}^{N_{\nu_o}} \frac{\partial G}{\partial R_{s_i}^n} \delta_{i,i_{\nu_o}} + \frac{\partial}{\partial R_{s_i}^n} \sum_{n=1}^{N_t} \sum_{i=1}^N \sum_{\nu_w=1}^{N_{\nu_w}} \Psi_{\nu_w}^n R_{w_{\nu_w}}^n \delta_{i,i_{\nu_w}} = 0, \quad (B.4)
\end{aligned}$$

and where the terms that include δS_{g_i} yield

$$\begin{aligned}
R_{S_{g_i}}^n = & - \sum_{j \in J_i} (\Psi_{p_i} - \Psi_{p_j})^n [(\frac{k k_{rw}}{\mu_w \beta_w})_{i,j} \frac{\partial P_{cwo_i}}{\partial S_w} \\
& - u_{w_{i,j}}(\frac{k}{\mu_w \beta_w})_{i,j} \frac{\partial k_{rw_{i,j}}}{\partial S_w} (p_i - p_j - g \rho_{w_{i,j}}(z_i - z_j) - P_{cwo_i} + P_{cwo_j})]^n \\
& - \sum_{j \in J_i} (\Psi_{S_{o_i}} - \Psi_{S_{o_j}} R_{s_{i,j}}(\Psi_{S_{g_i}} - \Psi_{S_{g_j}}))^n \\
& \times [u_{o_{i,j}}(\frac{k}{\mu_o \beta_o})_{i,j} \frac{\partial k_{ro}}{\partial S_g} (p_i - p_j - g \rho_{o_{i,j}}(z_i - z_j))]^n \\
& - \sum_{j \in J_i} (\Psi_{S_{g_i}} - \Psi_{S_{g_j}})^n [(\frac{k k_{rg}}{\mu_g \beta_g})_{i,j} \frac{\partial P_{cog_i}}{\partial S_g} \\
& + u_{g_{i,j}}(\frac{k}{\mu_g \beta_g})_{i,j} \frac{\partial k_{rg_{i,j}}}{\partial S_g} (p_i - p_j - g \rho_{g_{i,j}}(z_i - z_j) + P_{cog_i} - P_{cog_j})]^n
\end{aligned}$$

$$\begin{aligned}
& + \Psi_{p_i}^n \frac{\partial Q_{w_i}}{\partial S_w} - \Psi_{S_{o_i}}^n \frac{\partial Q_{o_i}}{\partial S_g} - \Psi_{S_{g_i}}^n \frac{\partial Q_{g_i}}{\partial S_g} \\
& - V_i \left(\frac{\phi}{\beta_w} \right)_i^n \left(\frac{\Psi_{p_i}^{n+1}}{\delta t^{n+1}} - \frac{\Psi_{p_i}^n}{\delta t^n} \right) - V_i \left(\frac{\phi}{\beta_o} \right)_i^n \left(\frac{\Psi_{S_{o_i}}^{n+1}}{\delta t^{n+1}} - \frac{\Psi_{S_{o_i}}^n}{\delta t^n} \right) \\
& - V_i \left[\left(\frac{\phi R_s}{\beta_o} \right)_i^n - \left(\frac{\phi}{\beta_g} \right)_i^n \right] \left(\frac{\Psi_{S_{g_i}}^{n+1}}{\delta t^{n+1}} - \frac{\Psi_{S_{g_i}}^n}{\delta t^n} \right) \\
& + \sum_{n=1}^{N_t} \sum_{i=1}^N \sum_{\nu_o=1}^{N_{\nu_o}} \frac{\partial G}{\partial S_{g_i}^n} \delta_{i,i_{\nu_o}} + \frac{\partial}{\partial S_{g_i}^n} \sum_{n=1}^{N_t} \sum_{i=1}^N \sum_{\nu_w=1}^{N_{\nu_w}} \Psi_{\nu_w}^n R_{w_{\nu_w}}^n \delta_{i,i_{\nu_w}} = 0 \quad (B.5)
\end{aligned}$$

for $i \in \bar{N}$ and $n = N_t, N_t - 1, \dots, 1$ with terminal constraints

$$\Psi_{p_i}^{N_t+1} = 0 \quad (B.6)$$

$$\Psi_{S_{o_i}}^{N_t+1} = 0 \quad (B.7)$$

$$\Psi_{S_{g_i}}^{N_t+1} = 0. \quad (B.8)$$

The functional derivative of J_{LS} with respect to k_i , for $i \in \bar{N}$ is given by

$$\begin{aligned}
\frac{\delta \widetilde{J_{LS}}}{\delta k_i} = & - \sum_{n=1}^{N_t} \sum_{j \in J_i} \frac{\partial k_{i,j}}{\partial k_i} \\
& \times [(\Psi_{p_i} - \Psi_{p_i})^n \left(\frac{k_{rw}}{\mu_w \beta_w} \right)_{i,j}^n (p_i - p_j - \rho_{w,i,j} (z_i - z_j) - P_{cwo_i} + P_{cwo_j}) \\
& + (\Psi_{S_{o_i}} - \Psi_{S_{o_j}} + R_{s,i,j} (\Psi_{S_{g_i}} - \Psi_{S_{g_j}})) \left(\frac{k_{ro}}{\mu_o \beta_o} \right)_{i,j}^n (p_i - p_j - \rho_{o,i,j} (z_i - z_j)) \\
& + (\Psi_{S_{g_i}} - \Psi_{S_{g_j}})^n \left(\frac{k_{rg}}{\mu_g \beta_g} \right)_{i,j}^n (p_i - p_j - \rho_{g,i,j} (z_i - z_j) + P_{cog_i} - P_{cog_j})] \\
& - \Psi_{p_i} \frac{\partial Q_{w_i}^n}{\partial k_i} - \Psi_{S_{o_i}} \frac{\partial Q_{o_i}^n}{\partial k_i} - \Psi_{S_{g_i}} \frac{\partial Q_{g_i}^n}{\partial k_i} \\
& + \sum_{n=1}^{N_t} \sum_{i=1}^N \sum_{\nu_o=1}^{N_{\nu_o}} \frac{\partial G}{\partial k_i} \delta_{i,i_{\nu_o}} + \frac{\partial}{\partial k_i} \sum_{n=1}^{N_t} \sum_{i=1}^N \sum_{\nu_w=1}^{N_{\nu_w}} \Psi_{\nu_w}^n R_{w_{\nu_w}}^n \delta_{i,i_{\nu_w}} \quad (B.9)
\end{aligned}$$

The adjoint system equations are solved using the same direct method used in the CLASS simulator. From $\frac{\partial J_{LS}}{\partial k_i}$, $i = 1, \dots, \overline{N}$, the derivative of J_{LS} with respect to the spline coefficients $W_{l_x, l_y, k}$ can be computed using the following relationship

$$\frac{\partial J_{LS}}{\partial W_{l_x, l_y, k}} = \sum_{i_x=1}^{N_x} \sum_{i_y=1}^{N_y} \frac{\partial J_{LS}}{\partial k_{i,k}} \chi^{*4}\left(4 - l_x + \frac{x}{\delta x_s}\right) \chi^{*4}\left(4 - l_y + \frac{y}{\delta y_s}\right) \quad (B.10)$$

for $l_x = 1, \dots, N_{xs}$, $l_y = 1, \dots, N_{ys}$ and $i = i_x + N_x(i_y - 1)$ where $\chi^{*4}(\theta)$ is given in Eq. (30). The derivative of J_{ST} with respect to $W_{l,k}$ can be calculated analytically from the expression for the bicubic spline approximation given in Eqs. (27 - 30) as shown by Kravaris and Seinfeld⁴. Finally, the derivative of J_{SM} with respect to $W_{l,k}$ is computed by

$$\frac{\partial J_{SM}}{\partial W_{l,k}} = \frac{\partial J_{LS}}{\partial W_{l,k}} + \beta \frac{\partial J_{ST}}{\partial W_{l,k}}. \quad (B.11)$$

CHAPTER IV

CONCLUSIONS

The aim of this work has been to develop a three-dimensional, three-phase (gas, oil and water) history matching algorithm for use with an industrial Black Oil simulator, that does not require any *a priori* information on the parameter to be estimated, in which the absolute permeability distribution is estimated using measured well data, such as pressure, water cut, gas-oil ratio and flow rates of gas and liquid from individual completions. In general, the convergence rate for three-phase problems is slower than for two-phase ones which is due in part to the additional complexity of the physical behavior of three-phase reservoirs and to additional terms in least-squares objective function, in particular, the gas flow rate discrepancy term and the gas-oil ratio discrepancy term. Furthermore, an additional equation (gas material balance) must be solved in each grid cell for three-phase problems. Thus each iteration for a three-phase problem takes approximately 2.8 times as long as an iteration in a two-phase problem.

Two examples of three-phase reservoir behavior have been considered. In the first, free gas is present in the reservoir initially. In the second, no free gas is present initially, but arises in the system from a reduction in reservoir pressure to a pressure below the bubble point of the oil-phase. Thus, in this case, a transition between two- and three-phase behavior occurs. The estimation of the permeability distribution in cases where there is a transition between two- and three-phase behavior is considerably more difficult than in cases where only two- or three-phase behavior exists. In three-phase reservoirs, the presence of gas makes the system more compressible. As a result, the spatial variation in the permeability distribution is more

difficult to estimate in three-phase reservoirs than in two-phase cases with only oil and water.

The estimation of absolute permeabilities in three-phase reservoirs is not recommended since it requires excessive computational time, and, in addition, in most three-phase reservoirs transitions between two- and three-phase behavior occur. In two-phase reservoirs, the absolute permeability is estimated accurately with relative computational efficiency. Furthermore, the computational time could be lessened by decreasing the number of observation times, and correspondingly, the number of time steps used for solving both the simulator and adjoint equations. Since in both the two- and three-phase cases, the measured well data were matched accurately, even though the permeability distribution was not estimated as well in the three-phase case as in the two-phase case, how well the observation data are matched is not necessarily a measure of the accuracy of the permeability estimation.

APPENDIX A

Derivation of the History Matching Algorithms

1. Derivation and Solution of the Reservoir Equations

Consider the three-dimensional, unsteady flow of oil, water and gas in a petroleum reservoir. If the three phases are immiscible, then the mass conservation equations for the water, oil and gas phases are given by

$$\begin{aligned}
 R_w \equiv & -\frac{\partial}{\partial t}(\rho_w(p_o)\phi(p_o)S_w) - \nabla \cdot (\rho_w(p_o)v_w) \\
 & + \sum_{\nu=1}^{N_w} \rho_w(p_o)q_{w,\nu}\delta(x-x_\nu)\delta(y-y_\nu)\delta(z-z_\nu) = 0
 \end{aligned} \tag{A.1}$$

$$\begin{aligned}
 R_o \equiv & -\frac{\partial}{\partial t}(\rho_o(p_o, R_s)\phi(p_o)S_o) - \nabla \cdot (\rho_o(p_o, R_s)v_o) \\
 & + \sum_{\nu=1}^{N_o} \rho_o(p_o, R_s)q_{o,\nu}\delta(x-x_\nu)\delta(y-y_\nu)\delta(z-z_\nu) = 0
 \end{aligned} \tag{A.2}$$

$$\begin{aligned}
 R_g \equiv & -\frac{\partial}{\partial t}(\phi(p_o)(\rho_g(p_o)S_g + R_s\rho_o(p_o, R_s)S_o)) \\
 & - \nabla \cdot (\rho_g(p_o)v_g + R_s\rho_o(p_o, R_s)v_o) \\
 & + \sum_{\nu=1}^{N_g} \rho_g(p_o)q_{g,\nu}\delta(x-x_\nu)\delta(y-y_\nu)\delta(z-z_\nu) = 0
 \end{aligned} \tag{A.3}$$

for $0 < t < T$. The volume fractions of oil, water and gas with respect to the total fluid volume, S_o , S_w and S_g , are called oil, water and gas saturations respectively, and satisfy

$$S_w + S_o + S_g = 1 \tag{A.4}$$

The linear velocities of the three phases are represented by Darcy's Law for the flow in porous media,

$$v_o = - \frac{k(x, y, z)k_{ro}(S_w, S_g)}{\mu_o(p_o, R_s)} \nabla (p_o - g\rho_o(p_o, R_s)h(x, y)) \quad (A.5)$$

$$v_w = - \frac{k(x, y, z)k_{rw}(S_w)}{\mu_w(p_o)} \nabla (p_o - g\rho_w(p_o)h(x, y) - P_{cwo}(S_w)) \quad (A.6)$$

$$v_g = - \frac{k(x, y, z)k_{rg}(S_g)}{\mu_g(p_o)} \nabla (p_o - g\rho_g(p_o)h(x, y) + P_{cog}(S_g)) \quad (A.7)$$

where the absolute permeability $k(x, y, z)$ is a parameter characterizing the fluid conductivity of a porous medium, $\mu_o(p_o)$, $\mu_w(p_o)$ and $\mu_g(p_o)$ are the viscosities of oil, water and gas, respectively, and the relative permeabilities of oil, water and gas, $k_{ro}(S_w, S_g)$, $k_{rw}(S_w)$ and $k_{rg}(S_g)$, are functions of the water and gas saturations. The initial conditions are

$$p(x, y, z, 0) = p_0(x, y, z) \quad (A.8)$$

$$S_w(x, y, z, 0) = S_{iw} \quad (A.9)$$

$$S_o(x, y, z, 0) = S_{io} \quad (A.10)$$

and the no flux boundary conditions

$$\mathbf{n} \cdot \nabla (p_o - g\rho_o(p_o, R_s)h(x, y)) = 0 \quad (A.11)$$

$$\mathbf{n} \cdot \nabla (p_o - g\rho_w(p_o)h(x, y) - P_{cwo}(S_w)) = 0 \quad (A.12)$$

$$\mathbf{n} \cdot \nabla(p_o - g\rho_g(p_o)h(x, y) + P_{cog}(S_g)) = 0 \quad (\text{A.13})$$

hold on the boundary for $0 < t < T$. Eqs. (A.1 - A.13) are solved numerically using finite difference approximation. An industrial Black Oil simulator, CLASS, (Chevron Limited Applications Simulation System) is used to simulate a water-flood where water is pumped down injections wells to drive the oil in place toward other wells where it is produced.

Using a finite difference approximation of Eqs. (A.1) - (A.7), a nonlinear system of algebraic equations is generated as shown

$$\begin{aligned} R_{w_i} \equiv & - \sum_{j \in J_i} kh_{i,j} \left(\frac{k_{rw}}{\mu_w \beta_w} \right)_{i,j}^n (p_i - p_j - g\rho_{w,i,j}(z_i - z_j) - P_{cwo_i} + P_{cwo_j})^n \\ & - Q_{w_i}^n - \frac{V_i}{\Delta t^n} \left[\left(\frac{S_w \phi}{\beta_w} \right)_i^n - \left(\frac{S_w \phi}{\beta_w} \right)_i^{n-1} \right] = 0 \end{aligned} \quad (\text{A.14})$$

$$\begin{aligned} R_{o_i} \equiv & - \sum_{j \in J_i} kh_{i,j} \left(\frac{k_{ro}}{\mu_o \beta_o} \right)_{i,j}^n (p_i - p_j - g\rho_{o,i,j}(z_i - z_j))^n \\ & - Q_{o_i}^n - \frac{V_i}{\Delta t^n} \left[\left(\frac{S_o \phi}{\beta_o} \right)_i^n - \left(\frac{S_o \phi}{\beta_o} \right)_i^{n-1} \right] = 0 \end{aligned} \quad (\text{A.15})$$

$$\begin{aligned} R_{g_i} \equiv & - \sum_{j \in J_i} kh_{i,j} \left[\left(\frac{R_s k_{ro}}{\mu_o \beta_o} \right)_{i,j}^n (p_i - p_j - g\rho_{o,i,j}(z_i - z_j))^n \right. \\ & \left. + \left(\frac{k_{rg}}{\mu_g \beta_g} \right)_{i,j}^n (p_i - p_j - g\rho_{g,i,j}(z_i - z_j) + P_{cog_i} - P_{cog_j})^n \right] - Q_{g_i}^n \\ & - \frac{V_i}{\Delta t^n} \left[\left(\frac{R_s S_o \phi}{\beta_o} \right)_i^n - \left(\frac{R_s S_o \phi}{\beta_o} \right)_i^{n-1} + \left(\frac{S_g \phi}{\beta_g} \right)_i^n - \left(\frac{S_g \phi}{\beta_g} \right)_i^{n-1} \right] = 0 \end{aligned} \quad (\text{A.16})$$

for $n = 1, \dots, N_t$ and $i \in \bar{N}$ defined by

$$\begin{aligned}
\overline{N} &\equiv \{i \mid i = i_x + N_x(i_y - 1) + N_x N_y(i_z - 1), \\
&\quad i_x = 1, \dots, N_x, \ i_y = 1, \dots, N_y, \ i_z = 1, \dots, N_z\} \\
&= \{1, \dots, N\}
\end{aligned} \tag{A.17}$$

where $N = N_x N_y N_z$ and i_x , i_y and i_z denote the PDE grid blocks along the x -, y - and z -directions, and the index set J_i , defined for each $i \in \overline{N}$ by

$$J_i = \{j \mid j = i - N_x N_y, i - N_x, i - 1, i + 1, i + N_x, i + N_x N_y\} \cap \overline{N}, \tag{A.18}$$

is introduced for simplicity, with initial conditions

$$p_i^0 = p_0 \tag{A.19}$$

$$S_{w_i}^0 = S_{iw}. \tag{A.20}$$

A harmonic average is used for the absolute permeability

$$kh_{i,j} = \frac{2.0 \ UFACX_{i,j}}{\frac{\Delta x_j}{UX_j k_j} + \frac{\Delta x_i}{UX_i k_i}} \tag{A.21}$$

for $j = i - 1, i + 1$, where

$$UFACX_{i,j} = \frac{\frac{1}{4}(\Delta x_i + \Delta x_j)^2}{\frac{1}{4}(\Delta x_i + \Delta x_j)^2 + (\Delta z_i + \Delta z_j)^2} \tag{A.22}$$

and

$$UX_i = \Delta y_i \Delta z_i, \tag{A.23}$$

$$kh_{i,j} = \frac{2.0 UFACY_{i,j}}{\frac{\Delta y_j}{UY_j k_j} + \frac{\Delta y_i}{UY_i k_i}} \quad (\text{A.24})$$

for $j = i - N_x$, $i + N_x$, where

$$UFACY_{i,j} = \frac{\frac{1}{4}(\Delta y_i + \Delta y_j)^2}{\frac{1}{4}(\Delta y_i + \Delta y_j)^2 + (\Delta z_i + \Delta z_j)^2} \quad (\text{A.25})$$

and

$$UY_i = \Delta x_i \Delta z_i, \quad (\text{A.26})$$

and

$$kh_{i,j} = \frac{2.0}{\frac{\Delta z_j}{0.1 UZ_j k_j} + \frac{\Delta z_i}{0.1 UZ_i k_i}} \quad (\text{A.27})$$

for $j = i - N_x N_y$, $i + N_x N_y$, where

$$UZ_i = \Delta x_i \Delta y_i. \quad (\text{A.28})$$

Furthermore, upstream weighting is used for the relative permeabilities for the stability of the numerical integration given by

$$\begin{aligned} k_{r,o,i,j}^n &= k_{ro}(S_{w_i}^n, S_{g_i}^n) \text{ if } p_{o_i}^n \geq p_{o_j}^n \\ k_{r,o,i,j}^n &= k_{ro}(S_{w_j}^n, S_{g_j}^n) \text{ otherwise} \end{aligned} \quad (\text{A.29})$$

$$\begin{aligned} k_{r,w,i,j}^n &= k_{rw}(S_{w_i}^n) \text{ if } p_{w_i}^n \geq p_{w_j}^n \\ k_{r,w,i,j}^n &= k_{rw}(S_{w_j}^n) \text{ otherwise} \end{aligned} \quad (\text{A.30})$$

$$\begin{aligned} k_{r,g,i,j}^n &= k_{rg}(S_{g_i}^n) \text{ if } p_{g_i}^n \geq p_{g_j}^n \\ k_{r,g,i,j}^n &= k_{rg}(S_{g_j}^n) \text{ otherwise} \end{aligned} \quad (\text{A.31})$$

The viscosity, formation volume factor and fraction of gas dissolved in the oil-phase are treated similarly.

Several equation solver options are available for use with the CLASS simulator. Since convergence difficulties are encountered when using iterative techniques to solve the adjoint system of equations, a direct method is employed in this work.

2. Derivation of the Adjoint System

The least-squares objective function, J_{LS} , consists of three contributions for two-phase problems and five contributions for three-phase problems, where the pressure discrepancy term is given by

$$\sigma_p^2 = \frac{1}{N_o N_t} \sum_{n=1}^{N_t} \sum_{\nu=1}^{N_o} (p(x_\nu, y_\nu, z_\nu, t_n) - p_\nu^{obs^n})^2 \quad (A.32)$$

where $(x_\nu, y_\nu, z_\nu) \in V$, $\nu = 1, \dots, N_o$ denote the locations of the observations, i.e., the wells, and t_n , $n = 1, \dots, N_t$ are the observation times. Similarly, the mean-square errors in the water cut, the gas-oil ratio and the rates of liquid and gas production from individual layers are defined as,

$$\sigma_W^2 = \frac{1}{N_o N_t} \sum_{n=1}^{N_t} \sum_{\nu=1}^{N_o} (WCUT(x_\nu, y_\nu, z_\nu, t_n) - WCUT_\nu^{obs^n})^2, \quad (A.33)$$

$$\sigma_G^2 = \frac{1}{N_o N_t} \sum_{n=1}^{N_t} \sum_{\nu=1}^{N_o} (GOR(x_\nu, y_\nu, z_\nu, t_n) - GOR_\nu^{obs^n})^2, \quad (A.34)$$

$$\sigma_{Q_l}^2 = \frac{1}{N_o N_t} \sum_{n=1}^{N_t} \sum_{\nu=1}^{N_o} \sum_{k=1}^{N_l} (Q_l(x_\nu, y_\nu, z_\nu, t_n) - Q_{l,\nu}^{obs^n})^2 \quad (A.35)$$

and

$$\sigma_{Q_g}^2 = \frac{1}{N_o N_t} \sum_{n=1}^{N_t} \sum_{\nu=1}^{N_o} \sum_{k=1}^{N_l} (Q_g(x_\nu, y_\nu, z_\nu, t_n) - Q_{g,\nu}^{obs^n})^2 \quad (A.36)$$

where N_l is the number of layers completed in a given well. Thus, the least-squares objective function is given by the weighted sum of the five contributions

$$\begin{aligned} J_{LS} = & \int_0^T \int \int \int_V dx dy dz dt \frac{1}{N_t N_o} \times \\ & [W_p \sigma_p^2 + W_W \sigma_W^2 + W_G \sigma_G^2 + W_{Q_l} \sigma_{Q_l}^2 + W_{Q_g} \sigma_{Q_g}^2] \times \\ & \delta(x - x_\nu) \delta(y - y_\nu) \delta(z - z_\nu) \delta(t - t_n). \end{aligned} \quad (A.37)$$

By adjoining Eqs. (A.1) - (A.3) and in addition the well equations, the corresponding Hamiltonian of the conventional least-squares problem is

$$\begin{aligned} \widetilde{J}_{LS} = & J_{LS} + \int_0^T \int \int \int_V (\Psi_p R_w + \Psi_{S_o} R_o + \Psi_{S_g} R_g \\ & + \sum_{\nu=1}^{N_{wells}} \Psi_{wells_\nu} R_{wells_\nu}) dx dy dz. \end{aligned} \quad (A.38)$$

The corresponding finite difference approximations of Eqs. (A.37) and (A.38) are

$$\begin{aligned} J_{LS} = & \frac{1}{N_t N_o} \sum_{n=1}^{N_t} \sum_{i=1}^N \sum_{\nu=1}^{N_o} [W_p \sigma_{p_{i,\nu}} + W_W \sigma_{W_{i,\nu}} + W_G \sigma_{G_{i,\nu}} \\ & + W_{Q_l} \sigma_{Q_{l,i,\nu}} + W_{Q_g} \sigma_{Q_{g,i,\nu}}] \delta_{i,i_\nu} \end{aligned} \quad (A.39)$$

$$\begin{aligned} \widetilde{J}_{LS} = & J_{LS} + \sum_{n=0}^{N_t} \sum_{i=1}^N [\Psi_{p_i}^n R_{w_i}^n + \Psi_{S_{o_i}}^n R_{o_i}^n + \Psi_{S_{g_i}}^n R_{g_i}^n + \\ & + \sum_{\nu=1}^{N_{wells}} \Psi_{wells_\nu} R_{wells_\nu}]. \end{aligned} \quad (A.40)$$

From the first variation of Eq. (A.40), the adjoint equations are given by the following, where the terms that include δp_i^n yield

$$\begin{aligned}
R_{p_i}^n = & - \sum_{j \in J_i} (\Psi_{p_i} - \Psi_{p_j})^n \left[\left(\frac{k k_{rw}}{\mu_w \beta_w} \right)_{i,j} \left(1 - g \frac{\partial \rho_{w,i,j}}{\partial p} (z_i - z_j) \right) \right. \\
& + u_{w,i,j} (k k_{rw})_{i,j} \frac{\partial}{\partial p} \left(\frac{1}{\mu_w \beta_w} \right)_{i,j} (p_i - p_j - g \rho_{w,i,j} (z_i - z_j) - P_{cwo_i} + P_{cwo_j}) \Big]^n \\
& - \sum_{j \in J_i} (\Psi_{S_{o_i}} - \Psi_{S_{o_j}})^n \left[\left(\frac{k k_{ro}}{\mu_o \beta_o} \right)_{i,j} \left(1 - g \frac{\partial \rho_{o,i,j}}{\partial p} (z_i - z_j) \right) \right. \\
& + u_{o,i,j} (k k_{ro})_{i,j} \frac{\partial}{\partial p} \left(\frac{1}{\mu_o \beta_o} \right)_{i,j} (p_i - p_j - g \rho_{o,i,j} (z_i - z_j)) \Big]^n \\
& - \sum_{j \in J_i} (\Psi_{S_{g_i}} - \Psi_{S_{g_j}})^n \left[\left(\frac{k k_{rg} R_s}{\mu_g \beta_g} \right)_{i,j} \left(1 - g \frac{\partial \rho_{g,i,j}}{\partial p} (z_i - z_j) \right) \right. \\
& + u_{g,i,j} (k k_{rg})_{i,j} \frac{\partial}{\partial p} \left(\frac{R_s}{\mu_g \beta_g} \right)_{i,j} (p_i - p_j - g \rho_{g,i,j} (z_i - z_j)) \Big]^n \\
& - \sum_{j \in J_i} (\Psi_{S_{g_i}} - \Psi_{S_{g_j}})^n \left[\left(\frac{k k_{rg}}{\mu_g \beta_g} \right)_{i,j} \left(1 - g \frac{\partial \rho_{g,i,j}}{\partial p} (z_i - z_j) \right) \right. \\
& + u_{g,i,j} (k k_{rg})_{i,j} \frac{\partial}{\partial p} \left(\frac{1}{\mu_g \beta_g} \right)_{i,j} (p_i - p_j - g \rho_{g,i,j} (z_i - z_j) + P_{cog_i} - P_{cog_j}) \Big]^n \\
& - \Psi_{p_i}^n \frac{\partial Q_{wi}^n}{\partial p} - \Psi_{S_{o_i}}^n \frac{\partial Q_{oi}^n}{\partial p} - \Psi_{S_{g_i}}^n \frac{\partial Q_{gi}^n}{\partial p} \\
& + V_i S_{w_i} \frac{\partial}{\partial p} \left(\frac{\phi}{\beta_w} \right)_i \left(\frac{\Psi_{p_i}^{n+1}}{\delta t^{n+1}} - \frac{\Psi_{p_i}^n}{\delta t^n} \right) + V_i S_{o_i} \frac{\partial}{\partial p} \left(\frac{\phi}{\beta_o} \right)_i \left(\frac{\Psi_{S_{o_i}}^{n+1}}{\delta t^{n+1}} - \frac{\Psi_{S_{o_i}}^n}{\delta t^n} \right) \\
& + V_i [S_{o_i} \frac{\partial}{\partial p} \left(\frac{\phi R_s}{\beta_o} \right)_i + S_{g_i} \frac{\partial}{\partial p} \left(\frac{\phi}{\beta_g} \right)_i] \left(\frac{\Psi_{S_{g_i}}^{n+1}}{\delta t^{n+1}} - \frac{\Psi_{S_{g_i}}^n}{\delta t^n} \right) \\
& + \sum_{n=1}^{N_t} \sum_{i=1}^N \sum_{\nu_o=1}^{N_{\nu_o}} \frac{\partial G}{\partial p_i^n} \delta_{i,i_{\nu_o}} + \frac{\partial}{\partial p_i^n} \sum_{n=1}^{N_t} \sum_{i=1}^N \sum_{\nu_w=1}^{N_{\nu_w}} \Psi_{\nu_w}^n R_{w_{\nu_w}}^n \delta_{i,i_{\nu_w}} = 0, \quad (A.41)
\end{aligned}$$

where the terms that include $\delta S_{o_i}^n$ yield

$$\begin{aligned}
R_{S_{o_i}}^n = & - \sum_{j \in J_i} (\Psi_{p_i} - \Psi_{p_j})^n \left[\left(\frac{k k_{rw}}{\mu_w \beta_w} \right)_{i,j} \frac{\partial P_{cwo_i}}{\partial S_w} \right. \\
& - u_{w_{i,j}} \left(\frac{k}{\mu_w \beta_w} \right)_{i,j} \frac{\partial k_{rw_{i,j}}}{\partial S_w} (p_i - p_j - g \rho_{w_{i,j}} (z_i - z_j) - P_{cwo_i} + P_{cwo_j}) \Big]^n \\
& + \sum_{j \in J_i} (\Psi_{S_{o_i}} - \Psi_{S_{o_j}} + R_{s_{i,j}} (\Psi_{S_{g_i}} - \Psi_{S_{g_j}}))^n \\
& \times [u_{o_{i,j}} \left(\frac{k}{\mu_o \beta_o} \right)_{i,j} \left(\frac{\partial k_{ro}}{\partial S_w} + \frac{\partial k_{ro}}{\partial S_g} \right)_{i,j} (p_i - p_j - g \rho_{o_{i,j}} (z_i - z_j))]^n \\
& + \sum_{j \in J_i} (\Psi_{S_{g_i}} - \Psi_{S_{g_j}})^n \left[\left(\frac{k k_{rg}}{\mu_g \beta_g} \right)_{i,j} \frac{\partial P_{cog_i}}{\partial S_g} \right. \\
& - u_{g_{i,j}} \left(\frac{k}{\mu_g \beta_g} \right)_{i,j} \frac{\partial k_{rg_{i,j}}}{\partial S_g} (p_i - p_j - g \rho_{g_{i,j}} (z_i - z_j) + P_{cog_i} - P_{cog_j}) \Big]^n \\
& + \Psi_{p_i}^n \frac{\partial Q_{w_i}}{\partial S_w}^n + \Psi_{S_{o_i}}^n \frac{\partial Q_{o_i}}{\partial S_w}^n + \Psi_{S_{g_i}}^n \frac{\partial Q_{g_i}}{\partial S_g}^n \\
& - V_i \left(\frac{\phi}{\beta_w} \right)_i^n \left(\frac{\Psi_{p_i}^{n+1}}{\delta t^{n+1}} - \frac{\Psi_{p_i}^n}{\delta t^n} \right) + V_i \left(\frac{\phi}{\beta_o} \right)_i^n \left(\frac{\Psi_{S_{o_i}}^{n+1}}{\delta t^{n+1}} - \frac{\Psi_{S_{o_i}}^n}{\delta t^n} \right) \\
& + V_i \left[\left(\frac{\phi R_s}{\beta_o} \right)_i^n - \left(\frac{\phi}{\beta_g} \right)_i^n \right] \left(\frac{\Psi_{S_{g_i}}^{n+1}}{\delta t^{n+1}} - \frac{\Psi_{S_{g_i}}^n}{\delta t^n} \right) \\
& + \sum_{n=1}^{N_t} \sum_{i=1}^N \sum_{\nu_o=1}^{N_{\nu_o}} \frac{\partial G}{\partial S_{o_i}^n} \delta_{i,i_{\nu_o}} + \frac{\partial}{\partial S_{o_i}^n} \sum_{n=1}^{N_t} \sum_{i=1}^N \sum_{\nu_w=1}^{N_{\nu_w}} \Psi_{\nu_w}^n R_{w_{\nu_w}}^n \delta_{i,i_{\nu_w}} = 0, \quad (A.42)
\end{aligned}$$

where for an unsaturated reservoir, the terms that include δR_{s_i} yield

$$\begin{aligned}
R_{R_{s_i}}^n = & \sum_{j \in J-i} [\Psi_{S_{o_i}} - \Psi_{S_{o_j}} + R_{s_{i,j}} (\Psi_{R_{s_i}} - \Psi_{R_{s_j}})]^n \left[g \left(\frac{k k_{ro} \frac{\partial \rho_o}{\partial R_s}}{\mu_o \beta_o} \right)_{i,j}^n (z_i - z_j) \right. \\
& - u_{o_{i,j}} \left(k k_{ro} \frac{\partial}{\partial R_s} \left(\frac{1}{\mu_o \beta_o} \right) \right)_{i,j}^n (p_i - p_j - g \rho_{o_{i,j}} (z_i - z_j))^n \Big] \\
& - \sum_{j \in J_i} (\Psi_{R_{s_i}} - \Psi_{R_{s_j}})^n [u_{o_{i,j}} \left(\frac{k k_{ro}}{\mu_o \beta_o} \right)_{i,j}^n (p_i - p_j - g \rho_{o_{i,j}} (z_i - z_j))^n]
\end{aligned}$$

$$\begin{aligned}
& - \Psi_{S_{o_i}}^n \frac{\partial Q_{o_i}}{\partial R_s}^n - \Psi_{S_{g_i}}^n \frac{\partial Q_{g_i}}{\partial R_s}^n + V_i S_{o_i} \left(\frac{\phi}{\beta_o} \right)_i^n \left(\frac{\Psi_{R_{s_i}}^{n+1}}{\delta t^{n+1}} - \frac{\Psi_{R_{s_i}}^n}{\delta t^n} \right) \\
& + V_i S_{o_i} \frac{\partial}{\partial R_s} \left(\frac{\phi}{\beta_o} \right)_i^n \left[\frac{\Psi_{S_{o_i}}^{n+1}}{\delta t^{n+1}} - \frac{\Psi_{S_{o_i}}^n}{\delta t^n} + R_{s_i}^n \left(\frac{\Psi_{R_{s_i}}^{n+1}}{\delta t^{n+1}} - \frac{\Psi_{R_{s_i}}^n}{\delta t^n} \right) \right] \\
& + \sum_{n=1}^{N_t} \sum_{i=1}^N \sum_{\nu_o=1}^{N_{\nu_o}} \frac{\partial G}{\partial R_{s_i}^n} \delta_{i,i_{\nu_o}} + \frac{\partial}{\partial R_{s_i}^n} \sum_{n=1}^{N_t} \sum_{i=1}^N \sum_{\nu_w=1}^{N_{\nu_w}} \Psi_{\nu_w}^n R_{w_{\nu_w}}^n \delta_{i,i_{\nu_w}} = 0, \quad (A.43)
\end{aligned}$$

and where the terms that include δS_{g_i} yield

$$\begin{aligned}
R_{S_{g_i}}^n = & - \sum_{j \in J_i} (\Psi_{p_i} - \Psi_{p_j})^n \left[\left(\frac{k k_{rw}}{\mu_w \beta_w} \right)_{i,j} \frac{\partial P_{cwo_i}}{\partial S_w} \right. \\
& - u_{w_{i,j}} \left(\frac{k}{\mu_w \beta_w} \right)_{i,j} \frac{\partial k_{rw_{i,j}}}{\partial S_w} (p_i - p_j - g \rho_{w_{i,j}} (z_i - z_j) - P_{cwo_i} + P_{cwo_j}) \Big]^n \\
& - \sum_{j \in J_i} (\Psi_{S_{o_i}} - \Psi_{S_{o_j}} R_{s_{i,j}} (\Psi_{S_{g_i}} - \Psi_{S_{g_j}}))^n \\
& \times [u_{o_{i,j}} \left(\frac{k}{\mu_o \beta_o} \right)_{i,j} \frac{\partial k_{ro}}{\partial S_{g_{i,j}}} (p_i - p_j - g \rho_{o_{i,j}} (z_i - z_j))]^n \\
& - \sum_{j \in J_i} (\Psi_{S_{g_i}} - \Psi_{S_{g_j}})^n \left[\left(\frac{k k_{rg}}{\mu_g \beta_g} \right)_{i,j} \frac{\partial P_{cog_i}}{\partial S_g} \right. \\
& + u_{g_{i,j}} \left(\frac{k}{\mu_g \beta_g} \right)_{i,j} \frac{\partial k_{rg_{i,j}}}{\partial S_g} (p_i - p_j - g \rho_{g_{i,j}} (z_i - z_j) + P_{cog_i} - P_{cog_j}) \Big]^n \\
& + \Psi_{p_i}^n \frac{\partial Q_{w_i}}{\partial S_w}^n - \Psi_{S_{o_i}}^n \frac{\partial Q_{o_i}}{\partial S_g}^n - \Psi_{S_{g_i}}^n \frac{\partial Q_{g_i}}{\partial S_g}^n \\
& - V_i \left(\frac{\phi}{\beta_w} \right)_i^n \left(\frac{\Psi_{p_i}^{n+1}}{\delta t^{n+1}} - \frac{\Psi_{p_i}^n}{\delta t^n} \right) - V_i \left(\frac{\phi}{\beta_o} \right)_i^n \left(\frac{\Psi_{S_{o_i}}^{n+1}}{\delta t^{n+1}} - \frac{\Psi_{S_{o_i}}^n}{\delta t^n} \right) \\
& - V_i \left[\left(\frac{\phi R_s}{\beta_o} \right)_i^n - \left(\frac{\phi}{\beta_g} \right)_i^n \right] \left(\frac{\Psi_{S_{g_i}}^{n+1}}{\delta t^{n+1}} - \frac{\Psi_{S_{g_i}}^n}{\delta t^n} \right) \\
& + \sum_{n=1}^{N_t} \sum_{i=1}^N \sum_{\nu_o=1}^{N_{\nu_o}} \frac{\partial G}{\partial S_{g_i}^n} \delta_{i,i_{\nu_o}} + \frac{\partial}{\partial S_{g_i}^n} \sum_{n=1}^{N_t} \sum_{i=1}^N \sum_{\nu_w=1}^{N_{\nu_w}} \Psi_{\nu_w}^n R_{w_{\nu_w}}^n \delta_{i,i_{\nu_w}} = 0 \quad (A.44)
\end{aligned}$$

for $i \in \bar{N}$ and $n = N_t, N_t - 1, \dots, 1$ with terminal constraints

$$\Psi_{p_i}^{N_t+1} = 0 \quad (A.45)$$

$$\Psi_{S_{o_i}}^{N_t+1} = 0 \quad (A.46)$$

$$\Psi_{S_{g_i}}^{N_t+1} = 0. \quad (A.47)$$

The functional derivative of J_{LS} with respect to k_i , for $i \in \overline{N}$ is given by

$$\begin{aligned} \frac{\delta \widetilde{J_{LS}}}{\delta k_i} = & - \sum_{n=1}^{N_t} \sum_{j \in J_i} \frac{\partial k_{i,j}}{\partial k_i} \\ & \times [(\Psi_{p_i} - \Psi_{p_i})^n (\frac{k_{rw}}{\mu_w \beta_w})_{i,j}^n (p_i - p_j - \rho_{w,i,j}(z_i - z_j) - P_{cwo_i} + P_{cwo_j}) \\ & + (\Psi_{S_{o_i}} - \Psi_{S_{o_j}} + R_{s,i,j}(\Psi_{S_{g_i}} - \Psi_{S_{g_j}})) (\frac{k_{ro}}{\mu_o \beta_o})_{i,j}^n (p_i - p_j - \rho_{o,i,j}(z_i - z_j)) \\ & + (\Psi_{S_{g_i}} - \Psi_{S_{g_i}})^n (\frac{k_{rg}}{\mu_g \beta_g})_{i,j}^n (p_i - p_j - \rho_{g,i,j}(z_i - z_j) + P_{cog_i} - P_{cog_j})] \\ & - \Psi_{p_i} \frac{\partial Q_{wi}^n}{\partial k_i} - \Psi_{S_{o_i}} \frac{\partial Q_{oi}^n}{\partial k_i} - \Psi_{S_{g_i}} \frac{\partial Q_{gi}^n}{\partial k_i} \\ & + \sum_{n=1}^{N_t} \sum_{i=1}^N \sum_{\nu_o=1}^{N_{\nu_o}} \frac{\partial G}{\partial k_i} \delta_{i,i_{\nu_o}} + \frac{\partial}{\partial k_i} \sum_{n=1}^{N_t} \sum_{i=1}^N \sum_{\nu_w=1}^{N_{\nu_w}} \Psi_{\nu_w}^n R_w^n \delta_{i,i_{\nu_w}} \end{aligned} \quad (A.48)$$

The adjoint system equations are solved using the same direct method used in the CLASS simulator. The numerical scheme to solve the adjoint equations and compute the derivatives, $\frac{\partial J_{LS}}{\partial k_i}$, for $n = N_t, N_t - 1, \dots, 2, 1$ is as follows

Step 1 Let $\Psi_{S_{o_i}}^n = \Psi_{S_{o_i}}^{n+1}$, $\Psi_{p_i}^n = \Psi_{p_i}^{n+1}$ and $\Psi_{S_{g_i}}^n = \Psi_{S_{g_i}}^{n+1} \forall i \in \overline{N}$.

Step 2 Let $\Psi_{S_{o_i}}^{n,old} = \Psi_{S_{o_i}}^n$, $\Psi_{p_i}^{n,old} = \Psi_{p_i}^n$ and $\Psi_{S_{g_i}}^{n,old} = \Psi_{S_{g_i}}^n \forall i \in \overline{N}$.

Step 3 Solve Eqs. (A.45) - (A.48) using the direct method used by CLASS.

Step 4 If $|\Psi_{p_i}^n - \Psi_{p_i}^{n,old}|_\infty > \epsilon_o$ etc., then repeat Step 2.

Step 5 Compute the contribution of the n-th time step values of

$$\frac{\partial J_{LS}}{\partial k_i}, \quad i \in \overline{N}.$$

3. Calculation of the Derivatives of J_{SM} with respect to $W_{l,k}$

To apply the spline approximation of the absolute permeability to the history matching algorithms, an expression for the derivatives of J_{SM} with respect to spline coefficients, $W_{l,k}$, $l = 1, \dots, N_s$ is needed. From the derivatives of J_{LS} with respect to k_i , $i \in \overline{N}$, the derivatives of J_{LS} with respect to the spline coefficients can be calculated by

$$\frac{\partial J_{LS}}{\partial W_{l,k}} = \sum_{i_x=1}^{N_x} \sum_{i_y=1}^{N_y} \frac{\partial J_{LS}}{\partial k_i} b_{x,l_x,i_x} b_{y,l_y,i_y} \quad (A.49)$$

for $i \in \overline{N}$ where b_{x,l_x,i_x} and b_{y,l_y,i_y} are the cubic B-spline function,

$$b_{x,l_x,i_x} = \chi^{*4}\left(4 - l_x + \frac{x_{i_x}}{\Delta x_s}\right), \quad l_x = 1, \dots, N_{xs}, \quad i_x = 1, \dots, N_x \quad (A.50)$$

$$b_{y,l_y,i_y} = \chi^{*4}\left(4 - l_y + \frac{y_{i_y}}{\Delta y_s}\right), \quad l_y = 1, \dots, N_{ys}, \quad i_y = 1, \dots, N_y \quad (A.51)$$

$$\chi^{*4}(\theta) = \begin{cases} \frac{\theta^3}{6}, & \theta \in [0, 1]; \\ \frac{1}{6} + \frac{(\theta-1)}{2} + \frac{(\theta-1)^2}{2} - \frac{(\theta-1)^3}{2}, & \theta \in [1, 2]; \\ \frac{4}{6} - (\theta-2)^2 + \frac{(\theta-2)^3}{2}, & \theta \in [2, 3]; \\ \frac{1}{6} - \frac{(\theta-3)}{2} + \frac{(\theta-3)^2}{2} - \frac{(\theta-3)^3}{6}, & \theta \in [3, 4]; \\ 0, & \text{otherwise;} \end{cases} \quad (A.52)$$

where Δx_s and Δy_s are the grid spacings for the spline approximation and $l = l_x + N_{xs}(l_y - 1)$, $l = 1, \dots, N_s$ where $N_s = N_{xs} \times N_{ys}$. With this approximation, $k_k(x, y)$ is replaced by the set of unknown coefficients, $W_{l,k}$, $l = 1, \dots, N_s$, $k = 1, \dots, N_{LAY}$.

The derivatives $\frac{\partial J_{ST}}{\partial W_{l,k}}$, $l = 1, \dots, N_s$ and $k = 1, \dots, N_{LAY}$ can be calculated analytically⁴, and hence,

$$\frac{\partial J_{SM}}{\partial W_{l,k}} = \frac{\partial J_{LS}}{\partial W_{l,k}} + \beta \frac{\partial J_{ST}}{\partial W_{l,k}}. \quad (A.53)$$

4. Minimization Algorithm

In this dissertation, the partial conjugate gradient algorithm of Nazareth³⁹ is used for the minimization of absolute permeabilities, or rather, the coefficients of the bicubic spline function. In general, this method is preferable for large-scale problems that have an order of a hundred variables or more. Let x be an n -dimensional vector, $F(x)$ be a function to be minimized over x , and $g(x)$ be the gradient of $F(x)$ at x . Let d denote the descent direction vector, which will be determined during the minimization. To maximize the overall efficiency, the line search step is terminated early without an exact search, and to keep the conjugacy of the search direction, the new descent direction is calculated from two previously determined descent directions given by

$$d_{j+1} = -h_j + \frac{h_{j-1}h_j}{h_{j-1}d_{j-1}}d_{j-1} + \frac{h_jh_j}{h_jd_j}d_j \quad (A.54)$$

where $h_j = g_{j+1} - g_j$ and j is the minor iteration count. (See Fig. A-1.) In the examples reported in this dissertation, the algorithm required usually two line search iterations, although occasionally a few more, and 7-10 minor iterations. The number of major iterations is much more dependent on the particular problem, but on the whole, the three-step history matching algorithm reported in Chapter III required 100 solutions of the state and adjoint equations.

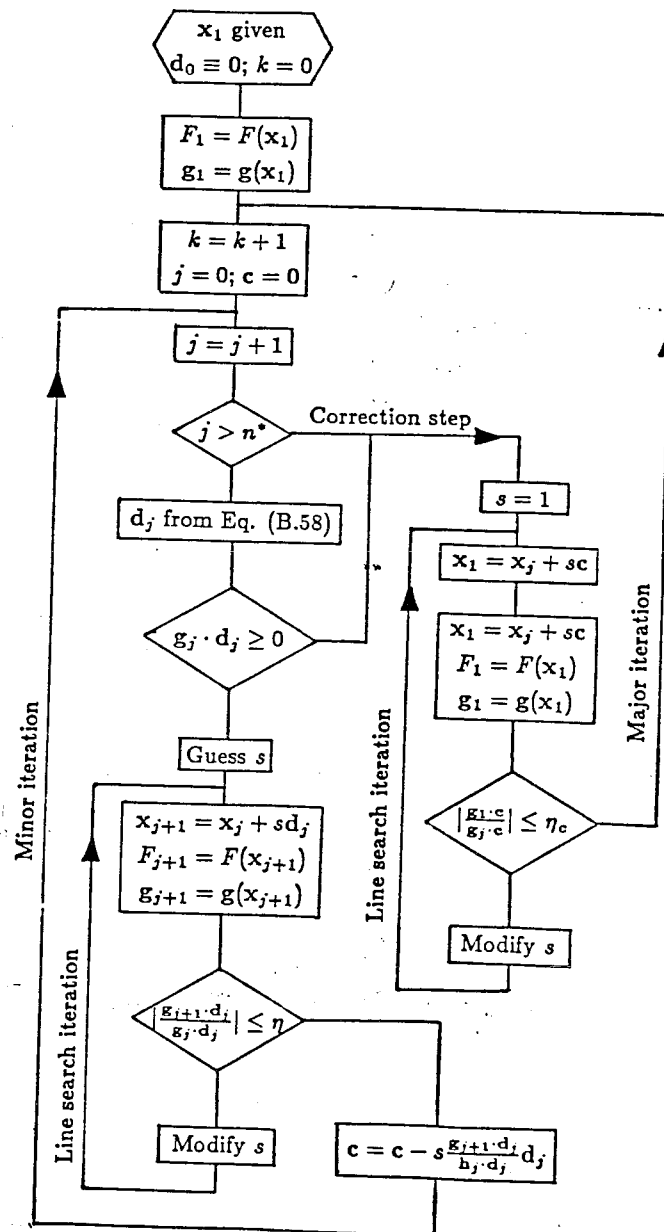


Fig. A-1 - Flow chart of Nazareth's partial conjugate gradient algorithm

APPENDIX B

User's Guide to the AUTOHM Program

1. Introduction

A new fully automatic, three-dimensional, three-phase history matching routine for estimating absolute permeabilities and well PI's is available for use with the industrial Black Oil simulator, CLASS. The algorithm uses the techniques of bicubic spline approximation, regularization and optimal control theory to make the algorithm computationally efficient and to alleviate the ill-posed nature of the mathematical problem of estimating spatially-varying parameters in a petroleum reservoir.

2. Discussion of Method

The AUTOHM program is run in three steps. In the first step, the best flat initial guess of the absolute permeability is estimated for each layer that minimizes, J_{LS} , the traditional least-squares objective function defined in Eqs. (A.32 - 39) using the secant method. In Step two, a multivariable estimation is performed which minimizes J_{LS} only. In the third step, the spatially-varying parameters are estimated using regularization techniques. In this step, the performance index is J_{SM} , the smoothing functional which is the weighted sum of J_{LS} and J_{ST} , the stabilizing functional where β , the regularization parameter, weights the relative importance of the two terms. The regularization parameter, β is calculated automatically at the end of Step 2 by $\beta = 0.1W_p \frac{\bar{\sigma}_p}{J_{ST}}$ for use in Step 3.

The algorithm has several restrictions. First, due to the use of bicubic spline approximation, each layer must have the same x- and y-dimensions; although, Δx and Δy can vary in the x- and y-directions, respectively. Secondly, the history matching algorithm assumes a particular set of injection and production rules. At the injection wells, water injection is allowed but not gas injection. At the producing wells, the total rate of liquid production must be specified. Finally, since a history match may be difficult if the production or injection rules change during the estimation, it is necessary to make sure they stay the same during the time period over which the minimization is performed.

3. Generation of the Input and Output Data Files for Use with the AUTOHM Program

A number of input files are necessary for running the AUTOHM program. These include the input files necessary for running CLASS as well as the history matching algorithm.

3.1 Input File for CLASS, *.DECK

The *.DECK file includes the input data necessary to run the CLASS simulator. The user must include this file as input during all steps of the history matching routine. A detailed discussion of the creation of the input file, *.DECK, needed to run the CLASS simulator can be found in the CLASS User and Programmer Guide. In using CLASS with all three steps of the minimization algorithm, the input file, *.DECK, must include time cards for all the observation times at which the user wishes to history match in order to assure that the simulator is solved at every observation time. It must be noted that although the absolute permeability is read as an input by CLASS from the *.DECK file, the history matching algorithm overrides

those values by reading them from other input files. In addition, the restrictions discussed in the previous section must be considered in creating the appropriate input *.DECK file.

3.2 Generation of the Observation Files from Program RSVRS.FOR

The observation data files needed for running AUTOHM depend upon the particular problem the user wishes to consider. In particular, the number and type of phases present and the dimensionality of the problem are factors that determine which sort of data files are needed. Several input data files are needed to run RSVRS.FOR. These input files and all the different kinds of observation data files and their usage are listed in this section. When program RSVRS.FOR is used with CLASS to generate a set of observation data to history match, the true absolute permeability distribution is entered in the input file for CLASS, *.DECK.

INPUT FILES

OBDAT.DAT \equiv Contains input data necessary to run the history matching algorithm. Must be created by the user for use with RSVRS.FOR as well as for all other steps of the minimization algorithm.

READ NOISY, KPENAL, IZONE, KPERM, NPI, NOBPT,
 NOBCOM, NOBWEL, NWLL, MAXCOM, NSRT,
 NGOR, NWCT

READ (MOBS(I), I = 1, NWLL)

READ (MOBCOM(I), I = 1, MAXCOM)

READ (MOBCEL(I), I = 1, NDATAP)

(NDATAP = # of active cells)

- NOISY = 0, Do not generate or use noisy observation data.
 = 1, Do generate and use noisy observation data.
- KPENAL = 1, Include JPEN, penalty terms used when assuming
 known values of the absolute permeability.
 2, Do not include JPEN.
- IZONE = 1, Use zonation approach.
 2, Use bicubic spline approach.
- KPERM = 0, Assume $k_{v_i} = 0$, i.e., layers are noncommunicating.
 1, Assume $k_{v_i} = 0.1k_i$.
- NPI = 1, Simultaneously estimate k 's and PI's.
 0, Estimate k 's only.
- NOBPT = Total # of observation cells; this does not include
 cells containing completions.
- NOBCOM = Total # of observation completions.
- NOBWEL = Total # of observation wells.
- NWLL = Total # of wells.
- MAXCOM = Total # of completions.
- NSRT = 1, Use the rate of liquid production from individual
 completions.
 2, Use the rate of total production from individual
 completions.
 3, Use both the rate of liquid production and gas production
 from individual completions.
- NGOR = 1, Use the gas-oil ratio from each completion.

2, Use the gas-oil ratio from each well.

NWCT = 1, Use the water cut from each completion.

2, Use the water cut from each well.

MOBS(NWLL) = 0, Well is not an observation well.

1, Well is an observation well.

MOBCOM(MAXCOM) = 0, Completion is not an observation comp.

1, Completion is an observation comp.

MOBCEL(NDATAP) = 0, Cell is not an observation cell.

1, Cell is an observation cell.

AWGT.DAT \equiv Contains a parameter used for calculating the weighting factors used in the least squares objective function; this number has a value between 0 and 1.
Must be created by the user.

NAMelist /AWGT0/ AWGT

READ (*,AWGT0)

AWGT(1) > 0, for all cases.

AWGT(2) > 0, for the two-phase oil and water case and for the three-phase case.

= 0, otherwise.

AWGT(3) > 0, for the two-phase oil and gas case and for the three-phase case.

= 0, otherwise.

AWGT(4) > 0, for all three-dimensional cases.

= 0, otherwise.

OUTPUT FILES

POB.DAT \equiv Contains reservoir pressure measurements in each active cell at each observation time in SI units.
Created by RSVRS.FOR. Needed for all estimation cases.

WRITE T, (POB(I), I = 1, NDATA)

BHPOB.DAT \equiv Contains bottom hole pressures in each well at each observation time in SI units. Created by RSVRS.FOR. Needed for all estimation cases.

WRITE T, (BHPOB(I), I = 1, NWLL)

WCTOB.DAT \equiv Contains water cut in each well at each observation time; only needed when both oil and water are present.
Created by RSVRS.FOR.

WRITE T, (WCTOB(I), I = 1, NWLL)

GOROB.DAT \equiv Contains gas-oil ratio in each well at each observation time; only needed when both oil and gas are present.
Created by RSVRS.FOR.

WRITE T, (GOROB(I), I = 1, NWLL)

SRTOB.DAT \equiv Contains liquid rate of production from each comp. at each observation time; 3-D cases only.
NSRT = 1 or 3.
Created by RSVRS.FOR.

WRITE T, (SRTOB(I), I = 1, MAXCOM)

SRTTOB.DAT \equiv Contains total rate of production from each comp.
at each observation time; 3-D cases only. NSRT = 2.
Created by RSVRS.FOR.

WRITE T, (SRTTOB(I), I = 1, MAXCOM)

SRGOB.DAT \equiv Contains gas rate of production from each comp.
at each observation time; 3-D, 3-phases cases only.
NSRT = 3. Created by RSVRS.FOR.

WRITE T, (SRGOB(I), I = 1, MAXCOM)

OBSTEP.DAT \equiv Contains the # of observation times for each
type of data. Created by RSVRS.FOR.

WRITE NTOP, NTOBH, NTOW, NTOG, NTOR

$$\text{NTOP} = \# \text{ of reservoir pressure observations}$$
$$\text{NTOBH} = \# \text{ of wellbore pressure observations}$$
$$\text{NTOW} = \# \text{ of water cut observations}$$
$$\text{NTOG} = \# \text{ of gas-oil ratio observations}$$
$$\text{NTOR} = \# \text{ of rate of production observations}$$

WGTDAT.DAT \equiv Contains the weighting factors used to calculate J_{LS} .
Created by RSVRS.FOR.

```

NAMELIST      /HMALG0/  WGTTP, WGTWCT, WGTGOR, WGTSTRT,
                        WGTSTRTT, WGTSTRG

```

WRITE (*,HMALG0)

WGTPP = weighting factor for pressure data.

WGTWCT= weighting factor for water cut data.

WGTGOR = weighting factor for gas-oil ratio data.

WGTSRT = weighting factor for liquid production data.

WGTSRTT= weighting factor for total production data.

WGTSRG = weighting factor for gas production data.

3.3 Input and Output Files for Step 1 of the AUTOHM Program, RSVR1.FOR

In Step 1 of the history matching algorithm, we wish to find the best uniform value of the absolute permeability for each layer which minimizes J_{LS} . The secant method is the minimization technique used in this step of the algorithm since we are only estimating a few parameters. In general, we have found that when starting with an initial guess that is much lower than the true permeability values the minimization algorithm works much more efficiently. Since the true permeability distribution is not known *a priori*, we suggest starting the algorithm with a very small value.

INPUT FILES

OBDAT.DAT	≡	Created by the user and discussed in Section 3.2.
POB.DAT	≡	Created by RSVRS.FOR and discussed in Section 3.2.
BHPOB.DAT	≡	Created by RSVRS.FOR and discussed in Section 3.2.
WCTOB.DAT	≡	Created by RSVRS.FOR and discussed in Section 3.2.
GOROB.DAT	≡	Created by RSVRS.FOR and discussed in Section 3.2.
SRTOB.DAT	≡	Created by RSVRS.FOR and discussed in Section 3.2.
SRTTOB.DAT	≡	Created by RSVRS.FOR and discussed in Section 3.2.

SRGOB.DAT \equiv Created by RSVRS.FOR and discussed in Section 3.2.

OBSTEP.DAT \equiv Created by RSVRS.FOR and discussed in Section 3.2.

WGTDAT.DAT \equiv Created by RSVRS.FOR and discussed in Section 3.2.

TIMES.DAT \equiv Contains end time for the simulation run.

READ TEND

TEND = End time for the simulation run.

MINIMU.DAT \equiv Contains input data for running RSVR1.FOR.

Created by the user.

READ NFC

READ EPS

NFC = Total # of function calls allowed, i.e., # of times both the simulator equations and the adjoint system are solved.

EPS = Tolerance for convergence.

PRM0.DAT \equiv Contains the uniform initial guess of the absolute permeability for each layer. Created by the user.

READ (PRMU(I), I = 1, NZ)

NZ = # of layers

PRMU(NZ) = Uniform initial guess for each layer in SI units.

OUTPUT FILES

PRM1.DAT \equiv Contains the best estimate of the uniform permeability for each cell in the reservoir.

Created by RSVR1.FOR.

WRITE (PRM(I), I = 1, NDATA)

PRM(NDATA) = Permeability for each grid cell.

RUNDAT.DAT \equiv Contains the values of PRMU(NZ), JLS and GLSKU(NZ), the derivative of JLS wrt PRMU(I), for each iteration of the minimization algorithm.

Created by RSVR1.FOR.

WRITE (PRMU(I), I = 1, NZ)

WRITE JLS

WRITE (GLSKU(I), I = 1, NZ)

PRMU(NZ) = Uniform permeability value for each layer.

JLS = Objective function.

GLSKU(NZ) = Gradient of JLS wrt PRMU(I)

3.4 Input and Output Files for Step 2 of the AUTOHM Program, RSVR2.FOR

In Step 2 of the history matching algorithm, we wish to estimate the spatially-varying absolute permeability distribution which minimizes J_{LS} starting with the best uniform values for each layer estimated in Step 1. The conjugate gradient method without exact line search is the minimization technique used in this step of the algorithm.

INPUT FILES

OBDAT.DAT \equiv Created by the user and discussed in Section 3.2.

POB.DAT \equiv Created by RSVRS.FOR and discussed in Section 3.2.

BHPOB.DAT \equiv Created by RSVRS.FOR and discussed in Section 3.2.

WCTOB.DAT \equiv Created by RSVRS.FOR and discussed in Section 3.2.

GOROB.DAT \equiv Created by RSVRS.FOR and discussed in Section 3.2.

SRTOB.DAT \equiv Created by RSVRS.FOR and discussed in Section 3.2.

SRTTOB.DAT \equiv Created by RSVRS.FOR and discussed in Section 3.2.

SRGOB.DAT \equiv Created by RSVRS.FOR and discussed in Section 3.2.

OBSTEP.DAT \equiv Created by RSVRS.FOR and discussed in Section 3.2.

WGTDAT.DAT \equiv Created by RSVRS.FOR and discussed in Section 3.2.

TIMES.DAT \equiv Contains end time for the simulation run.

READ TEND

TEND = End time for the simulation run.

MINIM.DAT \equiv Contains input data for running RSVR2.FOR and
RSVR3.FOR. Created by the user.

READ NFC

READ NLS

READ NITE

READ EPS

READ ETA, ETAC

NFC = Total # of function calls allowed, i.e., # of times both the

simulator equations and the adjoint system can be solved.

NLS = Total # of line searches allowed. Usually 5-10.

NITE = Total # of iterations before corection step of the minimization technique is performed.

EPS = Tolerance for convergence.

ETA, ETAC = Convergence tolerances for the correction step.

PRM1.DAT \equiv Contains the uniform initial guess of the absolute permeability for each layer. Created by RSVR1.FOR.
Used when IZONE = 2 only.

READ (PRM(I), I = 1, NDATA)

PRM(NDATA) = Starting guess of the permeability for Step 2.

SPLINE.DAT \equiv Contains the dimensions of the spline grid.
Used only when IZONE = 2.

NAMelist /NLSPL/ NXs, NYS, TOL

READ (*,NLSPL)

NXS = x-dimension of the spline grid; $NXS \leq NX$.

NYS = y-dimension of the spline grid; $NYS \leq NY$.

TOL = Tolerance for solving over-determined system generated by calculating the spline coefficients from the permeability.

WKDAT.DAT \equiv Used only when KPENAL = 1;
i.e., when the bicubic spline approach is used, and when some of the permeability values are assumed known. This is accomplished by adding a penalty

term to the performance index, J_{PEN} .

Created by the user.

READ NKNOW

READ (MKNOW(I),I=1,NDATAP)

READ (WGHTK(I),I=1,NKNOW)

READ (PRMK(I),I=1,NKNOW)

NKNOW = Total # penalized permeability values.

MKNOW(NDATAP) = 0, Non-penalized permeability value.
Cell number of the penalized value.

WGHTK(NKNOW) = Weighting factors for the penalized
permeability values.

PRMK(NKNOW) = Penalized permeability values.

ZONE.DAT \equiv Used only if IZONE = 1;
i.e., when the zonation approach is used.
This file is created by the user.

READ NZONE

READ (NPZONE(I),I=1,NDATAP)

NZONE = Total # zones \leq NDATAP.

NPZONE(NDATAP) = Zone number associated with an active cell.

PZONE1.DAT \equiv Used only if IZONE = 1;
i.e., when the zonation approach is used.
This file is created by the user.

READ (KZONE(I),I=1,NDATAP)

READ (PRMZON(I),I=1,NZONE)

KZONE(NDATAP)= 1, permeability of zone is known.
 2, permeability of zone is unknown.
 PRMZON(NDATAP) = Initial value of the permeability of each zone.

OUTPUT FILES

PRM2.DAT \equiv Contains the best estimate of the spatially-varying permeability when minimizing JLS, REGPRM, the regularization parameter, and the spline coefficients and the PI's when PI's are estimated as well.
 Created by RSVR2.FOR when IZONE = 2.

WRITE (PRM(I), I = 1, NDATAP), REGPRM,
 (W(I), I = 1,NA)

PRM(NDATAP) = Permeability for each grid cell.

REGPRM = Regularization parameter calculated in RSVR2.FOR
 for use in Step 3.

W(NA) = Spline coefficient for each spline grid cell and the PI's.
 NA = NXS*NYS + # of PI's to be estimated.

PRM2.DAT \equiv Contains the best estimate of the spatially-varying permeability when minimizing JLS, REGPRM, the regularization parameter, and the spline coefficients and the PI's when PI's are estimated as well.
 Created by RSVR2.FOR when IZONE = 2.

WRITE (PRM(I), I = 1, NDATAP), REGPRM,
 (W(I), I = 1,NA)

PRM(NDATAP) = Permeability for each grid cell.

REGPRM = Regularization parameter calculated in RSVR2.FOR
for use in Step 3.

W(NA) = Spline coefficient for each spline grid cell and the PI's.
NA = NXS*NYS + # of PI's to be estimated.

PZONE2.DAT \equiv Contains the best estimate of the spatially-varying
permeability when minimizing JLS, REGPRM, the
regularization parameter, and the KZONE(NDATAP).
Created by RSVR2.FOR when IZONE = 1.

WRITE (KZONE(I), I=1, NDATAP), REGPRM,
(PRMZON(I), I = 1, NZONE)

PRMZON(NZONE) = Permeability for each zone.

REGPRM = Regularization parameter calculated in RSVR2.FOR for use in Step 3.

RUNDAT.DAT \equiv Contains the values of the gradient, the objective
function and the permeability for each iteration.

WRITE (PRM(I), I = 1, NDATAP)

WRITE IFC

WRITE (W(I), I = 1, NA)

WRITE JLS

WRITE JPEN

WRITE JLS, JLSPP, JLSWCT, JLSGOR, JLSSRT OR JLSSRTT,
JLSSRG

WRITE JST, (SBLV(I), I = 1, 4)

WRITE ITE, ILS, J

WRITE JSM, < G,D >, || G ||, || D ||, S

IFC	=	Current number of function calls, i.e., number of times the simulator and adjoint equations have been solved.
JPEN	=	Penalty function used when known permeability data is included in the estimation.
JLSPP	=	Pressure terms in the objective function.
JLSWCT	=	Water cut terms in the objective function.
JLSGOR	=	Gas-oil ratio terms in the objective function.
JLSSRT	=	Total or liquid production rate terms in the objective function.
JLSSRG	=	Gas production rate terms in the objective function.
JST	=	Stabilizing functional.
SBLV(4)	=	Magnitude of the four terms in the stabilizing functional.
ITE	=	Current number of iterations.
ILS	=	Current number of line searches.
JSM	=	Smoothing functional.
$\langle G, D \rangle$	=	Norm of G^*D .
$\ G \ $	=	Norm of G , the gradient.
$\ D \ $	=	Norm of D , the search direction.
S	=	Step length.

3.5 Input and Output Files for Step 3 of the AUTOHM Program, RSVR3.FOR

In Step 3 of the history matching algorithm, we wish to estimate the spatially-varying absolute permeability distribution which minimizes J_{SM} the smoothing functional discussed in Section 2, starting with the permeability values estimated in Step 2.

INPUT FILES

OBDAT.DAT	≡	Created by the user and discussed in Section 3.2.
POB.DAT	≡	Created by RSVRS.FOR and discussed in Section 3.2.
BHPOB.DAT	≡	Created by RSVRS.FOR and discussed in Section 3.2.
WCTOB.DAT	≡	Created by RSVRS.FOR and discussed in Section 3.2.
GOROB.DAT	≡	Created by RSVRS.FOR and discussed in Section 3.2.
SRTOB.DAT	≡	Created by RSVRS.FOR and discussed in Section 3.2.
SRTTOB.DAT	≡	Created by RSVRS.FOR and discussed in Section 3.2.
SRGOB.DAT	≡	Created by RSVRS.FOR and discussed in Section 3.2.
OBSTEP.DAT	≡	Created by RSVRS.FOR and discussed in Section 3.2.
WGTDAT.DAT	≡	Created by RSVRS.FOR and discussed in Section 3.2.
TIMES.DAT	≡	Contains end time for the simulation run.

READ TEND

TEND = End time for the simulation run.

MINIM.DAT	≡	Contains input data for running RSVR2.FOR and RSVR3.FOR. Created by the user.
------------------	---	---

READ NFC

READ NLS

READ NITE

READ EPS

READ ETA, ETAC

NFC = Total # of function calls allowed, i.e., # of times both the
 simulator equations and the adjoint system can be solved.

NLS = Total # of line searches allowed. Usually 5-10.

NITE = Total # of iterations before correction step of the minimization
 technique is performed.

EPS = Tolerance for convergence.

ETA, ETAC = Convergence tolerances for the correction step.

PRM2.DAT ≡ Contains the best estimate of the spatially-varying
 permeability when minimizing JLS, REGPRM, the
 regularization parameter and the spline coefficients
 and the PI's when PI's are estimated as well.

Created by RSVR2.FOR when IZONE = 2.

READ (PRM(I), I = 1, NDATA), REGPRM,
 (W(I), I = 1,NA)

PRM(NDATA) = Permeability for each grid cell.

REGPRM = Regularization parameter calculated in RSVR2.FOR
 for use in Step 3.

W(NA) = Spline coefficient for each spline grid cell and the PI's.
 NA = NXS*NYS + # of PI's to be estimated.

SPLINE.DAT ≡ Contains the dimensions of the spline grid.
 Used only when IZONE = 2.

NAMelist /NLSPL/ NXS, NYS, TOL

READ (*,NLSPL)

NXS = x-dimension of the spline grid; $NXS \leq NX$.
 NYS = y-dimension of the spline grid; $NYS \leq NY$.
 TOL = tolerence for solving over-determined system generated by
 calculating the spline coefficients from the permeability.

WKDAT.DAT \equiv Used only when $KPENAL = 1$;
 i.e., when the bicubic spline approach is used, and
 when some of the permeability values are assumed
 known. This is accomplished by adding a penalty
 term to the performance index, J_{PEN} .
 Created by the user.

READ NKNOW
 READ (MKNOW(I),I=1,NDATAP)
 READ (WGHTK(I),I=1,NKNOW)
 READ (PRMK(I),I=1,NKNOW)

 NKNOW = Total # penalized permeability values.
 MKNOW(NDATAP) = 0, Non-penalized permeability value.
 Cell number of the penalized value.
 WGHTK(NKNOW) = Weighting factors for the penalized
 permeability values.
 PRMK(NKNOW) = Penalized permeability values.

ZONE.DAT \equiv Used only if $IZONE = 1$;
 i.e., when the zonation approach is used.
 This file is created by the user.

READ NZONE
 READ (NPZONE(I),I=1,NDATAP)

NZONE = Total # zones \leq NDATA.

NPZONE(NDATA) = Zone number associated with an active cell.

PZONE2.DAT \equiv Contains the best estimate of the spatially-varying permeability when minimizing JLS, REGPRM, the regularization parameter, and the KZONE(NDATA).
Created by RSVR2.FOR when IZONE = 1.

READ (KZONE(I), I=1, NDATA), REGPRM,
(PRMZON(I), I = 1, NZONE)

PRMZON(NZONE) = Permeability for each zone.

REGPRM = Regularization parameter calculated in RSVR2.FOR
for use in Step 3.

OUTPUT FILES

PRM3.DAT \equiv Contains the best estimate of the spatially-varying permeability when minimizing JLS, REGPRM, the regularization parameter, and the spline coefficients and the PI's when PI's are estimated as well.
Created by RSVR3.FOR.

WRITE (PRM(I), I = 1, NDATA), REGPRM,
(W(I), I = 1, NA)

PRM(NDATA) = Permeability for each grid cell.

REGPRM = Regularization parameter calculated in RSVR2.FOR
for use in Step 3.

W(NA) = Spline coefficient for each spline grid cell and the PI's.
NA = NXS*NYS + # of PI's to be estimated.

PZONE3.DAT \equiv Contains the best estimate of the spatially-varying permeability when minimizing JLS and REGPRM, the regularization parameter.

Created by RSVR3.FOR when IZONE = 1.

WRITE (PRMZON(I), I = 1, NZONE), REGPRM

PRMZON(NZONE) = Permeability for each zone.

REGPRM = Regularization parameter calculated in RSVR2.FOR for use in Step 3.

RUNDAT.DAT \equiv Contains the values of the gradient, the objective function and the permeability for each iteration.

WRITE (PRM(I), I = 1, NDATA)

WRITE IFC

WRITE (W(I), I = 1, NA)

WRITE JLS

WRITE JPEN

WRITE JLS, JLSPP, JLSWCT, JLSGOR, JLSSRT OR JLSSRTT,
JLSSRG

WRITE JST, (SBLV(I), I = 1, 4)

WRITE ITE, ILS, J

WRITE JSM, < G,D >, || G ||, || D ||, S

IFC = Current number of function calls, i.e., number of times the simulator and adjoint equations have been solved.

JPEN = Penalty function used when known permeability data is included in the estimation.

JLSPP = Pressure terms in the objective function.

JLSWCT = Water cut terms in the objective function.

JLSGOR	=	Gas-oil ratio terms in the objective function.
JLSSRT	=	Total or liquid production rate terms in the objective function.
JLSSRG	=	Gas production rate terms in the objective function.
JST	=	Stabilizing functional.
SBLV(4)	=	Magnitude of the four terms in the stabilizing functional.
ITE	=	Current number of iterations.
ILS	=	Current number of line searches.
JSM	=	Smoothing functional.
$\langle G, D \rangle$	=	Norm of $G \cdot D$.
$\ G \ $	=	Norm of G , the gradient.
$\ D \ $	=	Norm of D , the search direction.
S	=	Step length.

4. Implementation

Implementation of the AUTOHM program involves several steps. First, the observation data files and other input data files must be generated for use with Steps 1, 2 and 3 of the minimization algorithm. A detailed discussion of these files and what they contain is presented in the previous section. The appropriate FETCH and DISPOSE commands must be included in the job control files created for each step of minimization algorithm and in the job control file used for generating the observation data with CLASS.

The Cray load modules needed for running program RSVRS to generate observation data using CLASS are accessed under the following:

CLASSPROC,ID=AUTOHM,OWN=FJKE.

IOLIB,ID=AUTOHM,OWN=FJKE.

```

CLASSLIB,ID=AUTOHM,OWN=FJKE.
DIRECTSOLV,ID=RESMATH,OWN=RERF.
CGLGEN,ID=RESMATH,OWN=RERF.
CLASSLIB,ID=AUTOHM,OWN=FJKE.
CCLASS,ID=AUTOHM,OWN=JEMAR.
COMPOB,ID=AUTOHM,OWN=JEMAR.

```

The Cray load modules needed for running Step 1 of the minimization algorithm are accessed under the following:

```

CLASSPROC,ID=AUTOHM,OWN=FJKE.
IOLIB,ID=AUTOHM,OWN=FJKE.
CLASSLIB,ID=AUTOHM,OWN=FJKE.
DIRECTSOLV,ID=RESMATH,OWN=RERF.
CGLGEN,ID=RESMATH,OWN=RERF.
CLASSLIB,ID=AUTOHM,OWN=FJKE.
CCLASS,ID=AUTOHM,OWN=JEMAR.
COMADJ,ID=AUTOHM,OWN=JEMAR.
COMP1,ID=AUTOHM,OWN=JEMAR.

```

The Cray load modules needed for running Step 2 of the minimization algorithm are accessed under the following:

```

CLASSPROC,ID=AUTOHM,OWN=FJKE.
IOLIB,ID=AUTOHM,OWN=FJKE.
CLASSLIB,ID=AUTOHM,OWN=FJKE.
DIRECTSOLV,ID=RESMATH,OWN=RERF.
CGLGEN,ID=RESMATH,OWN=RERF.
CLASSLIB,ID=AUTOHM,OWN=FJKE.

```

CCLASS,ID=AUTOHM,OWN=JEMAR.
 COMADJ,ID=AUTOHM,OWN=JEMAR.
 COMP2,ID=AUTOHM,OWN=JEMAR.

The Cray load modules needed for running Step 3 of the minimization algorithm are accessed under the following:

CLASSPROC,ID=AUTOHM,OWN=FJKE.
 IOLIB,ID=AUTOHM,OWN=FJKE.
 CLASSLIB,ID=AUTOHM,OWN=FJKE.
 DIRECTSOLV,ID=RESMATH,OWN=RERF.
 CGLGEN,ID=RESMATH,OWN=RERF.
 CLASSLIB,ID=AUTOHM,OWN=FJKE.
 CCLASS,ID=AUTOHM,OWN=JEMAR.
 COMADJ,ID=AUTOHM,OWN=JEMAR.
 COMP3,ID=AUTOHM,OWN=JEMAR.

The source code for the minimization algorithm is stored under the following:

JEMAR.SIMUL.FORT.

5. Definition of Programs

RSVRS

The main program used for generating observation data using CLASS.

RSVR1

The main program used for performing Step 1 of the the minimization algorithm in which the best uniform value of k is calculated for each layer.

RSVR2

The main program used for performing Step 2 of the the minimization algorithm in which a multivariable estimation is performed that minimizes J_{LS} , the traditional least-squares objective function.

RSVR3

The main program used for performing Step 2 of the the minimization algorithm in which a multivariable estimation is performed that minimizes J_{SM} , the smoothing functional, which is the weighted sum of J_{LS} and J_{ST} , the stabilizing functional.

6. Definition of Subroutines**AAMAIN**

This was the main program of class which is now a subroutine called by all steps of the minimization algorithm.

ADJCUM

Computes the time derivative terms of the matrix elements of the adjoint equations.

ADJEQ

Calls the routines that compute the matrix elements of the adjoint equations and puts these elements into sparse matrix format.

Calls ADJCUM, ADJWEL, ADTXS, SPARSE and WELADJ.

ADJGRD

Computes the gradient of J_{LS} wrt. the permeability from the

adjoint variables.

ADJGRD1

Computes the gradient of J_{LS} wrt. the PI's from the adjoint variables.

ADJSTP

Calls ADJEQ and the equation solver routines to solve adjoint equations.

ADJWEL

Computes the coefficients of the adjoint equations associated with the well equations.

ADTXS

Computes the directional derivative terms of the adjoint equations.

These terms are associated with the transmiscibility terms in the flow equations.

ATRANS

Updates the KH's after each iteration of the minimization algorithm.

BSPLM

Calls BSPL3.

BSPL3

Computes the bicubic spline function and its first, second and third derivatives.

EXTREM

Calculates the upper and lower bounds of the observation data needed to create noisy observation data.

GLSF

Sets the terminal constraints for solving the adjoint equations.

Calls ATRANS. Calls AAMAIN which solves the flow equations with the updated values of the KH's. Reads in data necessary for solving the adjoint equations. Calls ADJSTP, ADJGRD and ADJGRD1.

GSTF

Computes the stabilizing functional and its derivatives wrt. the permeability analytically from the bicubic spline function.

GSTF1

Computes the stabilizing functional and its derivatives wrt. the permeability using finite difference approximation.

HSEHLD

Solves the over-determined system of equations generated from calculating the bicubic spline coefficients, W, from the permeability.

JSTF

Computes the constant terms in the bicubic spline function.

MINZ

Updates the current values of the parameters during a multivariable minimization done in Steps 2 and 3. This minimization algorithm generates

a conjugate search direction and maintains finite termination when applied to quadratic functions without requiring exact line search. Calls VARY which updates the values of the gradient of J_{SM} wrt. the parameters.

Reference:

"A Conjugate Direction Algorithm without Exact Line Searches," Opt. Theory and Appl., 23, (1977), 373-387.

SECANT

Updates the current values of the parameters using the the secant method. This method is used in Step 1 where only one value of the parameter is estimated for each layer. Calls UNIF which updates the gradient of J_{LS} wrt. the parameters.

SHIFT1

Generates BX2 and BY2 which are associated with the bicubic spline function.

SHIFT2

Generates F2 which is associated with the bicubic spline function.

SPARSE

Stores the cell coefficients of the adjoint equations in sparse matrix A and the right hand side in matrix B.

UNIF

Computes the partial derivative of J_{LS} wrt. the flat permeability profile for each layer and the PI's for each for each completion. Calls GLSF.

VARY

Computes the derivative of J_{SM} wrt. the spline coefficients, W , and the PI's. Calls GLSF, GSTF and GSTF1.

WELADJ

Computes the well terms of the adjoint equations for the adjoint variables associated with pressure, saturations and R_g .

7. Discussion of Options

The AUTOHM program can be used to estimate horizontal permeabilities alone, PI's alone or PI's and horizontal permeabilities simultaneously. The vertical permeabilities in each cell are either assumed to be a tenth of the horizontal permeabilities of that cell in which case the layers are communicating, or they are assumed to be zero in which case the layers are noncommunicating. RSVRS.FOR can be used to generate either noisy or non-noisy observation data. Either the zonation approach or the bicubic spline approach may be used for performing the multivariable minimization. This program allows the user to input known values of the permeability for both the zonation and bicubic spline approaches. When using the zonation approach, the known value is not estimated during the minimization procedure. When using the bicubic spline approach, since the coefficients of the bicubic spline function do not have a one-to-one correspondence with the permeability values in each grid cell, a penalty function, J_{PEN} , is added to the performance index to weight the known values of the permeability during the estimation procedure.